University of Arkansas, Fayetteville
ScholarWorks@UARK

Theses and Dissertations

12-2015

Field Amplified Sample Stacking on Amyloid Beta (1-42) Oligomers using Capillary Electrophoresis

Sadia Ali Paracha
University of Arkansas, Fayetteville

Follow this and additional works at: http://scholarworks.uark.edu/etd

 Part of the Other Chemical Engineering Commons

Recommended Citation
Paracha, Sadia Ali, "Field Amplified Sample Stacking on Amyloid Beta (1-42) Oligomers using Capillary Electrophoresis" (2015). *Theses and Dissertations*. 1388.
http://scholarworks.uark.edu/etd/1388

This Thesis is brought to you for free and open access by ScholarWorks@UARK. It has been accepted for inclusion in Theses and Dissertations by an authorized administrator of ScholarWorks@UARK. For more information, please contact scholar@uark.edu, ccmiddle@uark.edu.

Field Amplified Sample Stacking on Amyloid Beta (1-42) Oligomers
using Capillary Electrophoresis

A thesis submitted in partial fulfillment
of the requirements for the degree of
Master of Science in Chemical Engineering

By

Sadia Ali Paracha
Oklahoma State University
Bachelor of Science in Chemical Engineer, 2012

December 2015
University of Arkansas

This thesis is approved for recommendation to the Graduate Council.

_____
Dr. Christa Hestekin
Thesis Director

_____
Dr. Robert Beitle
Committee Member

_____
Dr. Josh Sakon
Committee Member

_____
Dr. Shannon Servoss
Committee Member

Abstract

According to recent literature, it is believed that the oligomeric form of amyloid beta (Aβ) is the leading cause of Alzheimer's disease (1; 8; 10; 12-18). Additionally, recent studies have eluded to the impact of Alzheimer's disease (AD) both economically and socially in today's society where an increase of about 71% of AD related deaths were recorded between 2000 and 2013 (7). Since the oligomeric forms of Aβ vary in size, shape and some believe conformation, it is vital to utilize a separation technique, such as capilllary electrophoresis (CE) to further understand Aβ aggregation. By understanding Aβ aggregation, treatment of AD or preventive care measurements could be additionally developed.

Therefore in this study, field amplified sample stacking (FASS) technique on the CE was utilized to provide higher resolution in oligomeric $A\beta_{1-42}$ detection without causing significant changes to the aggregation. It was observed that the FASS technique provided smaller peak widths and increased peak heights on the CE compared to the non-FASS conditions. Furthermore by conducting thioflavin-t (ThT) assays, it was observed changing the buffer concentrations in accordance to the FASS technique conditions did not effect the overall aggregation. Thioflavin-t (ThT) assays were also conducted in order to determine an agitation rate where the oligomers of $A\beta_{1-42}$ were observed on the CE.

The oligomeric species observed were believed to be less than or equal to 100 kDa. Additionally, Congo red and Orange G inhibition were conducted to confirm oligomeric $A\beta_{1-42}$ species were observed on the CE. Both inhibition studies alongside TEM imaging proved the aggregates observed on the CE in the 27 hour aggregation were smaller than proto-fibrils. Future work on natural compound inhibition studies using CE are recommended to see how those inhibitors target $A\beta_{1-42}$ species that are less than or equal to 100 kDa.

Acknowledgements

"Everyone is my teacher. Some I seek. Some I subconsciously attract. Often I learn simply by observing others. Some may be completely unaware that I'm learning from them, yet I bow deeply in gratitude."-Eric Allen

I am grateful to have the opportunity to complete my Master of Science in Chemical Engineering at the University of Arkansas. I still remember the first time I met Dr. Havens and he told me I was accepted to the Master's Program. Though that day you made me cry, you later became an inspirational professor who made me fall in love with chemical engineering all over again. I also remember joining Dr. Christa Hestekin's research group. As I look back I am so grateful to have had the pleasure of learning from such as amazing advisor and great mentor. Not only have you taught me so much about capillary electrophoresis and how to be a researcher, you have been a listening ear when I needed, a strong backbone when I doubted, a great advice giver when I asked and just an amazing person to learn from. As an engineer, I am inspired by your passion and as a person, by your strength.

I would also like to give my special thanks to Tammy Lutz-Rechtin. It was truly a crazy and super awesome experience to be trained by you. I could not have asked for a better friend and am blessed to have someone like you in my life. You have the amazing ability to help a person develop their skills and enable others through your wealth of knowledge and passion. Additionally, I would like to thank Phillip Turner and Betty Martin for not only training me but also teaching about their research/ work of interest. I have learnt so much by these individuals that I feel like I always need to surround myself by such people who challenge my brain yet at the same time help me grow.

Additionally, I would like to thank my committee members: Dr. Beitle, Dr. Sakon and Dr. Servoss. Not only were you an amazing group to have in a committee, I also had the pleasure of

using your equipment, sometimes chemicals, learning from you as a student, and also learning from your questions during our meetings. I could not have asked for a more supportive group of people to be in my committee.

I would also like to thank Dr. Jamie Hestekin for using his conductivity meter and Dr. Mourad for using the TEM. I, the author, greatly appreciate the use of Arkansas Nano & Bio Materials Characterization Facility at the University of Arkansas, supported by the National Science Foundation and the State of Arkansas. Additionally, I would like to thank all my professors both in undergrad and grad school. I know what I know and am the type of student I am because of your love to teach and to help students like me learn.

Second to last, I would like to thank all the Cheme graduate students and new friends I have made in UofA for being awesome and helping me enjoy my experience thoroughly! The BELL graduate office hall is not only filled with awesomeness- it was a home away from home. I would also like to thank Jackie, Janet, Harold, Jim, Amber and George for helping out with my purchases, CE issues and computer requested. You all are really amazing and it was nice hearing your stories. Additionally, I would like all to thank the janitorial staff at BELL. I remember my long nights in BELL and it would not have been as normal and fun without you all and Dr. Silano who talked to me and made me feel safe.

Lastly, I would like to thank my family and friends. Without my family, I know for a fact I would not have come to UofA and I am truly grateful for this experience. You all have had to put up with my numerous “pray for me” moments. I know how amazing (hint hint) those moments were and I know I could not have made it without all of you. I would also like to thank Allah. I know everything happens for a reason and am grateful Allah gave me a reason to grow here and learn from everyone.

Dedication

I would like to dedication this thesis to my family. Each of you have a special and different place in my heart and I hope you know exact how important I think you all are. Thank you!!

Table of Content

Table of Figures

Appendix Figures

Appendix Tables

Nomenclature

AD	Alzheimer's Disease	**C_i**	Concentration of species
APP	Amyloid precursor protein	**PPE**	Personal Protection Equipment
Aβ	Amyloid beta	**HFIP**	1,1,1,3,3,3-hexafluoro-2-propanol
CE	Capillary electrophoresis	**NaOH**	Sodium hydroxide
EOF	Electro-osmotic flow	**NBT**	Nitro blue tetrazolium chloride
UV	Ultra-violet	**TBS-T**	Tris-buffer saline (Tween)
PEO	Poly(ethylene oxide)	**DMSO**	Dimethyl sulfoxide
ThT	Thioflavin-t	**DMF**	Dimethylformamide
TEM	Transmission electron microscopy	**BCIP**	5-bromo-4-chloro-3-indolyl phosphate
MWCO	Molecular weights cutoff filters	**$MgCl_2$**	Magnesium chloride
FASS	Field amplified sample stacking	**RES**	Resolution
BGE	Background electrolyte	**w**	Bi-Gaussian widths of CE peak
V	Electrostatic potential	**X**	Migration time of CE peaks
F	Faraday's constant (9.648×10^4 C/mol)	**ROS**	Reactive oxygen species
$u_{m,i}$	Electrophoretic mobility	**RNS**	Reactive nitrogen species
u	Fluid velocity	**EGCG**	Epigallocatechin 3-gallate
D_i	Diffusion coefficient	**AFM**	Atomic force microscopy
z_i	Valence		

Chapter 1: Introduction

As discoveries within the human proteome have increased, misfolded proteins and mutation of numerous proteins are being linked with various disorders (such as Alzheimer's, Parkinson, Diabetes II, etc.) in today's world (1-5). Misfolded proteins have the potential to interact with one another creating toxic aggregates, amyloidosis, that is most commonly known for fibril accumulation and an increase in β-sheet contents (1-2). An example of a disease associated with amyloidosis is Alzheimer's disease. Alzheimer's disease (AD) is a devastating progressive neurodegenerative disease without a viable preventative treatment. AD is the most common form of dementia and is believed to be caused by disruption in neurotransmitters (4; 6). With a growing increase in the life span of people, it is believed AD patient cases will also increase, creating a huge economic and social impact in the near future (3; 7).

Though the exact mechanism of the disease is still unclear, AD consists of β-sheet structures with a wide range of cytotoxic aggregated amyloid beta (Aβ) and hyperphosphorylated tau proteins throughout the damaged brain tissues (1;8-10). Linkage between hyperphosphorylation of tau and Aβ has placed tau disruption (causing formation of neurofibrillary tangle) in cognitive decline as a downstream process of Aβ pathology (3; 9-12). Furthermore, recent studies suggest that the small soluble Aβ oligomers form is the likely neurotoxic agent that is associated with the progress of AD (1; 8; 10; 12-18).

Understanding Aβ oligomer aggregation through capillary electrophoresis (CE) can help for future work in analyzing the affects natural compound inhibitors have on Aβ aggregation and therefore, help find preventive treatment. In order to study the Aβ oligomer species, background information on Aβ, Aβ aggregation, and separation techniques needed to understand the peptide aggregation will be provided in this chapter. In Chapter 2, the specific research hypothesis and

results will be discussed in detail. Finally in Chapter 3, future research utilizing CE on analyzing Aβ aggregation with natural compound inhibitors will be recommended.

1.1 Amyloid Beta

The amyloid beta forming proteins are generated when amyloid precursor protein (APP) is cleaved by the β- and ϒ-secretases. Found on chromosome 21, APP is a single transmembrane protein that is not just limited to the brain (10; 19). This protein consists of a cysteine-rich domain in the extracellular domain and intracellular domain that are cleaved to produce both amyloid forming and non-amyloid forming proteins (10; 20). Though the exact functionality of APP is still unclear, it is believed that changing the expression of APP affects activities in the brain (10; 21-22). Therefore, it is important to understand the protein further in order to avoid other detrimental side effects within the human body.

The β-secretase cleavage occurs in APP at the N-terminus of Aβ peptide; whereas, the ϒ-secretase cleaves in the intracellular domain, creating the C-terminus of Aβ peptide. Aβ consist of 36-42 residues with the most common cleavage being either at $A\beta_{1-40}$ or $A\beta_{1-42}$ (8;15). $A\beta_{1-40}$ is believed to be the predominant form; however, $A\beta_{1-42}$ is more pathogenic and predominantly found in the Aβ plaque (3; 8; 14-15; 17; 23-24). Even though $A\beta_{1-40}$ and $A\beta_{1-42}$ vary by two amino acids in the C-terminus, isoleucine and alanine, the difference causes variation in structural interactions as the peptide aggregates which leads for $A\beta_{1-42}$ having more forms of aggregate and higher toxicity (24; 25). Aβ specificity of intramolecular interaction is believed to be due to the hydrophilic residues whereas the hydrophobic amino acids are believed to help increase aggregation (26; 27). Furthermore, studies have been conducted showing how decreasing the $A\beta_{1-42}$ level has reduced the AD risk level (25; 28).

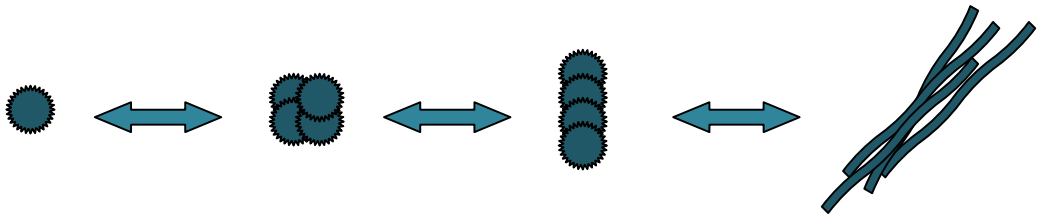

Figure 1.1-1: Overview of Aβ aggregation where the amyloid peptide aggregates from the monomeric form into soluble intermediates and proto-fibrils to eventually fibrils plaques.

As shown in Figure 1.1-1, the initial phase of the amyloid beta aggregation is the monomeric form of Aβ. These nontoxic Aβ monomers have been observed to interact with other oligomers or fibrils and also promote aggregation of the toxic residues (15). Amyloid beta monomer is believed not to be harmful. Kinetic studies have been conducted to demonstrate the conformational changes of amyloid beta from its alpha helical and/or random coil monomer structure to the formation of oligomers and eventually fibrils (26;29). The formation of oligomers is believed to be intracellular and can potential affect synapse functions, disruption of glutamate uptake, and prevent the ability to maintain proper memory (1; 3; 12; 30-31). Furthermore since the oligomer aggregates are quite unstable and time dependent, the exact shape, size, and pathological pathway are hard to determine (32; 33). Additionally with the varying size range of oligomers (from 10 kDa to 250 kDa), it is believed that the oligomers only vary in conformation when dealing with pre-fibrillar or fibrillary oligomers (32; 34). However, there are various types of oligomers as stated by Hamley and the aggregation pathway to determine which oligomeric species forms is dependent upon the experimental conditions and environment (3). Nonetheless, the fibrillary oligomers are believed to consist of similar conformation of fibrils; whereas, all other types of oligomers are believed to consist of a similar conformation with varying size range (32; 34).

1.1.1 Aggregates Formation

Though exact quantitative analysis of Aβ aggregation is still undetermined, it is believed that with the addition of aggregates, the Aβ aggregates change (in size, shape or conformation) in the presence of fibrils depending on both higher aggregates and monomer species within the solution (5; 35; 36). Recent studies have shown that AD can occur without the presence of fibril plaques (12). Therefore, increased research is being conducted on understanding the soluble intermediate aggregates of Aβ. Some techniques, such as native page, enzyme-linked immunosorbent assay, light scattering, mass spectrometry and size exclusion chromatography, have been reviewed in depth by Pryor et al. (2012) to show the various advantages and disadvantages for each technique (37). Furthermore, *in vitro* studies conducted have highlighted the difficulty in narrowing the type of intermediate aggregates that can be formed (such as ADDLs, oligomers smaller than 30 kDa, fibrillar oligomer, protofibrils) and also the ability to analyze Aβ without causing alternative aggregate pathways due to experimentation (3; 8; 12; 16; 24; 34). Consequently, by studying the soluble aggregates through CE, the separation of the Aβ species can further help understand the aggregation pathway of Aβ in a rapid manner under non-denaturing, non-organic conditions which should reduce interference with the Aβ kinetics.

1.2 Capillary Electrophoresis

Capillary electrophoresis (CE) separates proteins based on their shape, size and mass. Additionally, CE provides the opportunity to conduct separations with speed, automation, high resolution and efficiency (38; 39). Using glass narrow bore fused silica coated capillaries offers a high surface area to volume ratio which allows for heat to be dissipated more effectively.

In CE separation, the sample is injected in the fused silica capillary by hydrodynamic injection or electrokinetic injection. Hydrodynamic injection applies pressure to the sample to push

it into the capillary and typically provides an unbiased representation of the sample. Electrokinetic injection uses an electric potential different to drive sample into the capillary and creates a bias towards charged species in the sample. After the introduction of the sample, an electric field is applied across the capillary causing the sample ions to migrate based on their electrophoretic mobility which is detected using UV absorbance and translated into an electropherogram, a plot of UV absorbance versus time.

1.2.1 Electroosmotic Flow

The separation of molecules occurs when the molecules in the capillary move under an applied field with a certain velocity and direction depending on the charge and mass of the molecules (40). Furthermore, the silica capillary inner wall consists of negatively charged silanol groups that when ionized under an applied field attracts the positive ions in the buffer and create an electrical double layer (38). This double layer consists of both an immobile layer where the positive ions are interacting with the capillary (outer Helmholtz and inner Helmholtz plane) and a diffusive layer where the cations migrate toward the cathode creating a bulk flow (40; 41). The specific interaction of this electric double layer can be further described by the Stern-Gouy-Chapman model (41-43). Furthermore, this interaction between the capillary wall and sample movement under an applied field is called the electroosmotic flow (EOF). The EOF can be affected by changing the capillary length and the surface charges on the capillary wall due to the solution's pH, concentration, etc. (40; 43).

In cases dealing with non-charged species, EOF might be a beneficial. Furthermore due to the interaction with the silica capillary, the positive ions travel faster under EOF causing less dispersion depending on the sample charge. However, when a sample has a strong negative charge, such as Aβ, the EOF opposes its migration and therefore leads to a more diffused sample peak.

Additionally, interaction with the ions on the wall can lead to a greater loss of protein being detected. Therefore, it is important to control or eliminate EOF which will also help increase the migration time precision, resolution and detection of the sample (44). In order to control electroosmotic flow (EOF), the capillary wall/ sample interaction can be manipulated by creating an environment that effects the viscosity of the sample, wall's charge density or double layer thickness (38). The EOF can also be reduced or controlled by having online sample preconcentration (sample stacking, pH variation, increasing ionic strength etc.) and/or the capillary can be chemically modified or coated (38; 40; 43).

Capillary coatings are often used to provide a homogeneous, viscous layer on the surface of the capillary (38; 45). Polymer coatings, such as poly(ethylene oxide) (PEO), adsorb onto the positively charged layer at the capillary's surface by forming hydrogen bonds with silanol groups and provide a neutral surface for the ions within the capillary (38; 43; 45). This provides the ability to utilize buffers at higher range (from pH 4-8) reducing wall-peptide interaction in a hydrophilic environment. It is important to note that as the polymer molecular weight increases, the sample wall interaction reduces but the stability of the coating also reduces (45). Therefore, it is vital to establish a good coating adsorption parameter and follow proper coating protocols. For example in order to have good coating adsorption, the capillary needs to be thoroughly washed before coating to ensure silanol groups on the wall are fully protonated.

1.3 Other Techniques to Study Amyloid Oligomer Aggregates

As the interest in the amyloid oligomer has increased due its linkage with AD progression, researchers are currently utilizing various techniques in order to determine the shape, size and interaction with other compounds of these aggregates. Therefore in order to establish a basis, comparison and/or verification of the oligomer aggregation study using CE, thioflavin-T assays

(ThT assays), dot blot analysis, transmission electron microscopy (TEM) analysis and centrifugation of the aggregates were conducted.

1.3.1 Thioflavin-T Assay

Vassar and Culling (1959) were the first to demonstrate the increase in fluorescent intensity of thioflavin T (ThT) upon the aggregation of amyloid peptide (46; 47). ThT is a cationic benzothiazole dye that consists of both polar and hydrophobic regions. Though some believe the attachment of dimethylamino groups linked to the polar region creates micelles in aqueous solutions which bind to amyloid β-sheets, other researchers have shown that under the 'normal' ThT conditions, micelles do not form and therefore, the exact molecular interaction of ThT with Aβ is still undetermined (46-48). However, it is believed the closeness of the sidechains to the bound ThT within the binding channels of the β-sheets causes an increasing in fluorescent intensity in excitation from 385 to 450 nm and emission from 445 to 482 nm (47-49). This increase of intensity might be due to the inability of ThT to rotate about the shared carbon-carbon bonds between the benzylamine and benzathiole rings that occurs when ThT has free rotation and is not bound to Aβ (47).

Since thioflavin-T (ThT) is not believed to disturb Aβ aggregation, ThT assays are a commonly used *in vitro* method to help model the aggregation by analyzing the increasing in fluorescent intensity. The binding fluorescence intensity usually results in a sigmoidal curve where the initial phase is considered the lag phase (29; 50). This lag phase is dependent upon the concentration, temperature, ionic strength, pH, metal ions, and/or agitation of the peptide (26; 36; 51-52). The lag is also believed to consist of the smaller soluble amyloid species (from monomer to oligomer species). After the lag phase, a rapid elongation phase occurs in which there is a huge increase in ThT-amyloid binding and in turn an increase in fluorescent intensity. Once the

equilibrium (the plateau) of the overall aggregation is reached, the ThT-amyloid binding is believed to reach a point where most of the soluble aggregates are converted into insoluble fibrils, resulting in a decreasing in fluorescent intensity.

1.3.2 Dot Blot Analysis and Transmission Electron Microscopy (TEM) Imaging

One of the simplest qualitative methods to analyze amyloid beta aggregates is by conducting dot blots. Dot blot analysis can be conducted both by using either the direct or indirect method. The indirect method requires the use of both primary and secondary antibodies; however, in doing so, this method provides increased signal detection and therefore, better sensitivity. A small amount (1-5 μL) of Aβ is dotted on a nitrocellulose membrane due to small pore size and instantaneous binding ability with proteins. The primary antibody binds to the peptide due to protein specificity (either of sequence or conformation). The secondary antibodies are responsive to the primary antibodies where part of the antibody recognizes a certain epitope. Recent studies have shown that various primary antibodies, such as 6E10 and OC, can be utilized to detect the different Aβ species. 6E10 has been found to be reactive with amyloid amino acid residues 1-16 and is mostly used as a control for amyloid experiments (53). Furthermore, OC is a polyclonal antibodies that detects fibril oligomer or fibril conformation of Aβ (34; 54).

Another method utilized to further qualitatively understand the Aβ aggregates is transmission electron microscopy (TEM) imaging. Since TEM uses electrons instead of light, a greater resolution is achieved through this image magnifying technique. The Aβ is negatively stained and the fibril aggregates are well defined upon imaging (24; 55). Therefore, using TEM further confirms the qualitative analysis of dot blots, it provides an opportunity to distinguish the species detected by the antibodies in the dot blot analysis.

1.3.3 Centrifugation

In hopes of determining the size range of Aβ species observed on CE, ultra-centrifugation were utilized along with membrane filtration. Pryor et al. previously used centrifugation to help determine specific sizes of various Aβ species (37). Furthermore, upon conducting centrifugation experiments, relationship between the concentration, sedimentation and peptide shape have also been further explained in past studies (56-58). Since the fibril aggregates are insoluble, it is believed that these species cannot be detected on CE. Therefore, by using various molecular weights cutoff filters (MWCO) (300 kDa, 100 kDa, and 30 kDa), the sizes of the aggregates seen on CE can be determined**.** Most MWCO filters consist of hydrophilic membranes to reduce fouling and also provide up to about 90% rejection (59). Due to the random coil like behavior of peptides, the separation of the higher molecular weight vs. the filter cut-off molecular weight is dependent upon the concentration of peptide, pore size of membrane and the influence of the various molecular size species within the solution (59). Therefore, by using past studies as a basis for filtration, experiments utilizing membrane ultrafiltration might be able to help provide, a better understanding of the aggregates.

Chapter 2: Studying $A\beta_{1-42}$ Oligomer Aggregates

As stated in Chapter 1, understanding Aβ aggregation using a separation technique such as capillary electrophoresis (CE) can help in finding a future therapeutic treatment for AD. CE provides a rapid and high resolution analysis that requires small sample volumes. Previous work using CE with UV has been conducted using $A\beta_{1-40}$ (60). Therefore, this study focused on studying how field amplified sample stacking (FASS) could improve resolution of $A\beta_{1-42}$ oligomers without causing significant changes to the aggregation of the small soluble $A\beta_{1-42}$ aggregates.

The soluble oligomers should theoretically form during the lag time observed by the thioflavin t (ThT) assay and therefore, having an adequate lag time to analyze various aggregates of $A\beta_{1-42}$ on the CE was essential. The time for oligomer formation of $A\beta_{1-42}$ was estimated by conducting a ThT assay. Furthermore, the effects of field amplified sample stacking (FASS) in CE was examined to determine if FASS affects the aggregation of the sample as well as the resolution between aggregated species. The transmission electron microscope (TEM) analysis provided qualitative information about the conformation of the aggregates; whereas, the molecular weight cutoff centrifugal filters were utilized to estimate the molecular weights of the aggregated species detected by CE. Inhibitors (such as Congo red and Orange G) were also used to provide additional information about the conformation of the aggregated species. The FASS and non-FASS CE results were also compared to computational results.

2.1 Field Amplified Sample Stacking

One of the greatest advantages of CE, other than the fast analysis time, is the ability to utilize very little sample volume in order to investigate the separation of various Aβ aggregate species. In order to improve the detection, reproducibility and separation of such aggregates, various sample pre-concentration techniques can be utilized depending on the CE parameters

established (parameter detail in Appendix B). Sample pre-concentration techniques in CE consist of large volume sample stacking, PEO based sample stacking, isotachophoresis, or differences in pH or conductivity between the separation and load buffer (44; 61-63). One of the simplest ways to improve resolution and increase sensitivity up to at least 10 fold with peptide samples is field amplified sample stacking (40; 44; 61- 62; 64- 65). FASS helps increase detection on the CE while providing the opportunity to reduce $A\beta_{1-42}$ concentration. By analyzing $A\beta_{1-42}$ on the CE using FASS, the potential to observe more oligomeric peaks is increased and the peptide cost per analysis is decreased.

2.1.1 Theory

The interactions in CE consist of three major components: the electrodes, the capillary and the sample or ion transportation. According to Kohlrausch if the background electrolyte, BGE, volume is large than changes at the buffer/electrode interface can be avoided (66). The two main driving forces in a capillary are then the electroosmotic (EOF) flows and electrophoretic flows under an applied field. The electrophoretic flow depends on the local environment and in turn the bulk electroosmotic velocity of the separation buffer (as known as BGE). Since the electrophoretic flow depends on the local environment, the velocity is influenced by the electric field relative to the BGE. Additionally, the EOF depends on the strength of the interaction of the BGE with the capillary wall under an applied voltage. For an environment with normal polarity and reverse injection, where the EOF travels toward the cathode, the sample's negatively charged flow (electrophoretic mobility) has to be greater than the EOF in order to travel through the capillary and pass the detector. If the EOF is larger than the electrophoretic flow, the bulk flow will dictate the overall flow of the ions (43; 67). Since large EOF has the ability to promote laminar flow and zone broadening, it is believed that stacking efficiency can be increase with decreased EOF. Once

a specific separation environment is established (as stated in Appendix B), the capillary environment can be manipulated by one of the simplest method called field amplified sample stacking (FASS) to provide better resolution, reproducibility and detection (43; 68-69).

In order to disturb the local field strength as shown in Figure 2.1.1-1, FASS involves injecting a sample at a lower buffer concentration (load buffer) than the BGE when utilizing the same buffer for both the sample and BGE. The field strength and conductivity consist of a linear relationship where the field strength is inversely proportionality to conductivity. Therefore, the sample buffer with the lower concentration migrates faster under applied field until the ions reach the BGE ions. Since the BGE consists of a higher conductivity, it has lower resistance and in turn a lower field strength than the load buffer. This leads to the stacking effect of the sample ions where an increase in the concentration will occur in the sample zone. In turn this will lead to a better separation and less band broadening.

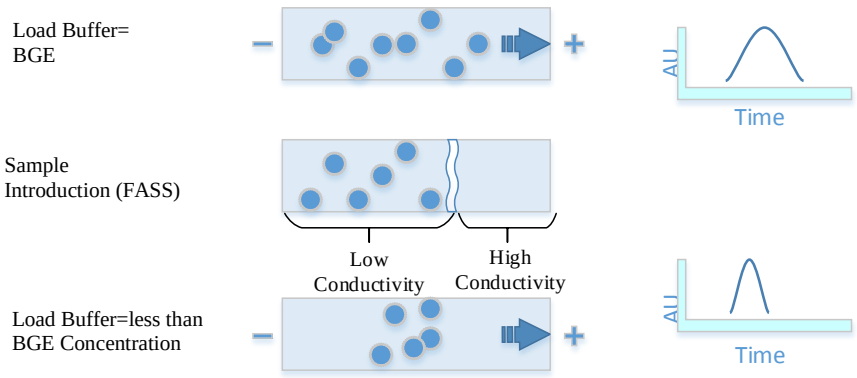

Figure 2.1.1-1: Effects of FASS where upon applying an electric field the sample focuses at an interface between the sample buffer (load buffer) and the separation buffer (BGE) due to the difference in conductivity (65).

In order to predict the effects of FASS, mathematical models have been developed where FASS has been studied in various EOF conditions (67; 70-71). The governing equation consists of

mass transport for a dilute electrolyte solution where molecular diffusion, electro-migration and convection effects are taken into account. This equation along with the flux equation, respectively, can be described as:

$$\frac{\partial C_i}{\partial t} + u\nabla C_i = \nabla\left(D_i\nabla C_i + z_i u_{m,i} F C_i \nabla V\right) \quad \text{[Equation 2.1.1]}$$

$$N_i = -D_i\nabla C_i - z_i u_{m,i} F C_i \nabla V \quad \text{[Equation 2.1.2]}$$

where F is Faraday's constant (9.648 X 10^4 C/mol), $u_{m,i}$ is the electrophoretic mobility, u is the fluid velocity, V is the electrostatic potential, z_i is the valence, D_i is the diffusion coefficient and C_i is the concentration of species. The subscript for the diffusion coefficient, valence charge and concentration can either account for the anion or cationic species (70). The electrophoretic mobility can be determined using the Nernst-Einstein relation where it is depend upon the diffusion coefficient, rate constant and temperature. Since the capillary is coated with a neutral polymer and the charge density is considered negligible, the electric field distribution often assumed to be constant and electrically neutral everywhere. Being electrically neutral helps reduce the complexity of the environment where the sum of the charge multiplied by the concentration of both the BGE and load buffer is approximately zero. Additionally, this assumption helps establish an electrically insulated capillary with a set temperature.

The initial condition consist of 0 volts where once the voltage is applied, the flow of the EOF will depend on the polarity and the strength of the applied voltage. Likewise, the boundary conditions along a single interface between the stationary and moving boundaries are as stated (70):$C_A(-L,t) = C_{Ao}$ and $C_A(L = injection\ end, t) = \gamma C_{Ao}$ where $\gamma = \frac{C_{LB}}{C_{BGE}}$, C_A =BGE concentration (Na+ focus), C_{BGE}=BGE concentration and C_{LB}= load buffer concentration. When considering the sample boundary conditions, the Danckwerts boundary condition is recommended where it is assumed that the injection point mass flux would be equal to the mass flux throughout

the capillary (72). By taking into account the Danckwerts boundary condition, a continuity of the sample at the inlet and outlet will be observed. Therefore, the mass balance will be satisfied. Furthermore, the initial conditions also described by Bharadwaj et al. highlight the importance of FASS by taking into account the concentration ratio of the BGE and load buffer as well as the sample gradient length (70). Both the concentration ratio and sample gradient length are believed to assist in determining the effect of stacking efficiency in the capillary.

2.2 Materials and Methods

Appendix D consists of a more detailed version of the protocols of all the methods described briefly below. It is important to note, all experiments were conducted utilizing proper safety and environmental regulations (wearing proper PPE, disposing chemicals in proper location etc.).

2.2.1 Sample Preparation

A 1 mg lyophilized powder of $A\beta_{1-42}$ sample from AnaSpec (San Jose, CA, USA) was pretreated using 1,1,1,3,3,3-hexafluoro-2-propanol (HFIP) as described by Pryor et al. 2014 (60). The pre-treated sample was separated into vials, dried and stored at -80°C. In order to analyze $A\beta_{1-42}$, the HFIP treated peptide was solubilized in 5 mM NaOH and kept on ice for 10 minutes. After 10 minutes, enough sodium phosphate buffer with pH=7.4 was added to the sample to reach the desired final concentration. The final $A\beta_{1-42}$ concentration utilized were 15 µM, 20 µM, 30 µM and 60 µM. The sample solution was kept on ice for an additional 20 minutes. When needed, samples were analyzed using a spectrophotometer at 277 nm to verify concentration (using Beer's law with extinction coefficient of 1280 L/(mol*cm)).

Furthermore, initial FASS experiments were performed using 1 mg/mL of bovine serum albumin (BSA) fraction V from Sigma-Aldrich as a model protein. The protein samples varied in sodium phosphate buffer concentration ranging from 10 mM to 100 mM.

Congo red and Orange G experiments were conducted using 16.7 μM stock solution of inhibitor where 2% of the total sample volume is the inhibitor. This concentration was based on the findings by Necula et. al and Pryor et al. (60; 73). Additionally, Congo red and Orange G were dissolved in water to make the stock solution in order to avoid any interference on the CE.

2.2.2 ThT Assay

The ThT assay, using RF-Mini 150 Recording Fluorometer (with excitation at 440±10 nm and emission at 490±10 nm), was conducted with a 5:1 molar ratio of the 14.29 μM ThT stock solution to 20 μM $A\beta_{1-42}$ (74). The ThT stock solution was prepared by mixing 1 mM ThT (powdered ThT from Sigma-Aldrich) with 100 mM sodium phosphate buffer (pH=7.4) or 40 mM Tris-HCl with 150 mM NaCl (pH=8.07). The initial concentration of $A\beta_{1-42}$ was 20 μM or 30 μM. The ThT stock solution concentration changed accordingly for the different amyloid beta concentration. For all ThT assays, agitation was performed utilizing a VWR micro plate shaker at 25°C and either 800, 600, 500, 400, or 300 RPM. The fluorescent intensity was determined by subtracting the background (ThT alone) from the sample fluorescent intensity.

2.2.3 CE Studies

All studies were conducted at 25°C using UV detection on P/ACE MDQ Glycoprotein System from Beckman Coulter, Inc. with a 214 nm filter, the total capillary length of 31 cm and the length to detector of 10 cm. The CE consisted of an interface with a computer utilizing the 32 Karat software for collecting the CE data. All fused silica capillary tubing were purchased from Polymicro Technologies with an inside diameter of 51 μm. The $A\beta_{1-42}$ samples were pressure

injected at 0.5 psi for various injection time depending on the sample concentration (detail stated in Appendix B Section II) and separated at 7 kV. The separation buffer (also called background electrolyte or BGE) for the CE was 100 mM sodium phosphate buffer with pH=7.4.

In order to coat the capillary, the capillary was equilibrated by conducting a pre-conditioning wash on a new capillary that included a 0.1 M NaOH rinse, a water rinse and a 0.1 M HCl rinse to potentially wash away adsorbed substances on the capillary wall and regenerate the capillary. The capillary was coated using 0.5% 2000 kDa poly(ethylene) oxide (PEO) purchased from Sigma Aldrich. The high molecular weight coating provided a strong hydrophilic/neutral environment for peptide separation and had great self-coating properties. In addition, a polymer separation matrix was used in each run to enhance the separation of the electrophoretic peaks. The polymer separation matrix consisted of 0.5% 50 kDa PEO dissolved in the 100 mM sodium phosphate buffer pH=7.4 and 0.1% of 0.1% 2000 kDa PEO. Once the capillary was coated, the capillary was utilized for at most 4 days depending on the amount of sample analyzed. Before each sample injection, the capillary was washed with filtered di-water to clean out contaminants and the coating was regenerated with the polymer matrix. The polymer coating can break down over time or have decreased efficiency due to protein adsorption. Therefore, a long wash followed by rinsing with polymer matrix (which contains a small amount of coating polymer) is believed to increase the lifetime of the capillary (75).

2.2.4 TEM Imaging

Three microliter of sample was placed on a parafilm at certain time points (stated in Section 2.2.6). At each time point, the 3 µL sample was transferred onto a 300 square grid nickel (VWR-Electron Microscope Science) by placing the grid onto the sample. Excessive sample was removed from the grid by taking the grid and tapping the side to a filter paper. Then the grid was negatively

stained with 3 µL of 2% uranyl acetate. Uranyl acetate is utilized in order to keep the peptide sample from changing its kinetics and also provide a strong background contrast to the peptide. Excess stain was also removed and sample grids were air dried. All samples were viewed using AmtV602 software interfaced with JEM-1011 Electron Microscope (JEOL) at 100 kV. The magnification utilized were 25000X, 50000X and 100000X.

2.2.5 Dot Blot Analysis

Nitrocellulose membranes were dotted with 5 µL $A\beta_{1-42}$ at 0, 2, 4, 7, 12, 18, 24, and 27 hours and air dried for 15-20 minutes after each time point. The membranes were then placed in a container that was placed within a zip lock bag that had drierite. The zip lock was then placed within a Tupperware and placed in a -20°C freezer. The drierite included an indicating dye which helped determine whether the zip lock contained moisture. Once aggregation was completed, the dried membranes were soaked in 5% milk with TBS-T and put on VWR Rocker at a tilt of 22 for an hour. Upon removing the milk solution and cleaning the membranes with TBS-T, the primary antibodies were placed on the membrane using a 1:2000 dilution for 6E10 and 1:4000 dilution for OC. The membranes were placed on the VWR Rocker overnight in the refrigerator with a tilt of 34 and washed three times using TBS-T. The washes consisted of 5 minute intervals. The secondary antibodies were added to the membranes after the last wash where 1:4000 dilution was utilized for the anti-mouse IgG on the 6E10 membranes and 1:4000 dilution was utilized for the anti-rabbit IgG on the OC membranes. This was placed on the VWR Rocker for 40-45 minutes and washed three times with TBS-T. The substrate solution was made by adding 0.1 mL of 50 mg/mL NBT (nitro blue tetrazolium chloride) in DMSO (dimethyl sulfoxide) and 0.05 mL of 50 mg/mL of BCIP (5-bromo-4-chloro-3- indolyl phosphate) in DMF (dimethylformamide) to 15 mL

TBS-T $MgCl_2$. Upon detection, this reaction was stopped by rinsing the membranes with 10% acetic acid and washed afterwards with distilled water.

2.2.6 Aggregation Study

After determining the agitation rate through ThT assays, all aggregation studies utilized a VWR micro plate shaker at 25°C and 300 RPM. At 0, 2, 4, 7, 12, 18, 24, and 27 hours, 20 µL of the $A\beta_{1\text{-}42}$ in either 100 mM (n=3) or 40 mM sodium phosphate buffer (n=4) was used for the CE experimentations and 3 µL was used for TEM imaging (n=1 for each buffer). Data collected by the CE was analyzed to determine the migration time and absorbance intensity. The CE data was translated from 32 Karat using Excel VBA program and compared using Origin® (64 bit) from OriginLab Corporation. A bi-Gaussian fit was used to calculate the migration time, peak area, width and height. The resolution, RES, was determined by (40):

$$RES = \frac{2(x_1 - x_2)}{(w_{1,1} + w_{1,2}) + (w_{2,1} + w_{2,2})} \quad \text{[Equation 2.2.3-1]}$$

where $w_{1,1}$, $w_{1,2}$ are the bi-Gaussian widths for the first peak and $w_{2,1}\ and\ w_{2,2}$ are the widths for the second peak and , $x_1\ and\ x_2$ are the migration time for the respective peaks.

Additionally, $A\beta_{1\text{-}42}$ samples were centrifuged using Nanosep MF centrifugal filters (Pall Life Science) where the filtrate was analyzed using the CE. The centrifugation process was conducted at 4°C. Initial experiments indicated that there was significant loss of the protein onto the filters and therefore the sample concentration was increased from 30 µM to 60 µM. The 60 µM $A\beta_{1\text{-}42}$ aggregated samples at 0 hour and 7 hours were analyzed. Additionally, 20 µL of the 60 µM $A\beta_{1\text{-}42}$ sample was studied using CE without centrifugation. This helped established a comparison with the filtered vs. unfiltered sample. The rest of the sample was filtered through either a 300 kDa, 100 kDa or 30 kDa filter.

Alongside conducting ThT assay at 300 RPM, a parafilm sheet was dotted with 3 μL of 30 μM $A\beta_{1-42}$ at 0, 12, 27, 51, and 79 hours for TEM imaging, n=2. This data was used to compare with the CE for both 100 mM and 40 mM sodium phosphate buffer pH=7.4 samples. Additionally, 20 μL of 30 μM $A\beta_{1-42}$ inhibited by either Congo red or Orange G was studied using the CE at 0, 2, 4, 7, 12, 18, 24 and 27 hours. TEM imaging was also conducted at 0, 12, 27, and 51 hours for both inhibitors, n=2.

2.3 Results

Several past studies have proven the various affects temperature, peptide concentration, agitation, and salt concentration etc. has on the aggregation of $A\beta_{1-42}$ (36; 46-47; 51). In order to thoroughly analyze various soluble intermediates of $A\beta_{1-42,}$ the agitation rate of the $A\beta_{1-42}$ aggregation study needs to be low enough to allow for a long lag time phase. As further discussed in Appendix A Section III, the agitation rate of 300 RPM was determined by conducting ThT assays where it was believed the soluble aggregates can be carefully examined and further understood by CE analysis. Furthermore since $A\beta_{1-42}$ was being examined on the CE where the FASS technique was going to be utilized, ThT assays for both 30 μM $A\beta_{1-42}$ samples with either 100 mM sodium phosphate or 40 mM sodium phosphate buffer were conducted. While conducting the ThT assays, the 100 mM sodium phosphate buffer produced a higher fluorescent intensity overall vs. the 40 mM sodium phosphate buffer (Figure A.3-3C). It is believed that the increase in fluorescent intensity was due to the higher concentration of β-sheet aggregates produced in the 100 mM sodium phosphate buffer. Furthermore, it was interesting to note that the overall aggregation time between the two buffers did not vary by much (Figure A.3-3A and B). As shown in Appendix A Section III, a sharp increase in fluorescent intensity was observed after 7 hours of aggregation while a huge statistical decrease in intensity was observed by 80 hours for both 100 mM and 40

mM sodium phosphate buffer samples. Therefore, it was believed that the $A\beta_{1-42}$ consist of insoluble fibril aggregates 80 hours into the aggregation.

Additionally as a confirmation of the ThT assay, TEM imaging for the 40 mM sodium phosphate buffer samples was also conducted simultaneously. Though 0 hour uranyl acetate spotting was observed, the aggregates in 12 and 27 hours appeared to be clumpier than the 0 hour. Moreover at 12 hours, protofibril like aggregates, similar to the TEM imaging of Ahmed et al. (Figure 2.3.1-4), also appeared (24). The 27 hour TEM images (Figure 2.3.1-1) showed how the interconnected fibril formation started to occur. It is important to note that TEM imaging does not provide a proper platform to distinguish or identify these 'clumpy' smaller aggregates. However as shown in Figure 2.3-1 D and E, at 79 hours larger fibrils were observed with more interconnected clusters than 51 hours. Furthermore, the clumpy like aggregates were not visualized to the extent as the previous time points at 51 hours and were non-existent at 79 hour. To further understand the earlier $A\beta_{1-42}$ aggregates, CE studies of up to 27 hours were conducted using an agitation rate of 300 RPM. Likewise, the effect the FASS technique had on CE separation and detection was also analyzed in hope to further improve CE separation technique.

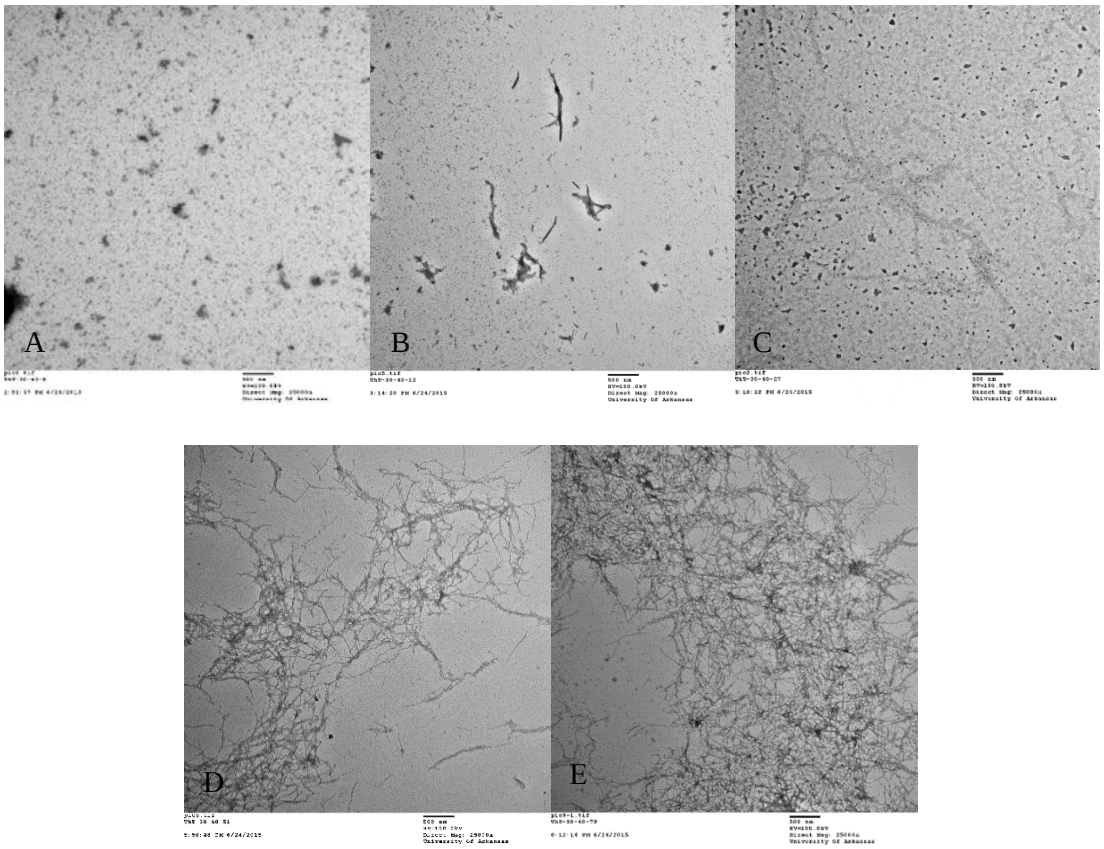

Figure 2.3-1: TEM imaging at A) 0 hour, B) 12 hour, C) 27 hour, D) 51 hour and E) 79 hour into the aggregation using JOEL with a magnification at 25000X and 100kV of 30 μM $A\beta_{1-42}$ with 500:10000 NaOH: 40 mM sodium phosphate buffer pH=7.4 ratio at 300RPM, 25°C.

2.3.1 Capillary Electrophoresis: FASS Technique

Various sodium phosphate buffer conductivities were determined to narrow the range of sample buffer concentrations to be used for FASS analysis (further discussed in Appendix B Section III). As shown in Appendix B Section III, initial experiments using FASS were conducted using 1 mg/mL BSA with sodium phosphate buffer concentration ranging from 10-50 mM. Upon comparing the data, further analysis of 100 mM, 40 mM and 30 mM sample buffer concentration were conducted on the CE. Figure 2.3.1-1 (below) showed not only improved detection using the FASS technique, the experiments also showed a higher reproducibility established by utilizing this technique.

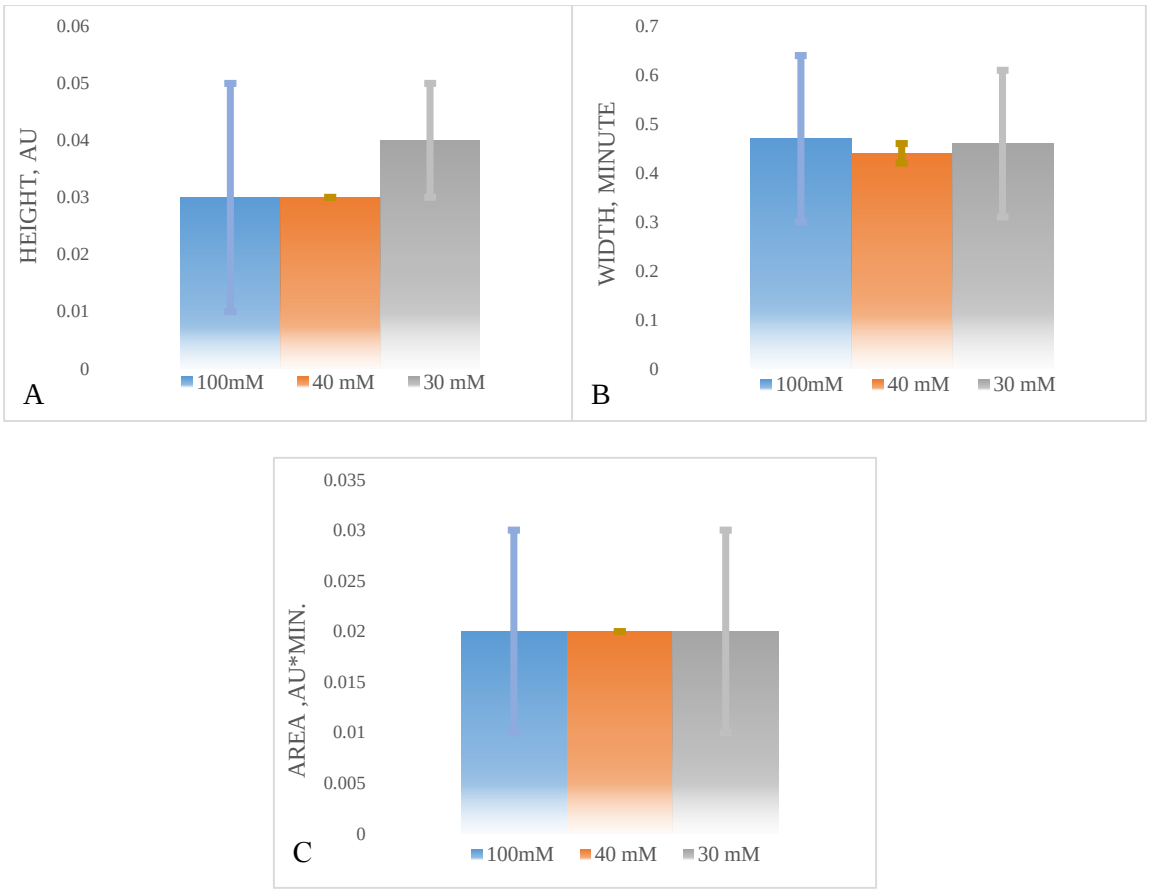

Figure 2.3.1-1: A) Height, B) Width, and C) Area data from CE analysis for 5% 2000 kDa PEO coated capillary with a separation matrix of 0.5% 50 kDa PEO + 0.1% of 0.1% of 2000 kDa PEO and BGE of 100 mM sodium phosphate buffer (pH=7.4) where the sample consisted of 1mg/ml of BSA at the varying buffer concentrations, n=3.

In Figure 2.3.1-1, the average area of the three varying buffer were equal which was expected because the BSA concentration was the same. However, in order to determine the optimal load buffer, it was necessary to look at the load buffer that produced the highest reproducibility, optimal detection, and less band broadening. Though the 30 mM sodium phosphate load buffer sample consisted of the best height detection, 40 mM sodium phosphate buffer was determined as the optimal option due to its ability to have high reproducibility and least amount of zone broadening. It is believed that when the concentration difference between the BGE and load buffer is high, then the sample can potentially behave similar to a laminar flow profile. This can affect

the way the sample travels in the capillary and cause width broadening. Therefore though increasing local field strength is beneficial, at a certain point it can cause negative effects as the 30 mM sodium phosphate buffer data confirmed. In order to further explore whether FASS was also better when analyzing $A\beta_{1-42}$, both 40 mM sodium phosphate and 100 mM sodium phosphate load buffer were utilized with the BGE being 100 mM sodium phosphate buffer. This provided an opportunity to see how the FASS method improved the separation and also the effect changing the load buffer has on the $A\beta_{1-42}$ as well.

Data collected with 30 μM $A\beta_{1-42}$ confirmed the importance of utilizing the FASS technique where there was less band broadening and higher height absorbance detection with the 40 mM sodium phosphate buffer sample vs. the sample with the same buffer as the BGE (Figure 2.3.2-1). In Figure 2.3.1-2, it is also important to note that the 'spike-like' peaks at or close to the 5 minute peak were usually not replicated in repeated experiments (especially at the same migration time) and were believed to be due to microscopic bubbles either in the sample or separation buffer. Additionally if there are precipitates in the sample, the CE might develop spikes on the baseline or start to have an unstable baseline.

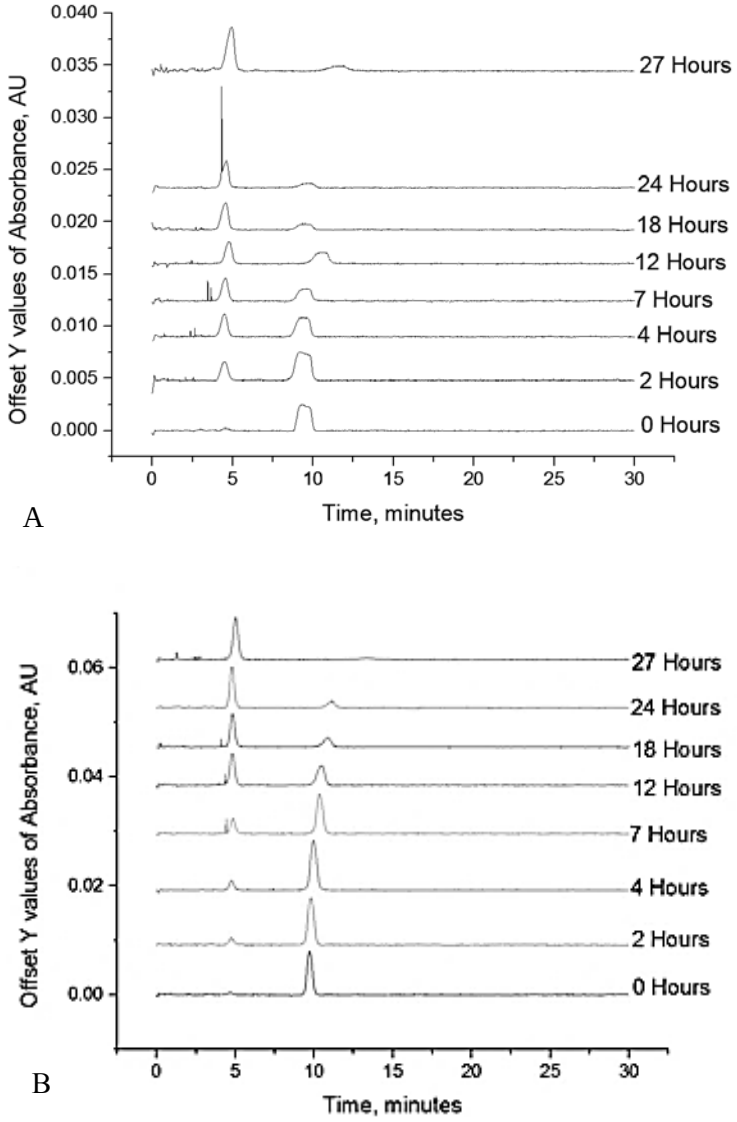

Figure 2.3.1-2: Representation electropherograms for the aggregation study at 300 RPM using A) 100 mM and B) 40 mM sodium phosphate load buffer at pH = 7.4 with a final concentration of 30 µM $A\beta_{1-42}$. Other conditions included: 25°C with 0.5% 2000 kDa PEO capillary coating and 100 mM sodium phosphate buffer (pH=7.4) as the BGE with a separation matrix of 0.5% 50 kDa PEO plus 0.1% of 0.1% of 2000 kDa PEO using a pressure injection of 0.5 psi for 13.3 seconds and 7 kV separation voltage.

Past studies have shown $A\beta_{1-42}$ aggregation contains larger forms of aggregates especially if it is dissolved in HFIP (76). As shown in Figure 2.3.1-2A and B, both aggregation studies consisted of the observation of more than one species of $A\beta_{1-42}$. Moreover, as the aggregation continued for 30 μM $A\beta_{1-42}$ samples using both 100 mM or 40 mM sodium phosphate buffer with pH=7.4, the peak at 10 minutes slowly decreased as the peak at 5 minute increased (shown in Figure 2.3.1-2). Therefore, it is believed that the 10 minute peak was smaller $A\beta_{1-42}$ aggregates then the 5 minute peak. A previous study by Wang et al. has shown that $A\beta_{1-42}$ aggregates exhibit a higher surface charge which would explain a faster migration (77).

By further comparing the peak areas, an understanding of the concentration of aggregates can be established. As observed in the $A\beta_{1-40}$ aggregation study by Pryor et al., amyloid peptide pre-treated with HFIP treatment increased in the smaller aggregates before the decrease was observed (60). This same pattern was observed for both 40 mM and 100 mM sodium phosphate $A\beta_{1-42}$ where an increase in the 10 minute peak is observed before it declined (Figure 2.3.1-3). In Figure 2.3.1-3A, the 10 minute aggregates of the 40 mM sodium phosphate buffer $A\beta_{1-42}$ appearred to increase until 4 hours into the aggregation and then decreased. Additionally at 12 hours, both the 5 and 10 minute peaks were statistically similar. This could represent a similar distribution of the aggregates at 12 hour where by 27 hours into the aggregation study, the 5 minute increased and 10 minute peak decreased. The 5 and 10 minute peak areas of 100 mM sodium phosphate amyloid sample (Figure 2.3.1-3B) are statistically different for all except the 7 hour time point. The 10 minute peak for the 100 mM sodium phosphate sample showed a clear decline in aggregates. Furthermore, the 5 minute peak leveled after the 7 hour time point. It is also interesting to note that both sample buffers consisted of a statistical difference compared to the 0 hour time point within 2 hours for the larger aggregates (5 minute peak). As stated in Chapter 1, the lag phase

is thermodynamically not favored. Therefore, it can be expected that the conversion of aggregates is preferably and continuous throughout the study.

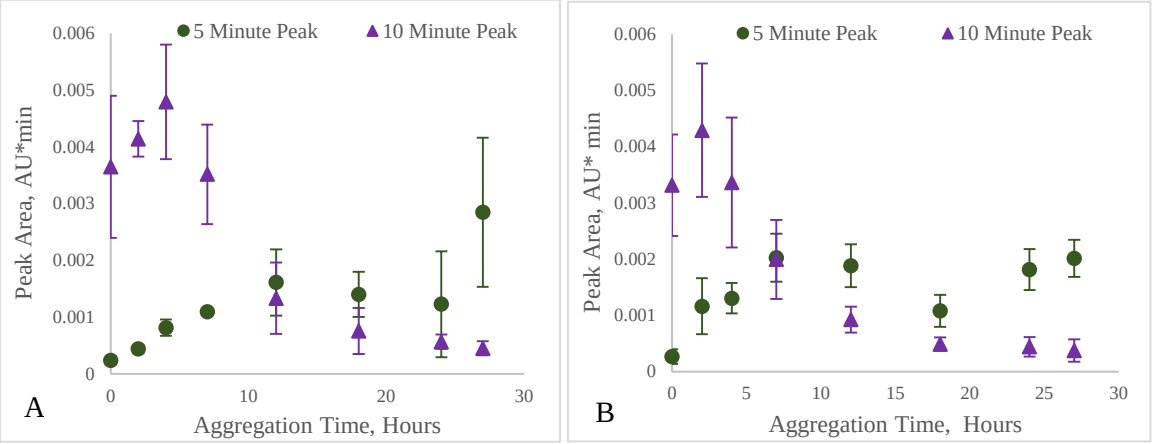

Figure 2.3.1-3: CE data of 30µM $A\beta_{1-42}$ with A) 40 mM load buffer, B) 100 mM load buffer with a 100 mM sodium phosphate pH=7.4 BGE buffer. The CE aggregation study is at 300RPM, 25°C with 0.5% 2000 kDa PEO capillary coating and a separation matrix of 0.5% 50 kDa PEO plus 0.1% of 0.1% of 2000 kDa PEO using a pressure injection of 0.5psi for 13.3 seconds and 7kV separation voltage, n=3.

When comparing the 5 minute peaks for each buffer concentration (Figure 2.3.1-4A), the majority of the time points were statistically similar peaks except for 2-7 hour time points. The statistical difference for the 5 minute peak between the 2-7 hour time points might be due to the variable nature of the aggregations which tend to lead to larger variance in the data. Additionally, the 30 µM $A\beta_{1-42}$ with the 40 mM sodium phosphate buffer also consisted of smaller peak area standard deviation than the 100 mM sodium phosphate buffer sample until 12 hours into the aggregation for the larger $A\beta_{1-42}$ aggregates (shown in Figure 2.3.1-4A). This is consistent with the BSA data that showed better reproducibility at the lower concentration of sample buffer.

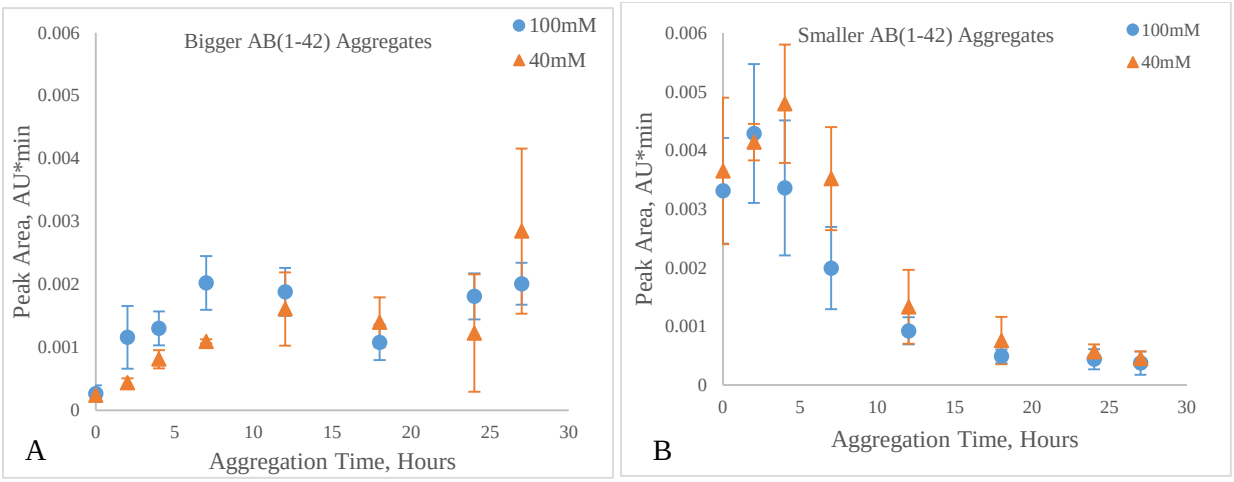

Figure 2.3.1-4: CE data of 30µM $A\beta_{1-42}$ with A) the bigger species of 30µM $A\beta_{1-42}$ comparison of the load buffers and B) the smaller species of 30µM $A\beta_{1-42}$ comparison of the load buffers consisting of sodium phosphate pH=7.4 and 100 mM sodium phosphate pH=7.4 BGE buffer. The CE aggregation study is at 300RPM, 25°C with 0.5% 2000 kDa PEO capillary coating and a separation matrix of 0.5% 50 kDa PEO plus 0.1% of 0.1% of 2000 kDa PEO using a pressure injection of 0.5psi for 13.3 seconds and 7kV separation voltage, n=3.

Once similar aggregation patterns were established between the ionic strengths, Origin® analysis of the data was conducted to compare the height, width and resolution of the peaks to understand the factors FASS method should effect the most. For CE detection, a signal that is greater than the noise by a factor of 3 is considered adequate. Therefore in hopes to analyze $A\beta_{1-42}$ using lower concentrations to reduce the peptide to cost ratio, it was important to be able to detect the peptide at lower limits of sample concentration. By utilizing the FASS method, the height increased for the smaller aggregates (Figure 2.3.1-5B) where 6 out of 8 time points (0, 2, 4, 7, 18, and 24 hours) consisted of a significant statistical difference of the sample with 40 mM sodium phosphate buffer compared to the 100 mM sodium phosphate buffer. Additionally though in Figure 2.3.1-4A some 100 mM sodium phosphate $A\beta_{1-42}$ appeared to have higher height detected, the statistical difference between the two buffers was not considered significant. For the larger $A\beta_{1-42}$ aggregates heights that did have a statistical difference, the 40 mM sodium phosphate

buffer consisted of the better detection (due to increased height). Furthermore, having less band broadening provided the opportunity for better separation. Therefore by comparing the width for both buffers, the smaller 30 μM $A\beta_{1-42}$ species with 40 mM sodium phosphate buffer consisted of a smaller peak width where up to 7 out of 8 of the widths were statistically different (Figure 2.3.1-5D). The bigger aggregates (Figure 2.3.1-5A) were statistically similar except for 4 out of 8 time points where the 100 mM sodium phosphate had the larger width. Therefore, the detection of 30 μM $A\beta_{1-42}$ using the FASS technique provided less broadening and in turn should provide better separation. Since resolution helps indicate the separation between the peaks, it was believed FASS would provide higher resolution as well. The lower buffer $A\beta_{1-42}$ consisted of a statistical higher resolution than the 100 mM sodium phosphate (Figure 2.3.1-5D). Therefore utilizing the FASS method with $A\beta_{1-42}$ provided better resolution, smaller width and larger height. This confirmed FASS helps increase peak separation and could be considered beneficial for analyzing numerous peaks that are close together.

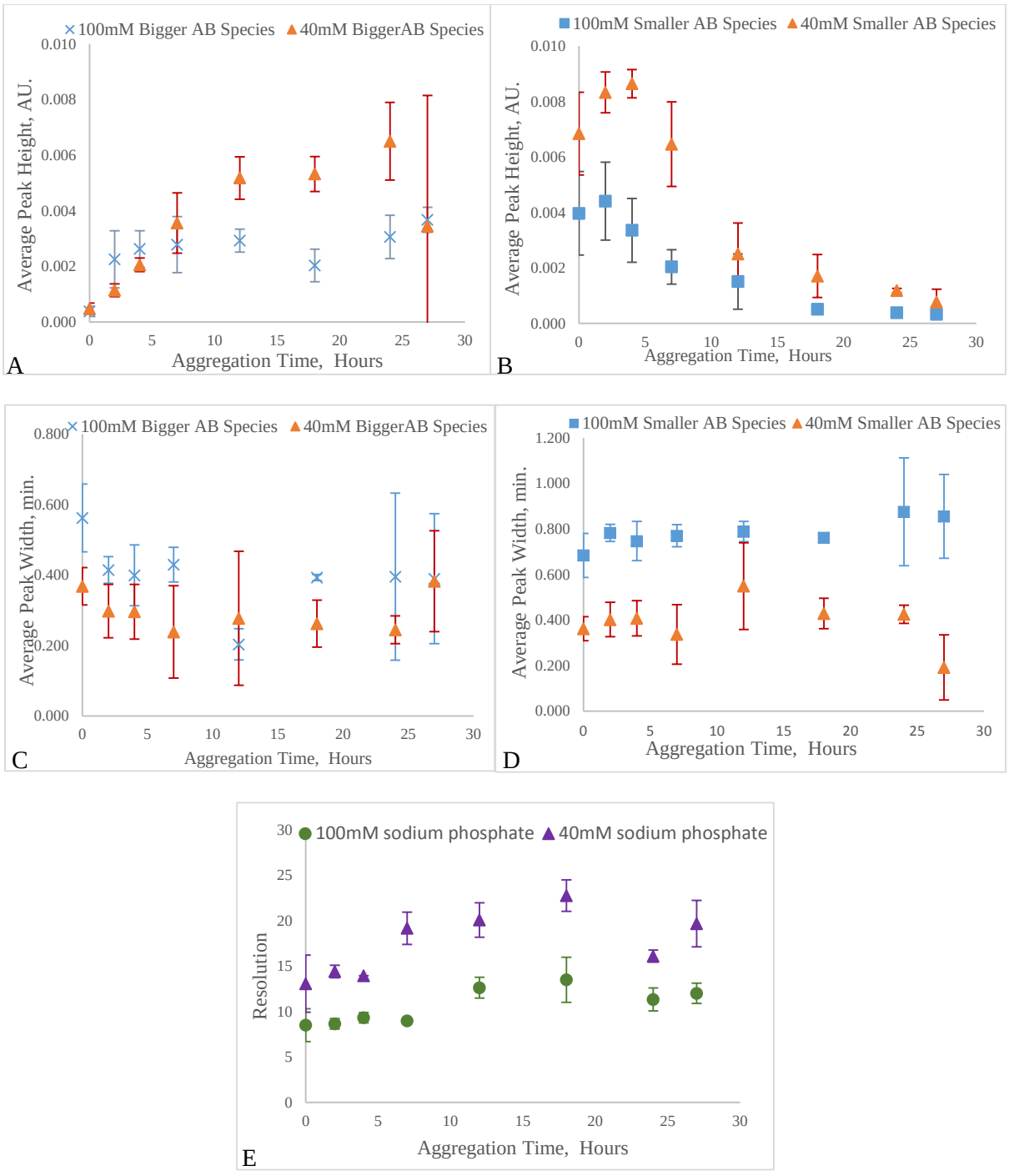

Figure 2.3.1-5: Average CE data of A) peak height for larger species of 30µM $A\beta_{1-42}$, B) peak height for smaller species of 30µM $A\beta_{1-42}$, C) peak width for larger species of 30µM $A\beta_{1-42}$, D) peak width for smaller species of 30µM $A\beta_{1-42}$, and E) resolution comparison of the load buffers consisting of 40 mM and 100 mM sodium phosphate pH=7.4 and BGE of 100 mM sodium phosphate buffer pH=7.4. The CE aggregation study is at 300RPM, 25°C with 0.5% 2000 kDa PEO capillary coating and a separation matrix of 0.5% 50 kDa PEO plus 0.1% of 0.1% of 2000 kDa PEO using a pressure injection of 0.5psi for 13.3 seconds and 7kV separation voltage, n=3.

2.3.2 MWCO Filtration

As shown in Figure 2.3.1-3A and B, the peak at 10 minute increased and then slowly decreased. Furthermore, since larger $A\beta_{1-42}$ aggregates (5 minute peak) were also detected, it was believed that the 10 minute peak was most likely not just monomeric. Therefore even though the ThT assay helped establish the lag time, it was important to see whether the $A\beta_{1-42}$ species observed by the CE is actually oligomers. In order to determine the molecular weight of the species observed by the CE, ultrafiltration with membrane filters were used. The concentration of $A\beta_{1-42}$ was increased to 60 μM due to peptide loss by the membrane and the aggregation study was conducted for the 0 hour and 7 hour time point. Since the increased concentration of $A\beta_{1-42}$ for ultrafiltration was larger and prone to aggregate faster according to past literature (5), CE study was also performed on 60 μM $A\beta_{1-42}$ to confirm the same 5 and 10 minute peaks were observed although in different amounts. Additionally, the larger aggregates at 7 hour were at least 6 times the concentration (peak area) as the 30 μM $A\beta_{1-42}$ whereas, the smaller aggregates were about 80% the size of the aggregates studied for the FASS technique. Therefore, the assumption of having larger aggregates at 60 μM $A\beta_{1-42}$ was adequate.

Upon conducting the centrifugation experiments of 60 μM $A\beta_{1-4}$, about 99% peptide loss was observed when comparing all filter experiment with the un-filtered experiments. Additionally by looking at Figure 2.3.2-1, it was observed that the bigger aggregates were more likely to stick to by the membrane. Therefore in order to analysis the filtered data, a qualitative analysis was conducted where if the peak was observed, it was believed to be within the MW range of the filter cutoff weight. At 300 kDa and 100 kDa (Figure 2.3.2-1B and C), both peaks at 5 and 10 minutes were observed. Additionally at 30 kDa, only the 10 minute peak was consistently observed (n=3). Therefore, the 10 minute aggregates were believed to be less than 30 kDa (Figure 2.3.2-1D).

Furthermore according to the 7 hour 100 kDa filter experiments, it was also believed that the peak observed at five minutes contains aggregates consisting of a range from 30-100 kDa (n=3). In other words, the 5 minute peak ranges between 7-22 mer and the 10 minute peak is up to 7 mers. Therefore, the $A\beta_{1-42}$ aggregates being analyzed by the CE range from higher molecular aggregates to small oligomer species throughout the aggregation and potentially smaller aggregates until 7 hours into the 30 µM $A\beta_{1-42}$ aggregation.

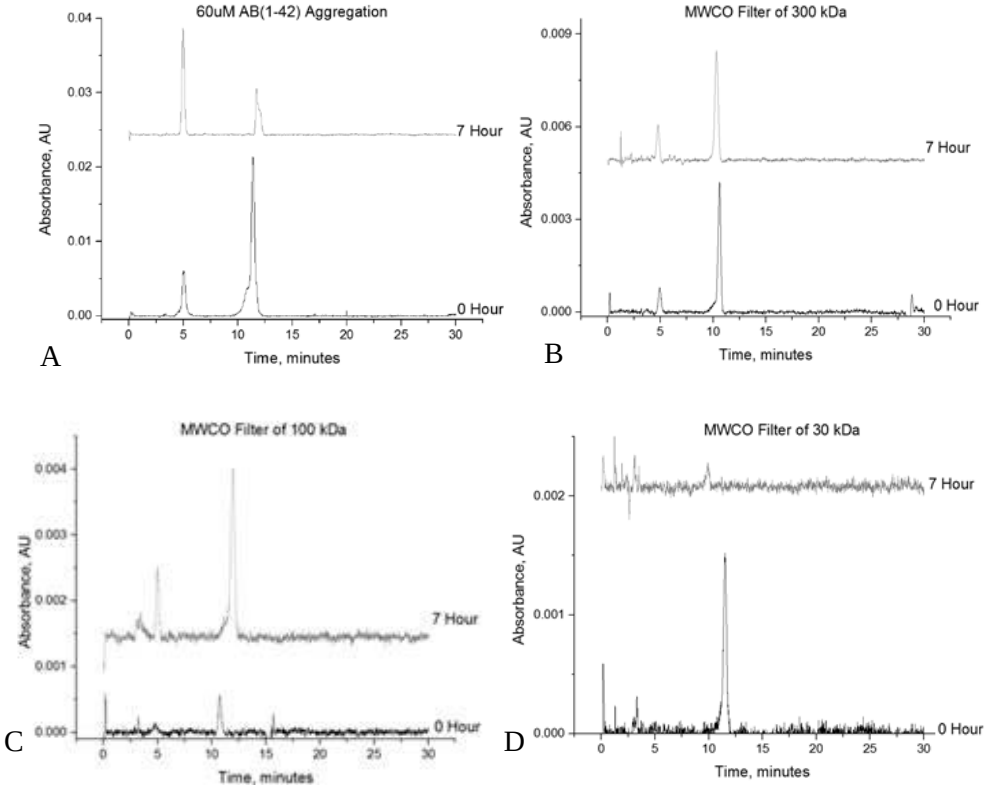

Figure 2.3.2-1: Representation electropherograms for A) unfiltered 60 µM $A\beta_{1-42}$ n=4, B) 60 µM $A\beta_{1-42}$ sample filtered by MWCO of 300 kDa, C) 60 µM $A\beta_{1-42}$ sample filtered by MWCO of 100 kDa and D) 60 µM $A\beta_{1-42}$ sample filtered by MWCO of 30 kDa, n=3 total for each filter. Other conditions included: 25°C with the aggregation study at 300 RPM and CE conditions of 0.5% 2000 kDa PEO capillary coating and 100 mM sodium phosphate buffer (pH=7.4) as the BGE with a separation matrix of 0.5% 50 kDa PEO plus 0.1% of 0.1% of 2000 kDa PEO using a pressure injection of 0.5 psi for 13.3 seconds and 7 kV separation voltage.

2.3.3 TEM Analysis

Oligomeric $A\beta_{1-42}$ species are believed to range from 10 kDa up to 250 kDa and range in conformation from pre-fibrillar oligomers (such as globular, paranuclei etc.) to fibrillar oligomer (3; 34; 78). Therefore, it is difficult to distinguish the type of oligomer $A\beta_{1-42}$ species just based on the molecular weight when analyzing the CE data. As stated in the previous section, the 10 minute peak consisted of aggregates smaller than 30 kDa. However since the 5 minute peak consisted of aggregates ranging from 30-100 kDa, TEM imaging was conducted to qualitatively help further confirm species analyzed by the CE are not fibril/ proto-fibril species. In Figure 2.3.3-1A and B, the TEM image further confirms that the 100 mM sodium phosphate consisted of slightly higher aggregates but was along a similar aggregation pathway as the 40 mM sodium phosphate buffer sample of 30 μM $A\beta_{1-42}$. The 12 hour (Figure 2.3.3-1A) showed how the 100 mM sodium phosphate buffer sample consisted of 'clumpier' aggregates than the 40 mM sodium phosphate buffer. This was observed more clearly at a higher magnification (100,000X) where image was enhanced to distinguish uranyl acetate staining compared to aggregate detection. Additionally, the 27 hour of the 100 mM sodium phosphate buffer consisted of more fibril strands compared to the 40 mM sodium phosphate sample (Figure 2.3.3-1B). While comparing 40 mM sodium phosphate buffer CE and ThT Assay TEM images, the overall aggregation study was fairly similar in the sense that the first inter-connected fibrils appeared at 27 hours into the aggregation (Figure 2.3.3-1B and D). Furthermore by looking at the TEM image of 51 hours (Figure 2.3-1), it can be concluded that majority of the aggregates converted into fibrils. Therefore not only do the TEM images confirmed majority of the aggregates during the 27 hours are smaller than fibrils, the TEM images also potentially helped correlate the ThT and CE data where both aggregation behaved similarly even though the experiments were set studying varying time points.

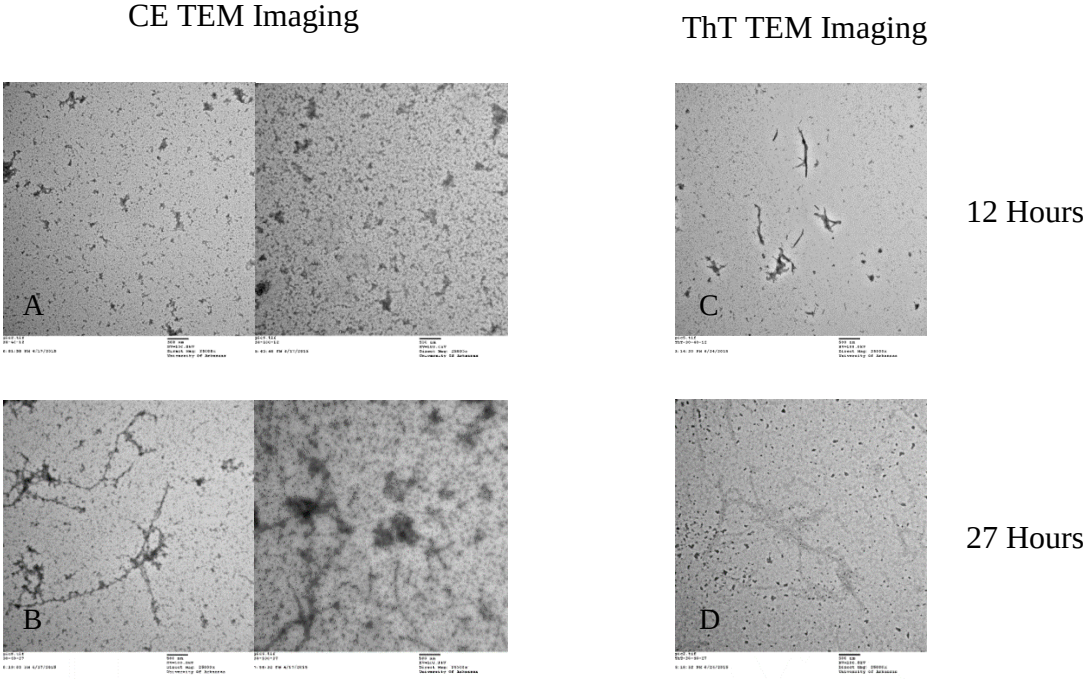

Figure 2.3.3-1: TEM imaging where data collected at CE time point intervals at A) 12 hour, and B) 27 hour of 30 μM $A\beta_{1-42}$ with 40 mM sodium phosphate buffer pH=7.4 (right images) or with 100 mM sodium phosphate buffer pH=7.4 (left images) and where data collected at ThT Assay time point intervals at C) TEM imaging for 12 hour and D) TEM imaging for 27 hour with 40 mM sodium phosphate sample buffer pH=7.4 using JOEL with a magnification of 25000X and 100kV. Aggregation study conducted using a mini-shaker at 300 RPM and 25°C.

Additionally by trying to correlate the CE and TEM imaging, it was observed by the CE that both 100 mM and 40 mM sodium phosphate buffer appeared to behave fairly similar except for the 7 hours bigger amyloid aggregates (Figure 2.3.1-4) when taking into account the standard deviation of the peak areas. It was believed since the peak area of the 100 mM sodium phosphate load buffer sample was larger than the 40 mM load buffer, the 100 mM sodium phosphate might consisted of larger aggregate species (Figure 2.3.1-4). Therefore by looking at the TEM images of the 7 hour time point, a better understanding of the aggregates was established. At 7 hours, there was an increased production of aggregates using the 100 mM sodium phosphate buffer compared to the 40 mM sodium phosphate buffer. The 30 μM $A\beta_{1-42}$ image with 40 mM sodium phosphate buffer consisted of fibril-like strands (blue arrow) in the mist of circular-like aggregates (orange

arrow) as well as some short linear strands (orange arrow). Additionally, the 100 mM sodium phosphate buffer sample also consisted of the circular like aggregates (green arrow) but was surrounded with more short linear strands (orange arrows) vs. the 40 mM load buffer. These circular aggregates (orange arrow in Figure 2.3.3-2) appeared to be similar to the round particles discussed by Ahmed et al. (24). Furthermore according to Ahmed et al., these circular aggregates (Figure 2.3.3-3) were oligomers. Additionally, in their studies it was found the average width of the oligomers to be 10-15 nm by utilizing AFM (atomic force microscope) (24). Therefore, TEM provided a platform to confirm the species observed by the CE with up to 100 kDa are some form of oligomers.

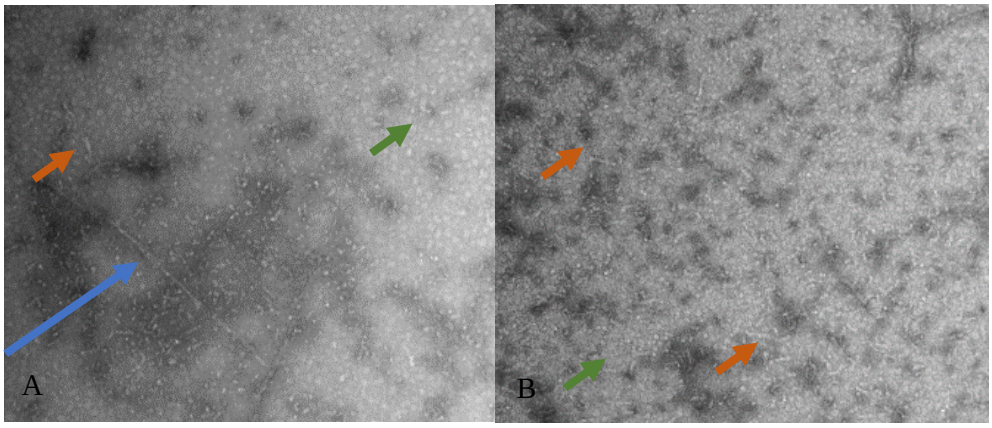

Figure 2.3.3-2: TEM imaging of A) 40 mM or B) 100 mM sodium phosphate sample buffer (pH = 7.4) after 7 hours of aggregation using a mini-shaker at 300 RPM and 25°C. TEM conducted using JOEL with a magnification of 100000X and 100 kV of 30 μM $A\beta_{1-42}$ with either 500:10000 NaOH: 40 or 100 mM sodium phosphate buffer. The green arrow represent the circular like aggregates, the orange show the short strand aggregates and blue arrows represent the long aggregates.

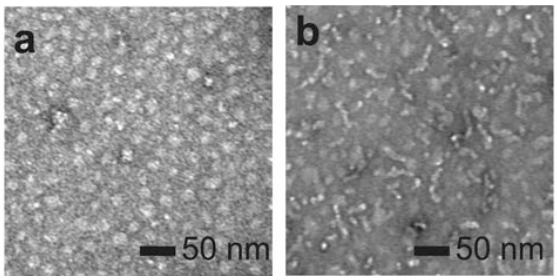

Figure 2.3.3-3: From Ahmed et al. Figure 2: "Characterization of Aβ42 oligomers, protofibrils and fibrils. (a) TEM of Aβ42 oligomers incubated at 4 °C for 6 h. (b) TEM of Aβ42 protofibrils incubated at 37 °C for 6 h" (24).

By looking at current literature the fibril-like strands could be categorized according to the secondary nucleation pathway where these aggregates were most likely an elongated nucleating fibril (36). The elongated nucleating fibrils consisted of sites for proto-fibrils and potentially grew into becoming larger fibrils. As shown in Figure 2.3.3-2, the protofibril were interacting with one another and appeared to be elongating (blue arrow). Therefore, the CE provided an opportunity to further analysis the smaller aggregates compared to ThT assays which detected the higher aggregate forms of $A\beta_{1-42}$ (increase of interaction with β-sheet) and the TEM images which showed the overall sample characteristics as a whole.

2.3.4 Congo red and Orange G Inhibition

Since the aggregates observed by the CE are believed to be up to 100 kDa, Congo red and Orange G inhibition studies were conducted to further investigate the nature of these aggregates. Congo red is believed to inhibit oligomer Aβ species or at least species smaller than fibrils (73; 79). Therefore, it was hypothesized that the 5 minute peak (larger aggregates) will be reduced using Congo red. However the Congo red inhibition of 30 μM $A\beta_{1-42}$ aggregation study at 300 RPM results produced mixed data (Figure 2.3.4-1). As shown by Figure 2.3.4-1, the set of electropherograms in on the left (A) show the expected behavior of suppression of the 5 minute

peak with increasing aggregation time. However, the set of electropherograms on the right (B) did not appear to be inhibited in the presence of the Congo red.

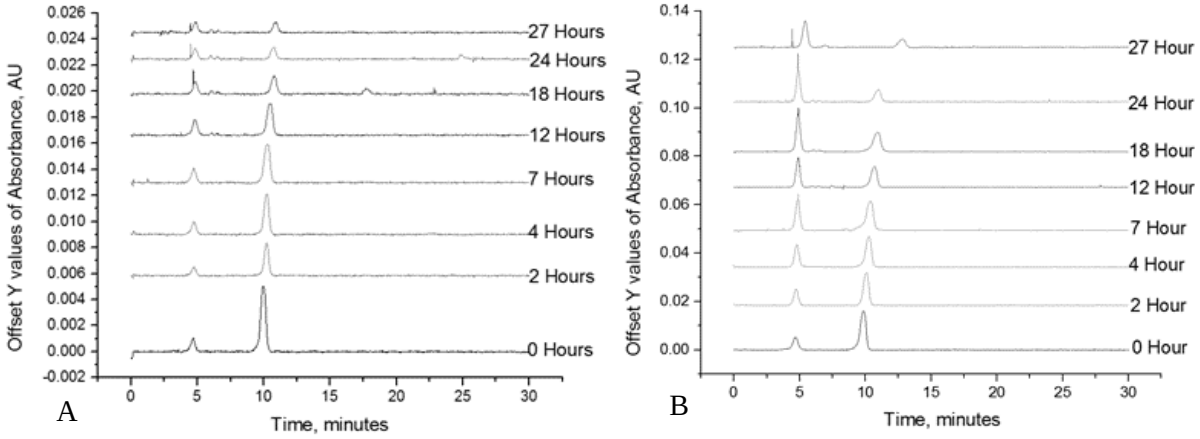

Figure 2.3.4-1: Electropherogram representation of A) n=2 and B) n=2 for Congo red inhibition of 30µM $A\beta_{1-42}$ with a 40 mM sodium phosphate sample buffer pH=7.4. The CE aggregation study was conducted at 300RPM, 25°C with CE 0.5% 2000 kDa PEO capillary coating and 100 mM sodium phosphate buffer (pH=7.4) as the BGE with a separation matrix of 0.5% 50 kDa PEO plus 0.1% of 0.1% of 2000 kDa PEO using a pressure injection of 0.5 psi for 13.3 seconds and 7 kV separation voltage

When taking a closer look at the peak areas (Figure 2.3.4-2B), a decrease in the $A\beta_{1-42}$ species < 30 kDa still occurred as the aggregation progresses. For the Set A electrophoresis experiments, there were statistically similar amount of small species present at all time points (Figure 2.3.4-2B) and statistically less of the bigger (30 – 100 kDa) $A\beta_{1-42}$ species were formed as the aggregation time increased (Figure 2.3.4-2A). However, for Set B electrophoresis experiments, the amount of smaller aggregates present initially was higher overall and a greater amount of bigger species were formed. There are several possible explanation for the differences between these two sets of data. First, Congo red is considered a weak inhibitor which could lead to variability in its ability to inhibit samples, especially in the presence of a significant amount of bigger aggregates at 0 hours (76). In addition for Set B, there was a larger amount of bigger species

initially present which could be acting as seeds for the growth of oligomers and thereby bypassing the species that Congo red was actually able to inhibit. Therefore, TEM imaging was also conducted to further understand what is happening during the aggregation.

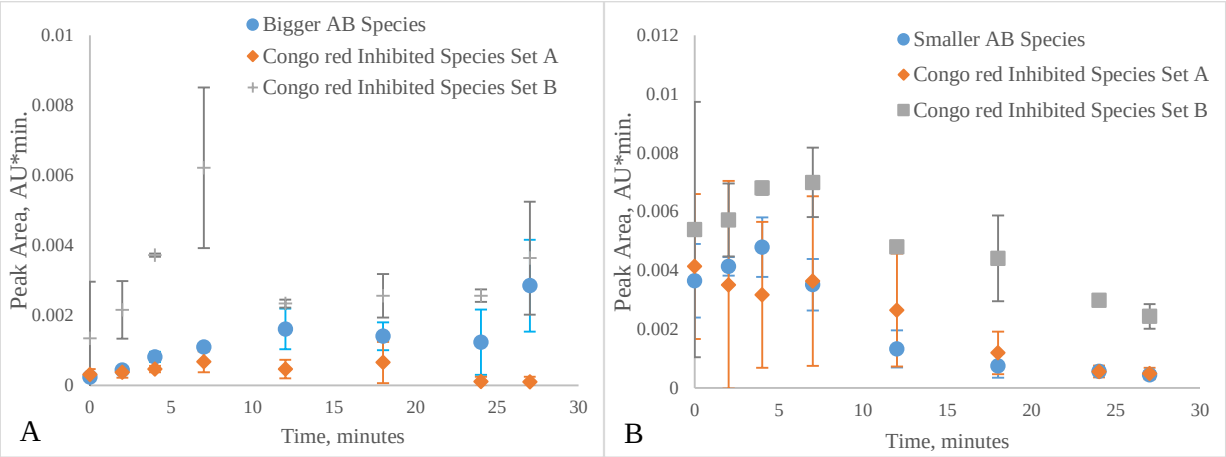

Figure 2.3.4-2: A) Bigger 30µM $A\beta_{1-42}$ aggregates and B) smaller 30µM $A\beta_{1-42}$ aggregates where Set A is from data similar to Figure 2.3.4-2A (n=2) and Set B is from data similar to Figure 2.3.4-2B (n=2). The aggregation study consisted of Congo red inhibtion at 300RPM, 25°C with 40 mM sodium phosphate pH=7.4 as the sample buffer. The CE setting consisted of 0.5% 2000 kDa PEO capillary coating and 100 mM sodium phosphate buffer (pH=7.4) as the BGE with a separation matrix of 0.5% 50 kDa PEO plus 0.1% of 0.1% of 2000 kDa PEO using a pressure injection of 0.5psi for 13.3 seconds and 7kV separation voltage.

As shown by the TEM images (Figure 2.3.4-3), the first fibril like aggregate was still observed at 12 hour where the fibril species development throughout the aggregation was similar to the un-inhibited aggregation of $A\beta_{1-42}$. Therefore, the results confirmed Necula et al. findings where Congo red does not inhibit fibril species (73). The major difference between the Congo red compared to the un-inhibited aggregation was the type of smaller aggregate species observed in the TEM. In Figure 2.3.4-3, it was interesting to note that the circular like species were a lot more abundant (Figure 2.3.4-3E) vs. the 'clumpy' species observed in the 12 hour un-inhibited aggregation study (Figure 2.3.4-3F). Additionally when the circular like aggregates were observed

in the un-inhibited study, protofibril (short strands) were also observed. In the Congo red aggregation study, however, the proto-fibrils (short strands) were not observed throughout the aggregation. Therefore data obtained by the CE further confirms Congo red to be a weak inhibitor and the TEM images eluded to the fact that Congo red does have the capability to bind to various Aβ species as described by Wu et al. (80).

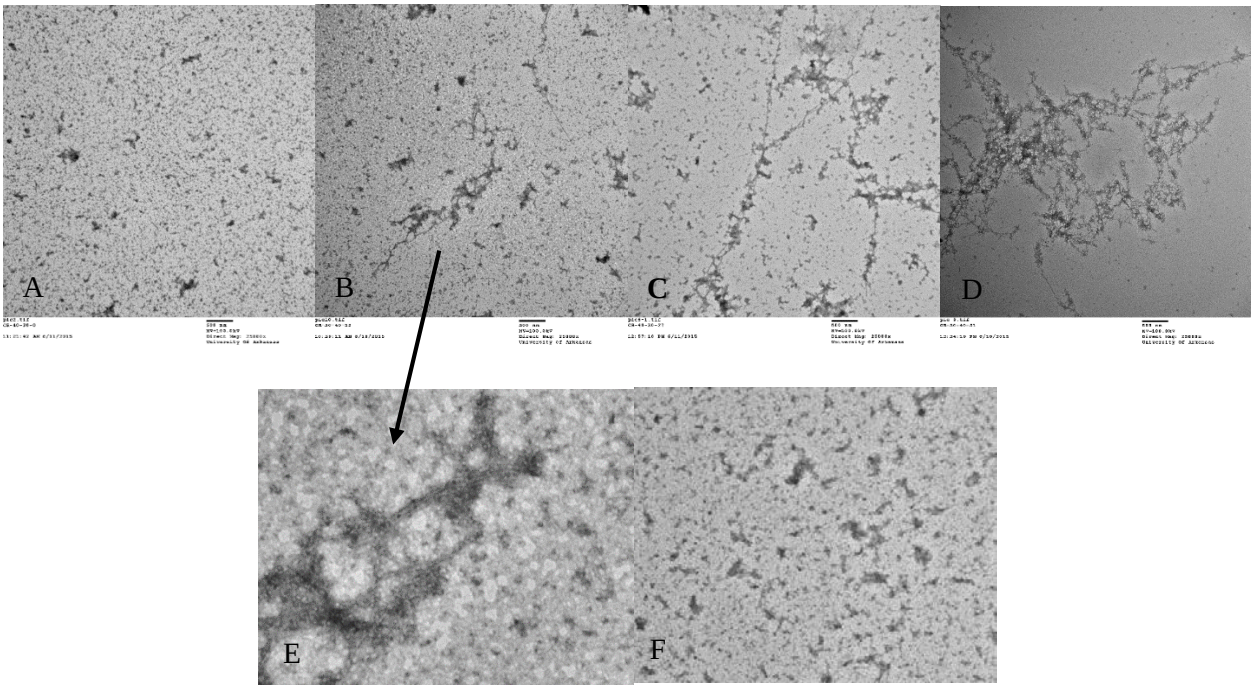

Figure 2.3.4-3: TEM imaging at A) 0 hour, B) 12 hour, C) 27 hour, and D) 51 hour into the Congo red inhibition aggregation of 30 μM $A\beta_{1-42}$ with 40 mM sodium phosphate sample buffer pH=7.4. The aggregation was conducted using a mini-shaker at 300RPM, 25°C and TEM imaging was produced using JOEL with a magnification of 25000X and 100kV, n=2. TEM image E is magnified version of B with a magnification of 50000X in order to visualize the 'circular' like aggregates and image F is an un-inhibited 12 hour TEM with magnification of 50000X.

Since in the TEM images an increase of the circular aggregates and decrease in the clumpier aggregates was observed, dot blot analysis of un-inhibited $A\beta_{1-42}$ were looked at for un-inhibited amyloid. Two distinct categorizes of oligomer identified are called pre-fibrillar oligomers and fibrillar oligomers (34). Furthermore it is believed that since fibril oligomer have a

conformation similar to fibrils but differ in size, OC can detect the fibrillar oligomer (34; 81). Upon using the OC antibody, positive detection was observed throughout the aggregation which have been reported to detect fibril oligomers (Figure 2.3.4-4B). 6E10 (a control) antibody was also positive for all time points (n=3). Positive results for the 6E10 confirmed the species being detection is Aβ. Hence it is hypothesized that Congo red might prefer inhibition of fibrillar oligomers and proto-fibrils better than the pre-fibrillar oligomer (80).

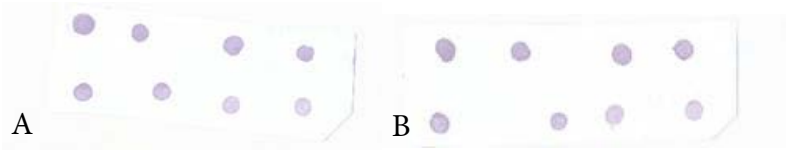

Figure 2.3.4-4: Dot blot analysis using A) 6E10 primary antibody, B)OC primary antibody for 30 μM $A\beta_{1-42}$ where the first row consisted of 0, 2, 4, 7 hour time points (starting from left to right) and the second row consisted of 12, 18, 24, and 27 hour time points (starting from left to right).

After Congo red inhibition and dot blot analysis, Orange G inhibition was conducted in hope to further ensure fibril species are not observed on CE. Orange G is commonly known to inhibit fibrils and is believed to bind Aβ in such a manner that does not stop monomers from aggregating but prolongs or eliminates fibril formation (73). Upon conducting Orange G inhibition, increases in $A\beta_{1-42}$ larger aggregates were observed (Figure 2.3.4-5) by CE with increasing aggregation time. Additionally, the smaller aggregate species increased and then slowly disappeared as the aggregation continued. The increase in the smaller $A\beta_{1-42}$ species from 0 hour to 2 hour into the aggregation was more prominent compared to the un-inhibited aggregation (Figure 2.3.1-1). However after 7 hours, the smaller aggregates (<30 kDa) began to decrease again which could indicate formation of another aggregate not shown on CE. Since the aggregation pattern using Orange G inhibition was similar to the un-inhibited aggregation study, the Orange G inhibition confirmed that the species detected by the CE are in fact not fibrils.

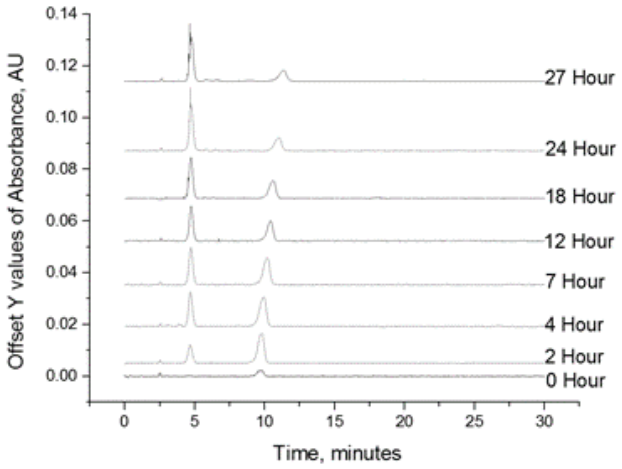

Figure 2.3.4-5: Electropherogram representation of 30 µM $A\beta_{1-42}$ of Orange G inhibition aggregation study at 300 RPM, 25°C with CE 0.5% 2000 kDa PEO capillary coating and 100 mM sodium phosphate buffer (pH=7.4) as the BGE with a separation matrix of 0.5% 50 kDa PEO plus 0.1% of 0.1% of 2000 kDa PEO using a pressure injection of 0.5 psi for 13.3 seconds and 7 kV separation voltage. The sample buffer consisted of 40 mM sodium phosphate buffer pH=7.4.

By looking at the specific peak areas (as shown in Figure 2.3.4-6), the inhibited $A\beta_{1-42}$ aggregate were in most cases greater in terms of concentration (peak area) than the un-inhibited species. The fact that the area and in turn concentration of the aggregates below 100 kDa was higher in the presence of the inhibitor further indicated the larger aggregate peaks (5 minute peak) were not fibrils but might be other forms of aggregates. The higher amounts of species detected in the present of Orange G also indicated their inability to be converted into larger species (fibrils) and therefore remained at higher concentrations in the species that were able to be detected by CE. It is important to note that Orange G also gives off a weak signal at the UV spectrum being used for peptide detection which could also be part of the increase in amount detected.

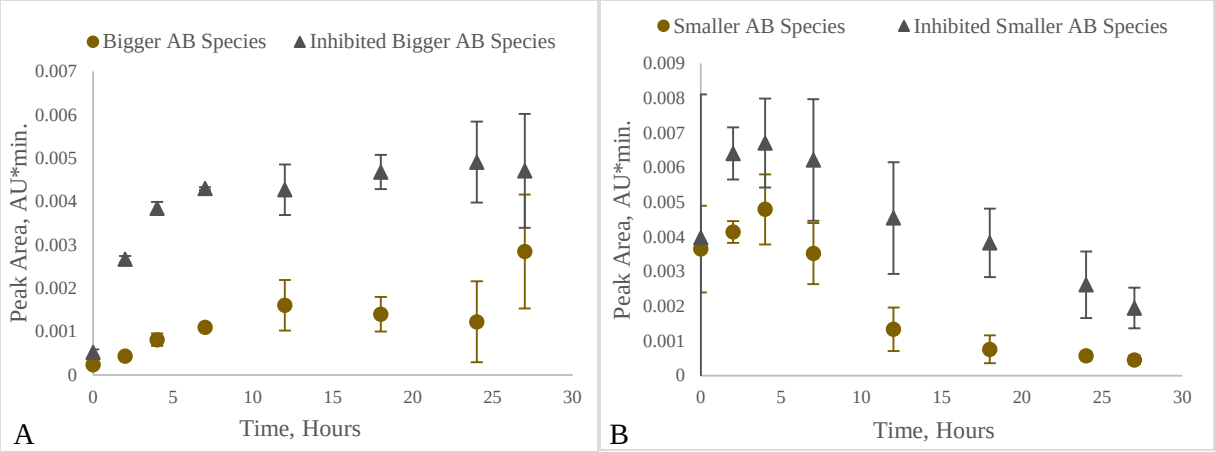

Figure 2.3.4-6: A) Inhibited Bigger 30µM $A\beta_{1-42}$ aggregates vs. un-inhibited and B) Inhibited smaller 30µM $A\beta_{1-42}$ aggregates vs. un-inhibited. The aggregation study consisted of Orange G inhibtion at 300RPM, 25°C with 40 mM sodium phosphate pH=7.4 as the sample buffer. The CE setting consisted of 0.5% 2000 kDa PEO capillary coating and 100 mM sodium phosphate buffer (pH=7.4) as the BGE with a separation matrix of 0.5% 50 kDa PEO plus 0.1% of 0.1% of 2000 kDa PEO using a pressure injection of 0.5 psi for 13.3 seconds and 7 kV separation voltage, n=3.

Since proto-fibrils and fibrils were observed at least within 7 hours into the un-inhibited aggregation, TEM imaging was also conducted to visualize the difference Orange G has on the aggregates. TEM imaging further confirms the increase in smaller aggregates where at 12 hour time point no proto-fibrils or fibril like species were observed (Figure 2.3.2-7B). Furthermore, the species at 12 hour appeared to be circular like aggregates (Figure 2.3.2-7E) that were earlier defined as oligomeric species. In the un-inhibited aggregated these circular like species reduced or appeared as ‘clumpy’ aggregates with fibrils observed. Additionally, the 0 hour TEM imaging barely had any if not any $A\beta_{1-42}$ aggregates visualized on the TEM. As the inhibited aggregation study continued, at 27 hours a few fibrils are observed in the TEM imaging where fibril species were observed. However, majority of the TEM image appeared to still consist of ‘clumpy’ aggregate like species. The fibrils observed at 27 hour might be due to inhibited degradation and/or the inability of Orange G to inhibit after a certain period of time. The interesting aspect of the

Orange G inhibited aggregation was the reduction of proto-fibril species where elongated proto-fibrils were observed (at 27 hours) but not the short stranded proto-fibrils at 12 hours. Therefore both the Congo red and Orange G data suggested that the CE aggregates are species smaller than proto-fibrils and most likely oligomers.

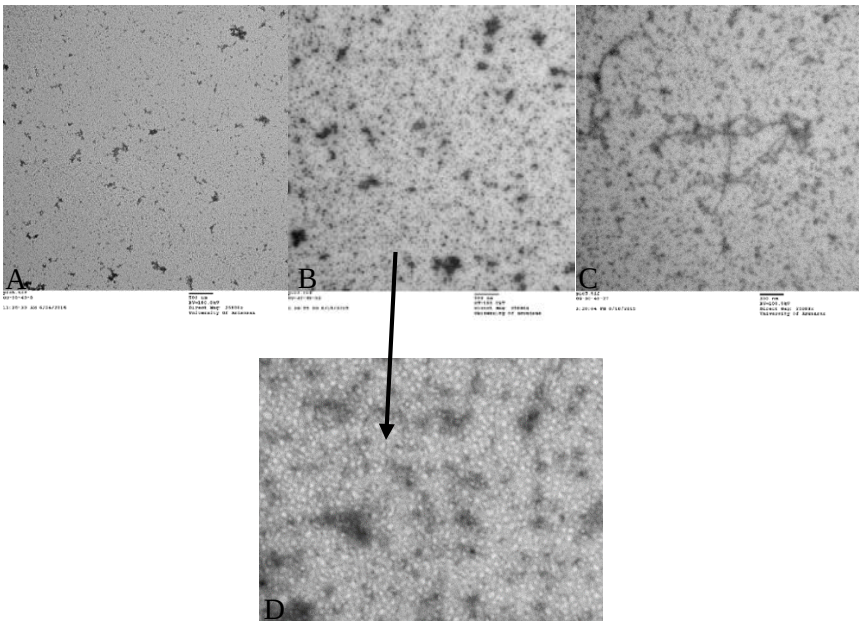

Figure 2.3.4-7: TEM imaging at A) 0 hour, B) 12 hour, C) 27 hour into the Orange G inhibition aggregation of 30 μM $A\beta_{1-42}$ with 40 mM sodium phosphate sample buffer pH=7.4. The aggregation was conducted using a mini-shaker at 300RPM, 25°C and TEM imaging was produced using JOEL with a magnification of 25000X and 100kV, n=2. TEM image D is magnified version of B with a magnification of 50000X in order to visualize the 'circular' like aggregates.

2.3.5 Computational Analysis

Since the sample concentration was much lower than the concentration of the sample buffer (μm compared to mM), it was assumed the electric field strength is greatly dependent on the sample buffer and BGE. Furthermore, the local electric field is believed to affect the stacking characteristics where in an ideal dynamic situation the sample concentration saturates at the ratio of load buffer divided by BGE (70). This situation was modeled by the simple control volume analysis where the sample BGE interface is located far from both ends of the capillary.

Therefore, the mass balance yields to:

$$\frac{dC_c}{dt} = \frac{F j_o z_c}{s_s \sigma_o \gamma} t(C_{co} - \frac{C_c(t)}{\gamma}) \quad \text{[Equation 2.3.5-1]}$$

and once the equation is rearranged it can be expressed as (70):

$$\frac{C_c(t)/C_{co}-1}{\gamma-1} = 1 - \exp(-\frac{j_o v_c F z_c}{s_s \sigma_o \gamma} t) \quad \text{[Equation 2.3.5-2]}$$

where j_o= current density, σ_o= electrical conductivity, s_s=sample gradient length, v_c=mobility of sample and z_c= charge of sample. The sample gradient length can be determined using (70):

$$E_s = \frac{\gamma V}{L_T(1+(\gamma+1)a)} \quad \text{[Equation 2.3.5-3]}$$

where V=voltage applied, Es=local electric field, L_T= total capillary length and a= fraction of capillary with load buffer. Once the variables are determined, various time points can be plugged into Equation 2.3.5-2 to determine the effect of lower conductive buffer compared to BGE for the sample buffer (as shown in Figure 2.3.5-1). Additionally, the data utilized to theorize the control volume analysis consist of assuming a monomeric amyloid peptide with a uniform current density and electrical conductivity.

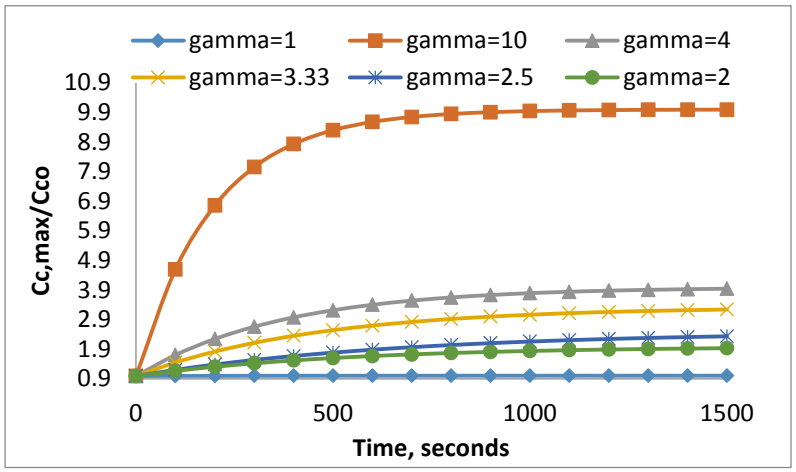

Figure 2.3.5-1: Change in concentration vs. time in accordance to the control volume analysis where ϒ=1 is for 100 mM, ϒ=2 is for 50 mM, ϒ=2.5 is for 40 mM, ϒ=3.33 is for 30 mM, ϒ=2 is for 20 mM and ϒ=10 is for 10 mM sodium phosphate sample buffer pH=7.4 with BGE of 100 mM

sodium phosphate buffer pH=7.4, V=7000 kV, local field strength is stated in Appendix B Section III and total capillary length is 31 cm.

As shown in Figure 2.3.5-1, the data developed by the theoretical input consisted of a graphical representation similar to Bharadwaj et al. where the concentration saturated at the gamma ratio (70). Therefore, the maximum enhancement of sample concentration using FASS was equal to the ratio of the buffer conductivity. Past studies have also shown that a local field strength between about 100-450 V/cm was an adequate separation environment (38; 75). As the difference between the BGE and load buffer increases, the higher end of the field strength is recommended where narrower peaks and better separation can occur (38; 43; 71). However, it is important to note that a huge difference between the concentrations of the sample buffer and separation buffer can also cause band broadening due to the increase in laminar flow characteristics created within the capillary. Therefore, it is important to establish the correct ratio difference between the two buffer systems. Even though a load buffer of 10 mM sodium phosphate provides highest concentration ratio, in practice this concentration might lead to zone broadening due to the huge difference in BGE and load buffer concentration. As the difference between the BGE and load buffer magnifies, the flow within the capillary behaves more like laminar flow, causing reduced resolution between peaks as well.

Additionally since the BSA data provided an approximate optimal load buffer of 40 mM sodium phosphate with the BGE at 100 mM sodium phosphate buffer pH=7.4, an idealized 2D computational simulation by Comsol® was developed to visualize the experimental difference of utilizing the FASS compared to non-FASS method with $A\beta_{1-42}$ (Figure 2.3.5-2). In order develop the 2D model, the affects due to the width of the capillary were ignored. The governing equations and boundary conditions stated in Section 2.1.1 were utilized to conduct the simulation. The

assumptions utilized consisted of no convection for the BGE due to neutral PEO coating on capillary. However, it is important to note that the BGE was assumed to be present in the capillary. This is possible since the separation matrix in the $A\beta_{1-42}$ consist of 5% of 50 kDa diluted in 100 mM sodium phosphate buffer. Furthermore, the theoretical diffusion coefficient for the peptide was assumed to be equivalent to the viscosity of water. The experimental diffusion coefficient was determined by utilizing $\sigma^2 = 2tD$ [Equation 2.3.5-4] where σ in this case is the variance, t is the migration time of the smaller aggregates and D is the diffusion coefficient of the amyloid (38). Additionally, the electric field distribution was also considered constant within the zones and the migration was based on the monomeric peptide charge of $A\beta_{1-42}$.

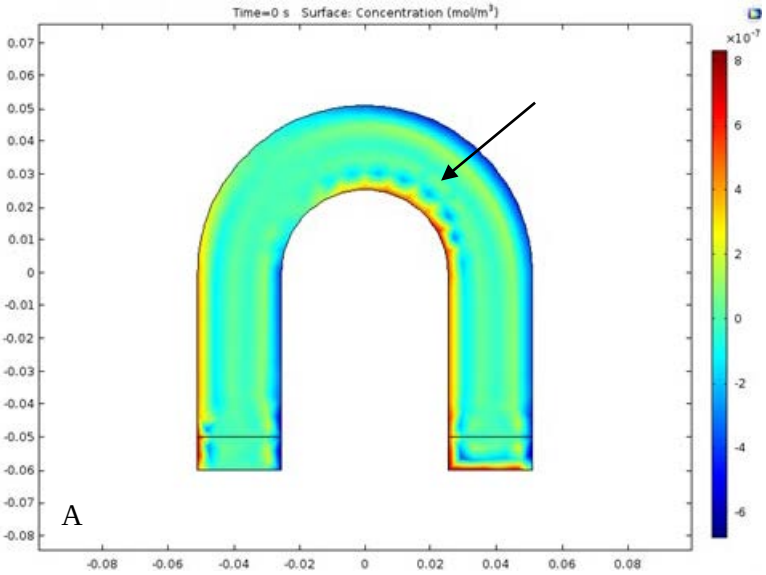

A

(Continued next page)

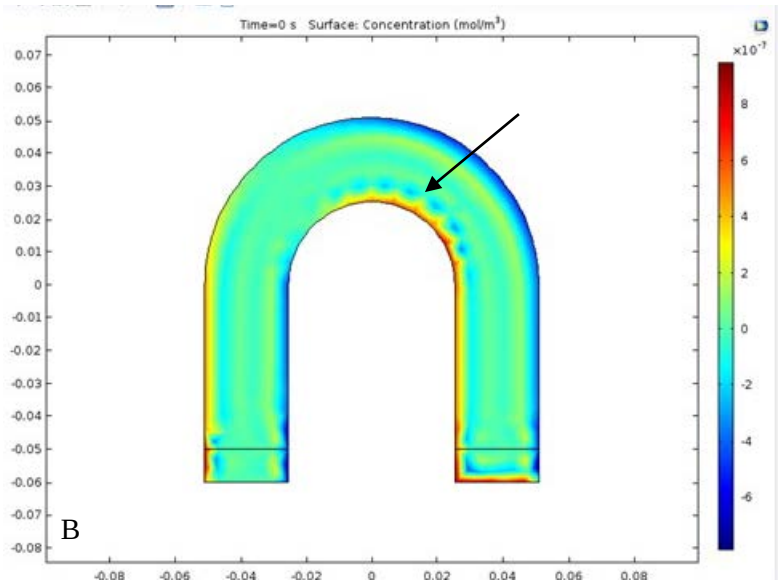

Figure 2.3.5-2: 2D Comsol® simulation of A) experimental 100 mM and B) experimental 40 mM sodium phosphate load buffer pH=7.4 with BGE of 100 mM sodium phosphate buffer where the concentration of $A\beta_{1-42}$ is 30µM. The applied voltage is 7000 V with Di for the 100 mM sodium phosphate buffer sample to be 0.025 cm^2/min and Di for the 40 mM sodium phosphate buffer sample to be 0.0066 cm^2/min.

The Comsol® simulation also required the sample velocity to run the model. The experimental velocity was determined using $\mu = \frac{LI}{tV}$ [Equation 2.3.5-6] where I is the length to detector, L is the total capillary length, t is the migration time and V is the voltage applied (40). Additionally, the $A\beta_{1-42}$ charge was assumed to similar to the charge of a monomeric Aβ (-2.9). By looking at Figure 2.3.5-2A and B, it can be observed that the two experimental surface concentrations are fairly similar. Since both the 100 mM and 40 mM sodium phosphate buffer migration time for the smaller aggregates did not change much, it can be expected that the computational data will be similar based on the calculated inputs in the simulation. The migration time affected the calculated velocity which would change if the intrinsic properties of Aβ were further understood and a true velocity profile was determined. Additionally, it is believed that the Nerst-Hartley-Gordon diffusion coefficient expression provides better data correlation for dilute

electrolyte solutions of experimental and theoretical data (82). The Nerst-Hartley-Gordon expression takes into account the relative viscosity of the solution as well as the concentration of the sample (82). Furthermore, for the experimental data aggregates of $A\beta_{1-42}$ at time 0 consisted of species larger than monomers. Again, causing a deviation of experimental data from the Comsol® computational analysis. However, the significance of the Comsol® simulation was that it offered the opportunity to explore the optimal sample injection end of the capillary as shown in Figure 2.3.5-2. By injecting the sample toward the end located closer to the detector, better detection of the sample was provided. The inflow was located in the side of the detection window (Figure 2.3.5-2A and B arrows) where higher detection is observed compared to injection in the farther end.

Since the surface concentration determined through Comsol® did not provide a foundation to determine the concentration of sample at the point of detection using FASS, fundamental understanding of electrochemistry process was observed and a replication of Bharadwaj et al. computational analysis was attempted (70). Since electrochemistry is considered a complex field, many scientists have utilized the dilute solution theory as a basis for transport analysis similar to Bharadwaj et al. (70, 83-84). Based on this theory, it is assumed that the species in the solution move due to migration, convection and diffusion as stated earlier. Additionally, the flux equation is based upon the average velocity of the solution (84). This is only true for extremely diluted solutions. Furthermore, Bharadwaj et al. utilized the Cottrell system concept where the experiment is believed to be controlled by diffusion (83). This is believed to be true due to the experimental data variance observed in the FASS technique vs. non-FASS technique. However upon attempting a replication of Bharadwaj et al.'s work, complications occurred either due to lack of knowledge, information and/or time spent on the governing equation's variables. Therefore, future work is needed to model the FASS technique using Aβ aggregates as the sample species.

2.4 Conclusion and Discussion

Recent studies have deduced the oligomeric species of Aβ to be the leading cause of AD. Hence in this study, it was confirmed that by using FASS on the CE better separation was reached and a better understanding of the $A\beta_{1-42}$ oligomer species without external interference with the aggregation occurred. In order observe the oligomer aggregates, the lag time was increased by changing the agitation rate. While conducting ThT assays, it was believed that the agitation rate of 300 RPM provided the optimal time range to analyze the oligomeric aggregates.

Upon establishing an adequate lag time to study the $A\beta_{1-42}$ aggregates, the optimal sample buffer for the FASS technique was determined to be 40 mM sodium phosphate pH=7.4 with the BGE at a concentration of 100 mM sodium phosphate pH=7.4. Then FASS conditions were compared with non-FASS conditions using $A\beta_{1-42}$ to further understand whether FASS is beneficial separation technique when observing Aβ oligomers. While comparing the FASS and non-FASS technique, it was establishment that the 5 minute peaks was the larger aggregates (30-100 kDa) compared to the 10 minute peak (< 30 kDa). According to the experimental data, the FASS technique provided maximum separation, reproducibility and Aβ detection.

While conducting the FASS technique using the CE, it was also important to ensure the $A\beta_{1-42}$ aggregation was not affected by varying sample buffer compared to the BGE. As shown by the CE data (Figure 2.3.1-2), the initial $A\beta_{1-42}$ species in the aggregation is not monomeric. This was believed to be due to the HFIP treatment conducted earlier to ensure aggregates with β-sheets were not present. Both the peak areas for the 100 mM and 40 mM sodium phosphate buffer were statistically similar for majority of the time points. Therefore, the assumption was accepted that the lower conductive sample buffer did not change the overall aggregation by much when

comparing with the 100 mM sodium phosphate buffer sample. Moreover, it was believed that the amyloid formation favored for this aggregation consisted of a process similar to Figure 2.4.1-1. According to Figure 2.4.1-1, the initial stage was the monomeric species where with the addition of monomers species ranging from dimers to oligomers were formed. The aggregation pathway was believed to vary according to the original aggregates in the solution.

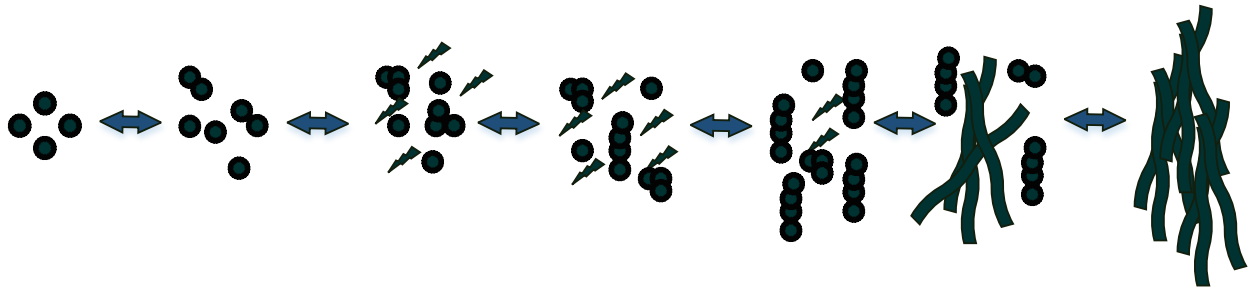

Figure 2.4-1: Aggregation $A\beta_{1-42}$ where the initial stages from monomer to oligomer species was observed with the addition of short strands of proto-fibrils. Eventually, the proto-fibrils strands elongate and were mixed with higher aggregates and short stranded proto-fibrils. The amyloid formation developed into producing nucleating fibrils and final various fibril formation occurred (85).

By conducting MWCO filter experimentations, it was established that the 5 minutes peak aggregates ranged from 30 – 100 kDa. Additionally, the 10 minute peak aggregates consisted of a molecular weight of up to 30 kDa. Since majority of the oligomer forms range from 30 to 250 kDa, the filter experiments helped prove that the aggregates were considered within the oligomer species range. By 51 hours into the aggregation study, majority of the aggregates were fibrils (if not all aggregates). The TEM imaging additionally proved that by 27 hours majority of the higher aggregates were not fibrils. However since some fibril species were observed in the TEM imaging at 27 hours, further experimentations were conducted to narrow the Aβ species detected using inhibition studies using Congo red and Orange G.

Since Congo red was believed to inhibit oligomeric species or species smaller than fibrils, it was assumed that the 5 minute peak would not increase. However, mixed results were produced using Congo red inhibition. Half of the CE data consisted of an increase in the concentration of the 5 minute species whereas the rest of the experiments did not. These results confirmed past literature studies where Congo red was considered a weak inhibitor (79-80). Additionally inhibition studies using Orange G, fibril inhibitor, was conducted to prove data observed by CE is not fibril. The Orange G TEM images confirmed fibril inhibition where the CE data highlighted the effects the inhibition might cause on the overall aggregation. For the Orange G inhibition, the CE results showed a higher detection of the inhibited species. It was believed the inhibition of fibril could potentially promote off pathway aggregates. Furthermore upon binding to Aβ, Orange G was believed to increase its absorbance and therefore, could potential effect the overall absorbance observed by the CE as well. The TEM imaging for both Congo red and Orange G believed to consist of adequate proto-fibrils inhibition where majority of the short stranded species decreased during the aggregation. Furthermore, both Congo red and Orange G aggregation consisted of an increase in the circular aggregate production. According to Ahmed et al., oligomer species observed by atomic force microscopy (AFM) can range from disc-shaped pentamer to globulomers (para-nucleus etc.) (24).

Since Congo red inhibition did not provide clear understanding of the data observed by the CE, it is recommended to conduct CE analysis using well known oligomeric inhibitors. This will further help distinguish the aggregates observed by the CE and also provide a clear picture of the aggregation study. Additionally upon attempting to conduct computational analysis, it is further recommended to utilize the dilute solution theory in order to develop a complete model showing the FASS technique using these conditions.

Chapter 3: Future Work with Natural Compound Inhibitors

With growing research being conducted on AD, finding the optimal analysis method while looking at the affects certain preventive treatment might have *in vitro* is essential before conducting *in vivo* research. Therefore by utilizing a separation method like CE, further understanding of un-inhibited and inhibited aggregates of Aβ can be determined and analyzed. Since current literature suggest the soluble Aβ oligomers to be the leading cause for AD, optimized separation conditions were determined using CE where $A\beta_{1-42}$ aggregates equal to or smaller than 100 kDa can be studied. Therefore, by utilizing the CE, an opportunity is provided to see whether certain inhibitors target these species and what happens to the aggregation after addition of a potential inhibitor.

Recent studies show how oxidative stress, caused by an imbalance between the defense mechanism and harmful reactive oxygen species (ROS) as well as reactive nitrogen species (RNS), can occur in the early stages of AD (3; 6; 86-88). In terms of Aβ, it is believed the mitochondria plays a key role in oxidative stress and the soluble oligomer $A\beta_{1-42}$ might potentially further promote oxidative damage (88). Though exact mechanism of oxidation for $A\beta_{1-42}$ is unknown, one explanation is that the oxidation of Met can lead to increase in ROS and RNS production, and activities that induce mitochondrial dysfunctions in AD patients (6; 86-88). Since in the previous chapter conditions were established to further study $A\beta_{1-42}$ aggregates less than 100 kDa, inhibitors known for their anti-oxidant characteristics will be discussed further in this chapter for future work in order further understand the affects these inhibitors might have on the aggregates by utilizing CE as a separation technique, especially the oligomer aggregates.

3.1 Natural Compound Inhibitors

Since it is believed that oxidative stress plays a major role in AD, there is reason to believe in the usefulness of polyphenol rich natural compound inhibitors. Numerous studies on determining the effects of certain inhibitors on AD have been conducted (3; 88). Polyphenols are flavonoids that consist of at least one phenol group and have major antioxidant properties. These flavonoids can be found in variety of organic foods such as fruits, vegetables, or plant derived beverages (89- 90). The polyphenols that will be recommended for future work consist of fisetin, quercetin, isorhamnetin, epigallocatechin 3-gallate (EGCG), and curcumin. Though past studies have been conducted using these inhibitors, no known study has been conducted using the CE with these inhibitors (88-90). Therefore, a study with CE may contribute further knowledge of how each inhibitor effects $A\beta_{1\text{-}42}$ aggregates less than 100 kDa and the overall aggregation.

According to past literature, fisetin, a flavonoid found in strawberries, inhibit fibrils and has been known to protect the nerve cells from oxidative stress (89; 91). It would be further interesting to see whether this rule also applies to fibril oligomers and whether the soluble intermediate aggregates increase due to fibril inhibition as observed by the Orange G data. Another antioxidant found in fruits (such as apples, apricots and blueberries) that is recommended is quercetin. Ansari et al. have shown quercetin to reduce cytotoxicity caused by $A\beta_{1\text{-}42}$ and have further developed a dose response study using quercetin (89-90). Also, both quercetin and isorhamnetin have been studied for their anti-inflammatory effects (89-90; 92). In addition to having anti-inflammatory effects, isorhamnetin is believed to potentially have an effect on AD since it is a component found in Ginkgo leaf which is used to treat early AD symptoms (93). Since isorhamnetin has been studied for its effect on neurite-inducing activity of nerve growth, it would be interesting to further study this compound with $A\beta_{1\text{-}42}$ (93). Furthermore understanding the

affects both quercetin and isorhamnetin have on $A\beta_{1-42}$ species less than 100 kDa through the CE will provide the opportunity to determine the aggregates these inhibitors affect and whether the overall aggregation for $A\beta_{1-42}$ will vary.

The other two recommended natural compounds, epigallocatechin 3-gallate (EGCG) and curcumin, are commonly found in many South Asians daily cuisine. Both of these natural compounds are also known for their anti-inflammatory characteristics where past studies have been conducted to also show the ability of both natural compounds to inhibit oligomers and/or fibrils amyloid (94-95). With the extensive research being conducting utilizing these inhibitors for AD, using CE to understanding how the aggregates less than 100 kDa behave would not only provide insight on the effect of these inhibitor on the aggregation of $A\beta_{1-42}$ but would hopefully further highlight the importance of having these natural compounds in a person's diet.

3.2 Conclusion

CE provides an opportunity to not only understand the aggregation of the intermediate species of Aβ, but it is also a great separation technique that provides a platform to observe how various inhibitors can affect the overall aggregation, especially when combined with other techniques such as TEM or AFM. Alterations in $A\beta_{1-42}$ aggregates smaller than 100 kDa by using inhibitors like Congo red and Orange G were observed using CE. By establishing optimal separation conditions using the CE with $A\beta_{1-42}$, it is further recommended to continue understanding the affect natural compound inhibitors have on $A\beta_{1-42}$ aggregates that are smaller than 100 kDa. Natural compound inhibitors re-iterate the importance of having a healthy lifestyle in order to avoid or potentially reduce the risk of diseases such as AD.

References

1. *A universal method for detection of amyloidogenic misfolded proteins.* **Yam, Alice, Wang, Xuemei and et.al.** 2011, Biochemistry, pp. 4322-4329.

2. **Whitford, David.** *Proteins Structure and Function.* s.l. : Wiley, 2005. 426-435.

3. *The amyloid beta peptide: a chemist's prespecitve. Role in Alzheimer's and Fibrillization.* **Hamley, I.W.** s.l. : Chemical Reviews, 2012, Vol. 112.

4. *Alzheimer's disease is a synaptic failure.* **Selkoe, Dennis J.** s.l. : Science, 2002, Vol. 298.

5. *Kinetics of amyloid formation and membrane interaction with amyloidogenic proteins.* **Murphy, Regina.** 2007, ScienceDirect, pp. 1923-1934.

6. *Amyloid beta, mitochondrial dysfunction and synaptic damage: implications of cognitive decline in aging and Alzheimer's disease.* **Reddy, P. Hemachandra and Beal, M. Flint.** s.l. : Cell Press, 2007.

7. *2015 Alzheimer's disease facts and figures."* . s.l. : Alzheimer's Association , 2015.

8. *Oligomerization and Toxicity of amyloid beta-42 Implicated in Alzheimer's Disease.* **El-Agnaf, O., et al.** 2000, Biochemical and Biophysical Research Communications, pp. 1003-1007.

9. *Pathways linking Aβ and tau pathologies.* **LaFerla, Frank M.** s.l. : Biochemical Society Transactions, 2010, Vol. 38.

10. *Roles of amyloid precursor protein and its fragments in regulating neural activity, plasticity and memory.* **Turner, Paul, et al.** s.l. : Progress in Neurobiology, 2003, Vol. 70.

11. *Amyloid beta peptide induces tau phosphorylation and loss of cholinergic neurons in rat primary septal cultures.* **W.H., Zheng, et al.** s.l. : Neuroscience, 2002, Vol. 115.

12. *AB oliogomer-induced aberrations in synapse composition, shape, and density provide a molecular basis for loss of connectivity in alzheimer's disease.* **Lacor, Pascale N., et al.** Evanston : The Journal of Neuroscience, 2007, Vol. 27.

13. *Soluble protein oligomers in neurodegeneration: lessons from the Alzheimer's amyloid B-peptide.* **Haass, Christian and Selkoe, Dennis.** s.l. : Nature, 2007, Vol. 8.

14. *AB40 Oligomers identified as potential biomarker for thediagnosis of alzheimer's disease.* **Carol Man Gao, ALice Y. Yam, Xuemei Wang and et al.** 2010, PLoS ONe.

15. *AB monomers transiently sample oligomer and fibril like configurations: ensemble characterization using a combined MD/NMR approach.* **Rosenman, David and et al.** 2013, Molecular Biology, pp. 3338-3359.

16. *Amyloid b- protein oligomerization prenucleation interactions revealed by photo-induced cross linking unmodified protein .* **Bitan, Gal; Lomakin, Aleksey and Teplow, David B.** s.l. : The Journal of Biological Chemistry, 2001, Vol. 276.

17. *Structure and dynamics of small soluble AB(1-40) oligomers studied by top down hydrogen exchange mass spectrometry.* **Pan, Jingxi, and et al.** 2012, Biochemistry , pp. 3694-3703.

18. *Soluble amyloid b peptide concentration as predictor of synaptic change in alzheimer's disease.* **Lue, Lih-Fen, and et al.** 3, s.l. : Elsevier, 1999, Vol. 155.

19. *B-Amyloid precursor protein of alzheimer disease occurs as 110- to 135 kilodalton membrane associated proteins in neural and nonneural tissues.* **Selkoe, Dennis, and et al.** s.l. : Proc. Natl. Sci., 1988, Vol. 85.

20. *Amyloid Precursor Protein Processing and Alzheimer's Disease.* **O'Brien, Richard and Wong, Philip.** s.l. : Annual Reviews Neuroscience, 2011, Vol. 34.

21. *Amyloid B-protein precursor: new clues to the genesis of Alzheimer's disease.* **Selkoe, Dennis.** 1994, Neurobiology, pp. 708-716.

22. *Amyloid precursor protein increases cortical neuron size in transgenic mice.* **Oh, Esther S., and et al.** 8, s.l. : Neurobiology of Aging, 2009, Vol. 30.

23. *Visualization of Aβ42(43) and Aβ40 in senile plaques with end-specific Aβ monoclonals: evidence that an initially deposited species is Aβ42(43).* **Iwatsubo, Takeshi, and et al.** 1, s.l. : Neuron, 1994, Vol. 13.

24. *Structural conversion of neurotoxic amyloid B1-42 oligomers to fibrils.* **Ahmed, Mahiuddin, and et al.** 2010, Nature Structural & Molecular Biology, pp. 561-567.

25. *Amyloid B protein monomer folding: free energy surfaces reveal alloform specific differences.* **Yang, Mingfeng and Teplow, David.** 2, s.l. : Journal of Molecular Biology, 2008, Vol. 384.

26. *The toxicity in vitro of B-amyloid protein.* **Iversen, Leslie L., and et al.** 1995, Biochemistry Journal, pp. 1-16.

27. *Substitutions of hydrophobic amino acids reduce the amyloidogenicity of alzheimer's disease BA4 peptide.* **Hilbich, Caroline, and et al.** 2, s.l. : Journal of Molecular Biology, 1992, Vol. 228.

28. *A subset of NSAIDs lower amyloidogenic Aβ42 independently of cyclooxygenase activity.* **Weggen, Sascha, and et al.** s.l. : Nature, 2001, Vol. 414.

29. *Phosphorylation of amyloid beta (AB) peptides- a trigger for formation of toxic aggregates in Alzheimer's disease.* **Kumar, Sathish and Walter, Jochen.** 2011, AGING Journal, pp. 803-812.

30. *Soluble oligomers of amyloid-β peptide disrupt membrane trafficking of α-amino-3-hydroxy-5-methylisoxazole-4-propionic acid receptor contributing to early synapse dysfunction.* **Miñano-Molina, Alfredo J., and et al.** s.l. : The Journal of Biological Chemistry, 2011, Vol. 286.

31. *AB oligomer-induced aberrations in synapse composition, shape, and density provide a molecular basis for loss of connectivity in alzheimer's disease.* **Lacor, Pascale, and et al.** s.l. : The Journal of Neuroscience, 2007, Vol. 27.

32. *Atomic view of a toxic amyloid small oligomer.* **Laganowsky, Arthur, and et al.** s.l. : Science, 2012, Vol. 335.

33. *Annular Protofibrils are a structurally and functionally distinct type of amyloid oligomer.* **Kayed, Rakez, and et al.** s.l. : The Journal of Biological Chemistry, 2009, Vol. 284.

34. *Fibril specific, conformation dependent antibodies recognie a generic eptiope common to amyloid fibrils and fibrillar oligomers that is absent in prefibrillar oligomers.* **Kayed, Rakez, and et al.** s.l. : Molecular Neurodegeneration, 2007, Vol. 2.

35. **Roberts, Christropher.** Nonnative Protein Aggregation. [book auth.] Regina Murphy and Amos Tsai. *Misbehaving proteins: proteins (mis)folding, aggregation, and stability.* USA : Springer, 2006, pp. 17-.

36. *Novel mechanistic insight into the molecular basis of amyloid polymorphism and secondary nucleation during amyloid formation.* **Jeong, Jae Sun, and et al.** s.l. : Journal of Molecular Biology, 2013, Vol. 425.

37. *Unraveling the early events of amyloid b protein (AB) aggregation: techniques for the determination of AB aggregate size.* **Pryor, Elizabeth, Moss, Melissa and Hestekin, Christa.** s.l. : International Journal of Molecular Science, 2012, Vol. 13.

38. **Grossman, P. D., and Colburn, J. C.** *Capillary Electrophoresis: Theory and Practice.* London : Academic Press, Inc., 1992.

39. **Bosserhoff, Anja, and Hellerbrand, Claus.** Capillary Electrophoresis. s.l. : Elsevier, 2005.

40. **Landers, J. P.** *Handbook of Capillary Electrophoresis.* United States : CRC Press LLC, 1997.

41. *Electrophoresis in fused silica capillaries: the influence of organic solvents on the electroosmotic velocity and the zeta potential.* **Schwer, Christine, and Kenndler, Ernst.** s.l. : American Chemical Society, 1991, Vol. 63.

42. **Delahay, Paul.** *Double Layer and Electrode Kinetics.* s.l. : Interscience, 1965.

43. **Khaledi, M.** *High-Performance Capillary Electrophoresis: Theory, Techniques, and Application.* s.l. : John Wiley & Sons, Inc, 1998.

44. **Schwartz, Herb and Pritchett, Tom.** *Separation of Proteins and Peptides by Capillary Electrophoresis: Application to Analytical Biotechnology.* 1992.

45. *Polymer Wall Coatings for Capillary Electrophoresis.* **Judit Horvath, and Vladislav Dolnik.** 2001, Electrophoresis, pp. 644-655.

46. *Mechanism of thioflavin T binding to amyloid fibrils.* **Khurana, Ritu, and et al.** 2005, Journal of Structural Biology, pp. 229-238.

47. *Molecular mechanism of Thioflavin T binding to amyloid fibrils.* **Biancalana, Matthew and Koide, Shohei.** 2010, Elsevier, pp. 1405-1412.

48. *The binding of thioflavin-t to amyloid fibrils: localisation and implications.* **Krebs, M.R.H and Bromley, E.H.C., Donald, A.M.** s.l. : Journal of Structural Biology, 2005, Vol. 149.

49. *Fluorometric determination of amyloid fibrils in vitro using the fluorescent dye, thioflavin T1.* **Naiki, Ho., and et al.** 1989, Analytical Biochemistry, pp. 244-249.

50. *A mathematical model of the kinetics of B-amyloid fibril growth from the denatured state.* **Pallitto, Monica M. and Murphy, Regina.** 2001, Biophysical Journal, pp. 1805-1822.

51. *A three-stage kinetic model of amyloid fibrillation.* **Lee, Chuang-Chuang, and et al.** 2007, Biophysical Journal, pp. 3448-3458.

52. *In vitro characterization of conditions for amyloid b peptide oligomerization and fibrillogenesis.* **Stine, W. Blaine, and et al.** 13, s.l. : The American Society for Biochemistry and Molecular Biology, 2003, Vol. 278.

53. *Amyloid b protein immunotherapy neutralizes AB oligomers that disrupt synaptic plasticity in vivo.* **Klyubin, Igor, et al.** s.l. : Nature Medicine, 2005, Vol. 11.

54. *Conformation dependent antibodies target diseases of protein misfolding.* **Glabe, Charles.** s.l. : Trends in Biochemical Science, 2004, Vol. 29.

55. *Aggregation and fibril morphology of the arctic mutation of alzheimer's AB peptide by CD, TEM, STEM and in situ AFM.* **Norlin, Nils, and et al.** s.l. : Journal of Structural Biology, 2012, Vol. 180.

56. *Sedimentation velocity analysis of amyloid oligomers and fibrils.* **Mok, Yee-Foong and Howlett, Geofrey.** s.l. : Methods in Enzymology, 2006, Vol. 413.

57. *Sedimentation patterns of rapidly reversible protein interactions.* **Schuck, Peter.** s.l. : Biophysical Journal , 2005, Vol. 98.

58. *On computational approaches for size and shape distributions from sedimentation velocity analytical ultracentrifugation.* **Schuck, Peter.** s.l. : Eur. Biophys. J, 2010, Vol. 39.

59. **Howell, J.A., Sanchez, V. and Field, R. W.** *Membranes in Bioprocessing: Theory and Application.* s.l. : Chapman and Hall, 1993.

60. *Capillary electrophoresis for the analysis of the effect of sample preparation on early stages of AB1-40 aggregation.* **Pryor, N. Elizabeth, Moss, Melissa and Hestekin, Christa.** s.l. : Electrophoresis, 2014, Vol. 35.

61. *On-line preconcentration methods for capillary electrophoresis.* **Osbourn, Damon, Weiss, David and Lunte, Craig.** s.l. : Electrophoresis, 2000, Vol. 21.

62. *Recent applications of on-line sample preconcentration techniques in capillary electrophoresis.* **Kitagawa, Fumihiko and Otsuka, Koji.** s.l. : Journal of chromatography A, 2013.

63. *On-line sample preconcentration by sweeping and poly(ethylene oxide)-mediated stacking for simultaneous analysis of nine pairs of amino acid enantiomers in capillary electrophoresis.* **Lin, EP, and et al.** s.l. : Elsevier, 2013.

64. *Capillary electrophoresis of proteins 1999–2001.* **Dolník, Vladislav and Hutterer, Katariina M.** s.l. : Electrophoresis, 2001, Vol. 22.

65. *On-line sample concentration techniques in capillary electrophoresis: velocity gradient techniques and sample concentration techniques for biomolecules.* **Lin, Cheng-Huang and Kaneta, Takashi.** s.l. : Electrophoresis, 2004, Vol. 25.

66. *Electrophoresis: mathematical modeling and computer simulation.* **Bier, M., and et al.** s.l. : Science, 1983, Vol. 219.

67. *On-column sample concentration using field amplification in CZE.* **Chien, Ring-Ling and Burgi, Dean.** 8, s.l. : Analytical Chemistry, 1992, Vol. 64.

68. *Sample preconcentration by field amplification stcking for microchip based capillary electrophoresis.* **Lichtenberg, Jan, Verpoorte, Elisabeth and de Rooij, Nico F.** s.l. : Electrophoresis, 2001, Vol. 22.

69. *Sample stacking of an extremely large injection volume in hight performance capillary electrophoresis.* **Chien, Ring Ling and Burgi, Dean S.** s.l. : Analytical Chemistry, 1992, Vol. 64.

70. *Dynamics of field amplified sample stacking.* **Bharadwaj, Rajiv and Santiago, Juan.** s.l. : Journal of Fluid Mechanics, 2005, Vol. 543.

71. *Optimization in sample stacking for high performance capillary electrophoresis.* **Burgi, Dean and Chien, Ring-Ling.** s.l. : Analytical Chemistry, 1991, Vol. 63.

72. **Guiochon, Georges, Felinger, Attila and Shirazi, Dean.** *Fundamentals of Preparative and Nonlinear Chromatography.*

73. *Small molecule inhibitors of aggregation indicate that amyloid b oligomerization and fibrillization pathways are independent and distinct.* **Necula, Mihaela, and et al.** 14, s.l. : The Journal of Biological Chemistry, 2007, Vol. 282.

74. *Rationally designed peptoids modulate aggregation of amyloid abeta 40.* **Turner, Phillip J., and et al.** 2014, ACS Chemical Neuroscience, pp. 552-558.

75. *An optimized microchip electrophoresis system for mutation detection by tandem SSCP and heteroduplex analysis for p53 gene exons 5-9.* **Hestekin, Christa, and et al.** s.l. : Electrophoresis, 2006, Vol. 27.

76. **Pachahara, Sanjai Kumar, and et al.** *Hexafluoroisopropanol induces self-assembly of b-amyloid peptides into highly ordered nanostructures.* s.l. : Journal of Peptide Science, 2012.

77. *Structural, morphological, and kinetic studies of B amyloid peptide aggregation on self assembled monolayers.* **Wang, Quiming, and et al.** s.l. : J. Phys. Chem., 2011, Vol. 13.

78. *Water-soluble Abeta (N-40, N-42) oligomers in normal and Alzheimer disease brains.* **YM, Kuo, and et al.** s.l. : Journal of Bio.Chem., 1996, Vol. 271.

79. *Spectroscopic and calorimetric studies of congo red dye amyloid b peptide complexes.* **Yokoyama, Kazyushige, and et al.** 3, s.l. : Journal of Biophyscial Chemistry, 2010, Vol. 1.

80. *Binding of congo red to amyloid protofibrils of the alzheimer AB9-40 peptide probed by molecular dynamics simulations.* **Wu, Chun, Scott, Justin and Shea, Joan-Emma.** s.l. : Biophysical Journal, 2012, Vol. 103.

81. *Common Structure of Soluble Amyloid Oligomers Implies Common Mechanism of Pathogenesis.* **Kayed, Rakez, and et al.** s.l. : Science, 2003, Vol. 300.

82. **Horvath, A.L.** *Handbook of Aqueous Electrolyte Solutions.* s.l. : Ellis Horwood Limited, 1985.

83. **Britz, D.** *Digital Simulation in Electrochemistry.* s.l. : Springer, 2005.

84. **Tobias, Charles.** *Advances in Electrochemistry and Electrochemical Engineering.* s.l. : John Wiley & Sons, Inc., 1967.

85. **Cohen, Samuel, and et al.** *Nucleated polymerization with secondary pathways. I. time evolution of the principal moments.* s.l. : The Journal of Chemical Physics, 2011.

86. *Mictochondrial defects and oxidative stress in alzheimer disease and Parkinson disease.* **Yan, Michael, Wang, Xinglong and Zhu, Xiongwei.** s.l. : Free Radical Biology and Medicine, 2013, Vol. 62.

87. *Amyloid b peptide (1-42) induced oxidative stress in alzheimer disease: importance in disease pathogenesis and progression.* **Butterfield, Allan, Swomley, Aaron and Sultana, Rukhsana.** 8, s.l. : Antioxidants and Redox Signaling, 2015, Vol. 19.

88. *Abeta, oxidative stress in alzheimer disease: evidence based on proteomics studies.* **Swomley, Aaron, and et al.** s.l. : Biochimica et Biophysica Acta, 2014.

89. *Effects of naturally occurring compounds on fibril formation and oxidative stress of b-amyloid.* **Kim, Hee, and et al.** s.l. : Journal of Agricultural and Food Chemistry, 2005, Vol. 53.

90. *Protective effect of quercetin in primary neurons against AB(1-42): relevance to Alzheimer's disease.* **Ansari, Mubeen Ahmad, and et al.** s.l. : Journal of Nutritional Biochemistry, 2008, Vol. 20.

91. *Structural requirements for the flavonoid fisetin in inhibiting fibril formation of amyloid b protein.* **Akaishi, Tatsuhiro, and et al.** s.l. : Neuroscience Letters, 2008, Vol. 444.

92. *Anti-inflammatory effects of flavonoids: genistein, kaempferol, quercetin, and daidzein inhibit STAT-1 and NF-kB activations, whereas flavone, isorhamnetin, naringenin, and pelargonidin inhibit only NF-kB activation along with their inhibitory effect on i.* **Hamalainen, Mari, and et al.** ID:45673, s.l. : Hindawi Publishing Corporation, 2007, Vol. 2007.

93. *Isorhamnetin, a flavonol aglycone from Ginkgo biloba L., induces nueronal differentiation of cultured PC12 cells: potentiating the effect of nerve growth factor.* **Xu, Sherry, and et al.** ID 278273, s.l. : Hindawi Publishing Corporation, 2012, Vol. 2012.

94. *EGCG redirects amyloidogenic polypeptides into unstructured, off-pathway oligomers.* **Ehrnhoefer, Dagmar, and et al.** 6, s.l. : Nature Structural and Molecular Biology, 2008, Vol. 15.

95. *Curcumin Inhibits formation of amyloid b oligomers and fibrils, binds plaques, and reduces amyloid in vivo.* **Yang, Fusheng, and et al.** 7, s.l. : The Journal of Biological Chemistry, 2004, Vol. 280.

96. *Effect of Environmental Factors on the Kinetics of Insulin Fibril Formation: Elucidation of the Molecular Mechanism.* **Nielsen, Liza, and et al.** 20, s.l. : Biochemistry, 2001, Vol. 40.

97. *Amyloid-β protein oligomerization and the importance of tetramers and dodecamers in the aetiology of Alzheimer's disease.* **Bernstein, Summer L., and et al.** 4, s.l. : Nat. Chem, 2009, Vol. 1.

98. *P/ACE MDQ User's Guide.* Brea, CA : Beckman Coulter, Inc., 2009**.**

99. *Sample preconcentration by field amplification stacking for microchip based capillary electrophoresis.* **Lichtenberg, Jan, Verpoorte, Elisabeth and de Rooij, Nico F.** s.l. : Electrophoresis, 2001, Vol. 22.

100. *Field-amplified sample stacking in micellar electrokinetic chromatography for on-column sample concentration of neutral molecules.* **Z, Liu, and et al.** s.l. : Journal of Chromatography, 1994, Vol. 673.

101. *Fibrillar oligomers nucleate the oligomerization of monmeric amyloid b but do not seed fibril formation.* **Wu, Jessica, and et al.** s.l. : The Journal of Biological Chemistry, 2010, Vol. 285.

102. *NIH Image to ImageJ: 25 years of image analysis.* **Schneider, C.A., Rasband, W.S., Eliceiri, K.W.** s.l. : Nature Methods, 2012, Vol. 9.

Appendix A: Determining Sample Preparation and Agitation Rate

I. Pre-Aggregation Sample Preparation

Initial experimentation consisted of utilizing buffer system previously established in the laboratory. This helped provide a foundation where understanding the pre-aggregation steps was necessary. According to literature, minute changes in Aβ concentration, pH, agitation, salt content, temperature, etc. can have leading effect in the pathway of the aggregates (26; 34; 36; 51-52). Therefore by using Thioflavin-T assay, aggregation studies were conducted to determine the effect certain parameters have. These parameters consisted of:

1. Cutting pipette tips: This was believed to help suction in larger Aβ aggregates as the assay continues.
2. Having a cooler (about 4°C) environment for Aβ during the pre-aggregation steps: This was believed to not promote aggregation while creating the 'cell like' environment before starting aggregation.
3. Transferring the solution from one vial to another after put in the buffer to the solution: This was believed to ensure mixture of solution.
4. Changing the amount of time Aβ solution consist of just the NaOH or is in the buffer system before starting the aggregation: This was believed to establish an adequate cell like environment from the *in vitro* experiments.

Experimentations were conducted to further understand the advantages or disadvantage of each hypothesis relating to the specific parameters. It was quickly realized that though cutting the tips of the pipette provided better detection of the ThT-Aβ binding when establishing a comparison within the data, major inconsistent was seen. Furthermore, the difference in increase in intensity was not as significant as expected. Therefore, the inconsistent in data readings became a greater

issue and cutting the tips became a greater hindrance than benefit. Additionally, Figure A.1-1 (below) shows the affect the other parameters have on ThT binding to Aβ.

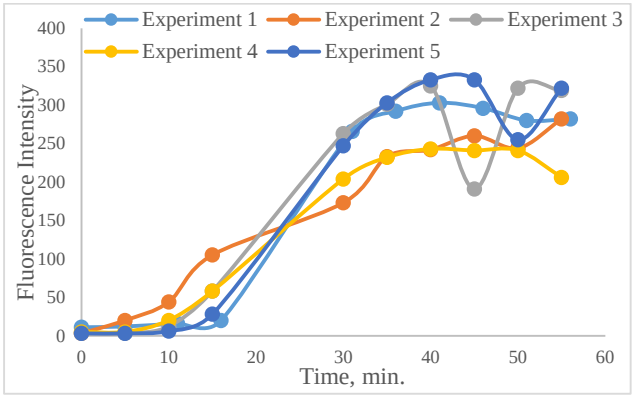

Figure A.1-1: Conducting ThT Assay at 800 RPM utilizing 20 µM Aβ1-42 in 40 mM Tris-HCl pH=8.07 and 150 mM NaCl at 25°C and 14.29 µM ThT stock solution (1 mM ThT diluted in 40 mM Tris HCl buffer) at a mol ratio of 5:1 of Aβ to ThT.

Figure A.1-1 represented five different experiments where Experiment 1, 3 and 5 consisted of adding NaOH 10 minutes before adding the buffer and the whole solution was kept on ice for a total of 30 minutes. Since the ice environment was not insulated and no lid was placed on the top of the container, the environment temperature is about 4°C. Experiment 2 consisted of adding NaOH and keeping it on ice for 10 minutes. After 10 minutes, the buffer was added and placed in room temperature for 10 minutes. It was interesting to note that though Experiment 2 started at a higher fluorescent intensity, its plateau consisted of a lower intensity than Experiment 1, 3, and 5. It was believed that keeping the solution at room temperature increased the aggregation rate (therefore higher initial fluorescent intensity) and produced insoluble fibrils faster than the other experiments. Consequently, keeping the pre-aggregation steps where solution was placed on ice (about a 4°C environment) provided slower aggregation and in turn, better chance of detecting the soluble intermediates shown in Chapter 1 Figure 1.1-1.

Finally, Experiment 4 dealt with changing the vials before taking the first ThT data point. The interesting aspect about this investigation was that it behaved quite similar to Experiment 2 where the fluorescent intensity at the plateau was lowered. By mixing the content in the vial, it ensures there is a uniform solution and the statistical difference until 10 minutes was not significant.

II. Determining Agitation Rate

Upon establishing the pre-aggregation step, it was important to re-evaluate the final thesis aim which is to study the oligomer form of Aβ and also the other soluble intermediate aggregates. Therefore, understanding what happens during the aggregation was important. Additionally, determining the optimal aggregation protocol to study the early aggregates in a timely manner was also beneficial in studying the sample using CE. Upon understanding how the addition of aggregates affected the overall aggregation, it was simple to conclude that the aggregation pathway cannot be determined thorough experiments looking at just monomer concentration vs. time (5; 34-35). This concept was verified through ThT assays conducted using 20 μM $A\beta_{1-42}$ (Figure A.2-1 below).

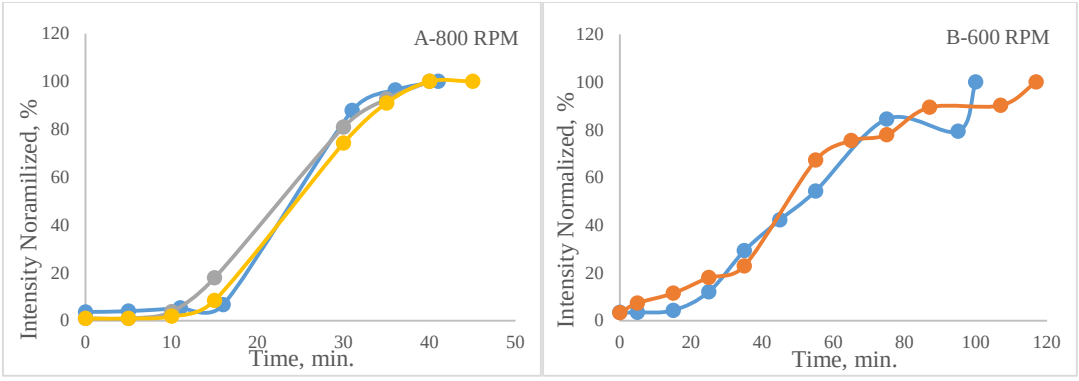

Figure A.2-1: ThT Assay where A) is conducted at 800 RPM and B) at 600 RPM agitation rate using 20 μM $A\beta_{1-42}$ with 40 mM Tris-HCl pH=8.07 plus 150 mM NaCl and ThT stock solution of a concentration of 14.29 μM. The data is normalized in accordance to the highest fluorescent intensity in each aggregation study.

Furthermore, the graphs (Figure A.2-1) confirmed how the agitation also affected the rate of aggregation (5; 36; 96). Since the lag phase was thermodynamically not favored, it led to a rapid elongation phase (29; 51). However, as Figure A.2-1 showed if the agitation rate is lowered, the lag time was increased and the conversion of amyloid monomer to oligomer to fibrils took a longer timeframe. Therefore, there were five different agitation rate (800, 600, 500, 400, and 300 RPM) at which the aggregation was analyzed. These studies consisted of utilizing the 100 mM sodium phosphate buffer only because it was believed the lower ionic strength buffer concentration should increase the smaller aggregate population, which was not a negative effect while analyzing using the CE.

As the agitation decreased, an increase in the lag time was observed. Figure A.2-2 (below) showed the agitation at 300 RPM to be a decent starting time to analysis the soluble intermediate aggregates since the amyloid concentration will vary either higher or lower than 20 μM when conducting CE analysis. Additionally, it was important to note the dip in fluorescent before the elongation phase. It was believed this dip in intensity represented the paranucleus form or globular oligomer of Aβ usually seen in $A\beta_{1-42}$ (3; 97). Furthermore taking into account the structural form of a paranucleus, it was believed that it is harder for the Aβ: ThT binding to occur which in turn caused the lower fluorescent intensity.

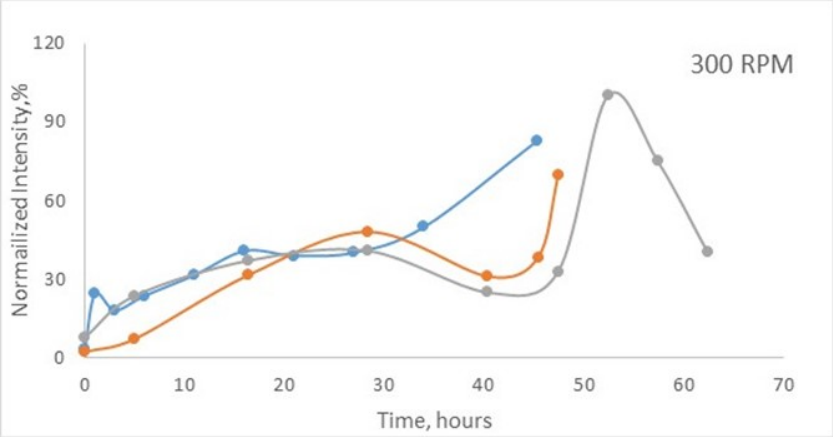

Sample Readings	
Time, Hrs.	**Standard Deviation**
noise	0.75
0	5.13
~16	7.55
~28	26.27

Figure A.2-2: Red, green, blue data are different experiments of ThT Assay using a Mini-Shaker at 25°C and 300RPM of 20μM $A\beta_{1-42}$ with 100 mM sodium phosphate pH=7.4 and ThT stock solution of 14.29μM; standard deviation of repeated points shown in table on the right; data is normalized in accordance to higher fluorescent intensity in aggregation study.

As shown in previous studies, it was believed the lower concentration of Aβ than 20 μM aggregated slower and the larger concentrations of Aβ led to shorter lag time (5; 36; 96). Therefore, since majority of the aggregation study in this thesis was conducted using 30 μM $A\beta_{1-42}$, ThT assays for 30 μM $A\beta_{1-42}$ was performed to understand the aggregation at 300 RPM (Figure A.2-3). Figure A.2-3 confirmed studies conducted in the past where the aggregation at 30 μM $A\beta_{1-42}$ was faster than the 20 μM $A\beta_{1-42}$; nonetheless, it was not faster by a great amount.

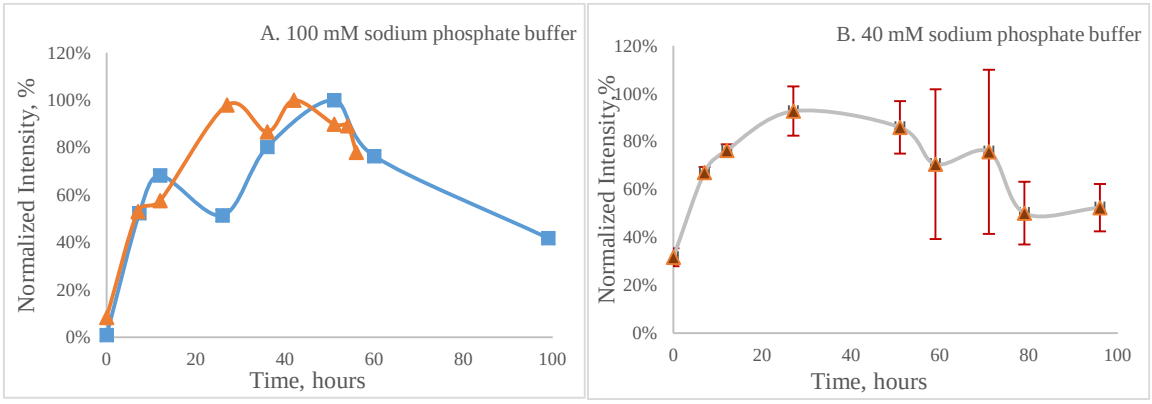

(Continued on next page)

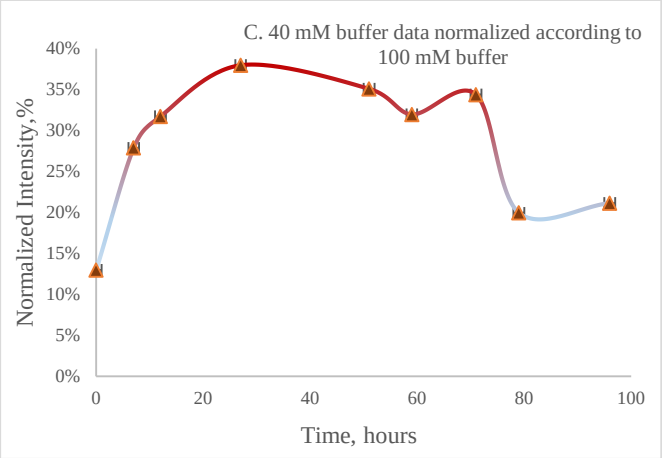

Figure A.2-3: Normalized data of (A) 100 mM sodium phosphate buffer, (B) 40 mM sodium phosphate buffer pH=7.4, n=2 using its highest fluorescent intensity for each aggregation study and (C) normalized data of 40 mM sodium phosphate buffer using 100 mM sodium phosphate buffer aggregation study's highest fluorescent data; initial concentration was 30 μM $A\beta_{1-42}$ with ThT stock solution of 16.67 μM at 25°C and 300 RPM.

Though the 40 mM sodium phosphate buffer experiments appeared to start at a higher normalized fluorescent intensity the actually experimentation consisted of an overall lower fluorescent intensity compared to the 100 mM sodium phosphate buffer assays (as shown in Figure A.2-3 C). Additionally, the difference between at time 0 between the two buffers might be a result of the peptide before starting the aggregation. Compared to the 20 μM $A\beta_{1-42}$, the 50 hour fluorescent intensity appeared to be the maximum intensity for all the experiments from where the fluorescent intensity started to decrease. Furthermore since the fluorescent intensity decreased by a huge percentage around 60 hours (Figure A.2-3) it was believed that an increase in insoluble $A\beta_{1-42}$ aggregates was observed. In Figure A.2-3, major variance occurred close to 27 hours when utilizing 100 mM buffer and since it appeared to be the start of the plateau using 40 mM sodium phosphate sample buffer, it was a good timeframe to analysis $A\beta_{1-42}$ aggregates using the CE and conduct experimentation at 300 RPM.

Appendix B: CE Parameters

CE analysis requires a greater understanding between the connection of the peptide concentration utilized and CE setup. Table B-1 below is an analysis of how some specific factors influence peptide separation and what factors to consider when developing an experimental method.

Specific Factors That Influence Peptide Separation Efficiency in CE	
Factors	**Influence Summary**
Capillary Length	Migration time and efficiency are linearly proportional where the resolution is proportional to square root of length; longer capillaries preferred for complex mixtures ➢ Due to past experiments, the capillary length was established as 31cm (60)
Capillary Inner Diameter	Resolution and efficiency are inversely proportional where mass loading and heat generation is proportional to diameter squared; smaller inner diameter capillaries allow higher voltage and ionic strength buffers ➢ All fused silica capillary tubing were purchased from Polymicro Technologies with an inside diameter of 51μm
Applied Voltage	At constant capillary length, efficiency and resolution is proportional where migration time is inversely proportional to voltage; on current vs. voltage graph need linearity or else excessive joule heating will occur (further details in Section I Appendix B)
Capillary Temperature	Current and amount of sample injection is proportional to temperature where viscosity and analysis time are inversely proportional to temperature ➢ Temperature set at 25°C (dealing with biological species- do not want to promote aggregation)
Buffer pH	Peptide charged groups pKa help establish pH range ➢ The separation buffer for the CE is 100 mM sodium phosphate buffer with pH=7.4. Sodium phosphate buffers pH usually does not change much with a change in temperature and can mimic the cell environment fluid.
Buffer Ionic Strength	Mobility and EOF are inversely proportional to ionic strength and can effect joule heating, detection sensitivity where peak shape is also proportional to ionic strength (further details in Section III Appendix B)
Pressure Injection	Though hydrodynamic injection is more precise than electrokinetic injection, in a coated capillary the viscosity of sample can be effected (further details in Section II Appendix B)
Detector	Ultraviolet (UV) light detection is utilized due to the ability to detect Aβ at 214 nm without any interference in analysis, provide detection with peptide content in micromolar range

Table B-1: Summary of factors effecting separation in CE (40; 43).

Another important parameter is the reducing or avoiding wall-analyte interaction. As mentioned in Chapter 1, neutral polymer coating can create the positively charged layer at the surface of the fused silica capillary and help avoid creating a double layer interaction between the capillary walls. This will also lead to better separation and better peptide detection.

I. Joule Heating

A nonlinear relationship between the voltage and current can create excessive joule heating in the capillary. Joule heating is when electric current runs through a conductor (such as a capillary filled with buffer) which leads to an increase in temperature. Though the high surface to volume ratio of the capillary helps reduce the generated heat through the capillary wall, temperature gradient and excessive joule heating can cause natural convection to occur where the local changes on viscosity or the sample's physical characteristics might be damaged (38). In turn, this will lead to poor resolution and separation.

As stated in Table B-1, the separation buffer be utilized is 100 mM sodium phosphate buffer which is considered a high ionic strength buffer. High ionic strength buffers are preferred in an uncoated capillary; however, high ionic buffer concentrations can make the current exceed the thermostat capacity at higher voltages which can potentially result in peak broadening and poor separation (38). In order to confirm utilizing 7 kV will be an adequate applied voltage for the separation, an Ohm's Law Plot was constructed using 100 mM sodium phosphate buffer pH=7.4. By constructing a current vs. voltage graph at the buffer concentration, the location of the point of non-linearity can be established. Hence, the voltage below that point can be utilized for future studies in hopes to avoid excessive joule heating. Figure B.1-1 (below), shows a linear regression (R^2=0.96) where major deviation from linearity occurs around 16 kV. Though the current/ voltage

relationship between 10-12 volts appears questionable, voltages below 15 kV could be utilized for the experiments.

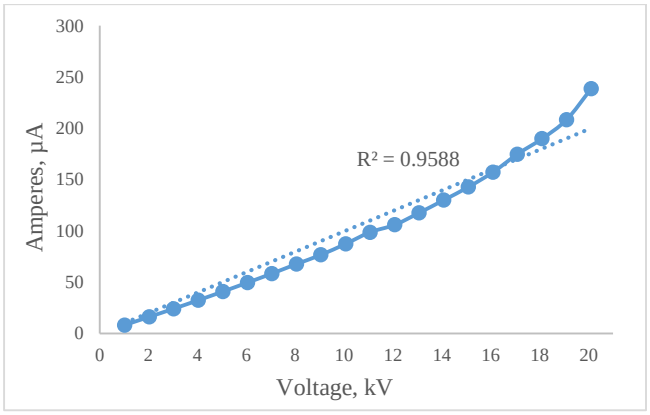

Figure B.I-1: Ohm's Law Plot analysis conducted utilizing 100 mM sodium phosphate buffer pH = 7.4 sample in 0.5% 2000 kDa PEO coated capillary with a pressure injection of 0.5 psi for 8 seconds; at each voltage n = 4 where the data points recorded were close to the set voltage.

Results shown in Figure B.1-1 were similar to literature for phosphate buffer system (40). Furthermore since 7kV was still a conservative applied voltage, it was utilized in hopes to provide fast separation with optimum resolution.

II. Pressure Injection

Unlike in electrokinetic injection, it is simplifier to quantify the injection amount utilizing pressure injection (43; 40). This helped set a basis of injection time and compare results by looking at previous work. In order to determine the necessary injection time, the flowrate of sample loading in the capillary or injection amount was determined by (40):

$$Q = \pi r^2 \left[\Delta P r^2 t_{inject}/(8\omega L)\right] C \qquad \text{[Equation B.II.1]}$$

where Q= flowrate, r= inner radius of capillary, P= pressure difference, t= injection time,

ω= viscosity of sample, L= length of capillary column

The sample is injected at 0.5 psi (as recommended by P/ACE MDQ User's Guide Beckman Coulter) (98). Therefore, the three unknowns are the flowrate, viscosity of sample and injection

time. In literature, data consisting of 50 μM $A\beta_{1-40}$ with a pressure injection of 8 seconds provides adequate separation and resolution (60). By using this as a basis and finding the flowrate, an estimation of the injection time needed can be calculated at various concentration. An important note to realize is that the viscosity of a peptide especially through a coated capillary is highly difficult to predict. Thus, a constant viscosity is determined assuming non-Newtonian flow at the point of injection since the flowrate into the capillary is believed to be constant and the viscosity is not dependent on the concentration. In turn, the injection time was determined at the varying concentrations.

For future experimentation, it is further recommended to determine whether injecting the separation buffer before and after the sample will help increase sample detection especially in a coated capillary.

III. Field Strength

As stated in Chapter 2, there is a linear relationship between the conductivity and field strength of a capillary under applied field where the difference between the field strength of the load buffer and BGE can be determined by (40; 99):

$$FS = \left(\frac{I}{A}\right) * \left[\left(\frac{1}{K_s} - \frac{1}{K_b}\right)\right] \qquad \text{[Equation B.III.1]}$$

According to Equation B.III.1, FS is the field strength, I=current, A=cross sectional area of capillary, Ks=conductivity of sample buffer (load buffer), and Kb=conductivity of separation buffer (BGE). Furthermore, the field strength can be looked in terms of local field strength in when considering the FASS method. Upon looking at Figure 2.1.1-1, it was observed that the local field strength affects the ions migration and zone broadening. The effect of the local field strength on the migration was especially true where molecular diffusion caused the zone broadening (67). With the CE parameters established as stated earlier in this appendix where neutral polymer

coating was utilized in the capillary to reduce EOF, it was important to understand exactly how the local field strength played into part when applying the FASS method.

As stated in the Section 2.2, before each sample was injected into the capillary, the capillary was rinsed with both water and a polymer rinse. As the water rinse cleaned the capillary of absorbed residues, the polymer rinse provided the opportunity to further stabilize the coating. It is important to known the neutral PEO coat was important in the capillary because the reduction of EOF due to coat is quite high and beneficial in terms of sample detection. Additionally, the polymer rinse was composed of the BGE buffer and therefore, helped create an environment in the capillary that has both the polymer coating and also BGE. Since the both the polymer coating and rinse concentration of the polymer was less than the critical micelles concentration (CMC), entanglement of the polymer with the sample was less likely to occur (38). However, the BGE is expected to affect the sample interaction in the capillary under an applied field. When applying the voltage, the current traveled from the positive electrode to the negative (normal polarity) where the electrode with the negative polarity was presumed to consist of ground potential. Therefore due to the polymer rinse, migration of BGE occurred within the capillary. The BGE conductivity difference with a load buffer of lower concentration creates a stationary zone that also differed in resistivity as stated in Chapter 2. Hence, it created a local field strength and provided an environment for FASS.

In order to narrow the sample buffer concentration and utilize Equation B.III.1, various sodium phosphate buffer conductivities were measured. As stated earlier, the BGE was 100 mM sodium phosphate buffer with pH=7.4. Therefore, the different conductivities and field strength of the various sodium phosphate buffer concentrations at and below 100 mM sodium phosphate are shown in Table B.III-1 (below).

Concentration	Average Conductivity, µS/cm	Field Strength, V/cm
100 mM	11280.0	225.0
75mM	9276.7	58.5
60 mM	7890.0	116.4
50 mM	6880.0	173.3
45mM	6340.0	211.1
40 mM	5766.7	259.0
30 mM	4636.7	388.1
25mM	3963.3	500.1
10 mM	1731.3	1494.1
5mM	993.3	2805.4
1mM	238.3	12550.5

Table B.III-1: Determine conductivities of various sodium phosphate buffer concentrations with pH=7.4 utilizing YSI Pro30 conductivity meter and finding the local field strenght in accordance to Equation B.III.1, n=3.

According to past studies using local field strength range of about 100-400 V/cm provides adequate separation and resolution (43; 75). By using bovine serum albumin fraction V (BSA) as a standard, experimentations were also conducted where the sample buffer varied from 10-50 mM sodium phosphate buffer (pH=7.4).

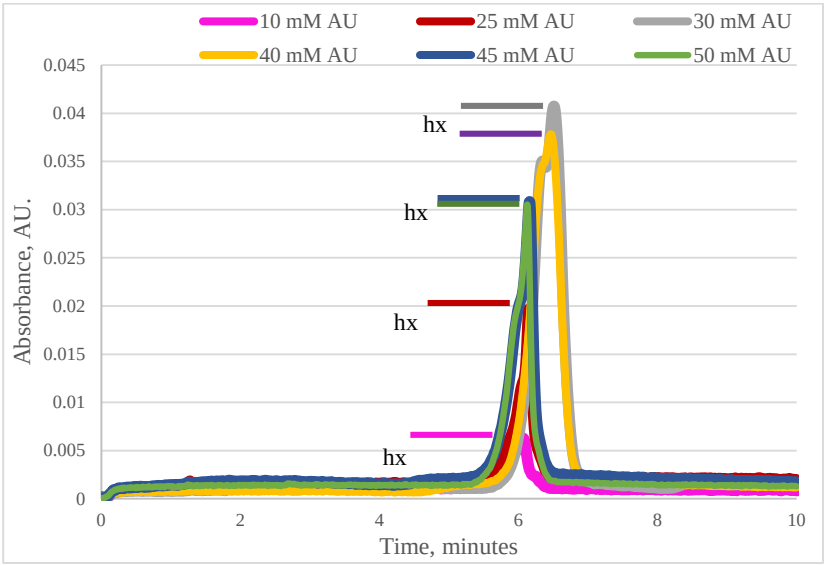

Figure B.III-1: 1mg/ml BSA using 10 mM (pink), 25 mM (red), 30 mM (gray), 40 mM (yellow), 45 mM (blue) and 50 mM (green) sodium phosphate buffer pH=7.4 as the load buffer, analyzed from CE data utilizing 0.5% 2000 kDa PEO coating, 8 second injection of 0.5 psi where

the BGE is 100 mM sodium phosphate buffer pH=7.4, hx line= max height corresponding to each peak.

By looking at Figure B.III-1, it was concluded that the two buffer with the best detection were either 30 mM or 40 mM sodium phosphate buffer with the BGE of 100 mM sodium phosphate buffer. Furthermore, experimentation utilizing 100 mM (control), 40 mM and 30 mM sodium phosphate was set as a good starting point to determine ideal FASS conditions.

It is recommended to further test Equation B.111.3 for future experiments to see whether adequate load buffer range for various buffers can be determined to utilize the FASS method.

Appendix C: Protocols

I. Prepare Sodium Phosphate Buffer

Objective: Make 100 mM sodium phosphate buffer

Method:

To make 0.10 M sodium phosphate dibasic and sodium phosphate monobasic in a 50 ml solution, first calculate the amount of grams needed of the two components for a 50 mL solution separately. The sample calculations are shown below:

Sodium Phosphate Dibasic:

$$\frac{0.10mol}{liter} * .05liter * 141.96\frac{gram}{mol} = 0.71\ grams$$

Sodium Phosphate Monobasic:

$$\frac{0.10mol}{liter} * .05liter * 156.01\frac{gram}{mol} = 0.78\ grams$$

Procedure:

Creating Solution-

1. Weight each gram amount in a weigh scale and put amount in two different sample tubes.
2. Put 50 mL of Nano-filtered DI water in the sodium phosphate dibasic sample tube and 50 mL in the sodium phosphate monobasic tube.
3. Make sure solution is mixed well.
4. Calculate the x amount of dibasic and y amount of monobasic sodium phosphate to make 100 ml solution for pH=7.4. This is based on the sodium phosphate buffer pH table at a concentration of 100 mM.

$$19ml\ of\ Monobasic + 81ml\ of\ Dibasic = 100ml$$

5. Since the final amount needed is 50 mL solution of the two combined, the equation in Step 4 can be manipulated to determine the needed amounts of the two components:

$$\frac{19ml\ of\ Monobasic}{2} + \frac{81ml\ of\ Dibasic}{2} = \frac{100ml}{2}$$

6. Get another sample tube and pipette to pipette the needed amounts of the two components for the 50 mL solution.

   Checking pH-

7. Turn on the pH meter and calibrate it:
   a. Clean the pH probe with DI Water and wipes
   b. Put pH probe in a pH of 4 and let the reading stabilize
   c. Set the readings to 4 by using the arrows and then press 'Yes'
   d. Repeat Steps a- c for a pH of 7 and 10 tubes.
   e. Clean pH probe again and put in sample (buffer in this case)
   f. Let the readings stabilize and read the final reading (sample pH)

II. Monomerization and storage of Amyloid Beta Peptide 1-42 by HFIP

Objective: 0.0271 mg $A\beta_{1-42}$ storage in -80°C refrigerator

Procedure:

1. Place 1,1,1,3,3,3-hexafluoro-2-propanol (HFIP) on ice in the hood and let it cool for a few minutes (about 15 minutes). HFIP is highly corrosive and very volatile. HFIP treatment was used to remove any pre-existing aggregates from the sample and due to its transparence in UV light. It is important to note, however, that HFIP has been reported to induce oligomer formation.
2. Take solid $A\beta_{1-42}$ that is stored in the -80°C freezer and place on ice in chemical hood fume.
3. Add enough HFIP to $A\beta_{1-42}$ that the final concentration is 1mM:

Have: 0.836mg AB Want: 1mM concentration

$$0.836\ mg\ AB * \frac{1\ mmol}{4514.1\ mg} = 0.000185197\ mmol$$

Therefore, total volume is 185 µL.

4. Rinse vial thoroughly and make sure well mixed in with the amyloid beta by pipetting solution in and out about 10 times.
5. Incubate on ice for 60 minutes, keeping the vial closed. Solution should be clear and colorless. Any traces of yellow color or cloudy suspension indicates poor peptide quality and should not be used.
6. Aliquot solution into non-siliconized micro-centrifuge tubes/vials with 0.0271 mg/vials (which means each tube has a total volume of 6 µL. Do not close tubes).
7. Allow HFIP to evaporate overnight in the hood at room temperature.
8. All traces of HFIP must be removed. The resulting peptide should be a thin clear film at the bottom of the tube. The peptide should not be white or chunky.
9. Store dried peptide films over desiccant at -80°C. These stocks should be stable for several months.

III. Nano-Drop Spectrometer

Objective: Determine the concentration of sample

Procedure:

1. Turn on the program, ND-1000 and click Protein A280.
2. Open the sampling arm and wipe the measuring pedestal with a Kim-wipes.
3. A message should pop up stating to measure water first. Get 2 µl of di-water and put it on the measuring pedestal and close the sample arm. Click ok. (Note: while putting in the amount on the measuring pedestal, put your hand close to the area to avoid bubbles etc.)

4. Make sure using proper wavelength and take the blank reading. Make sure the nano-drop is properly cleaned; therefore, measuring water and/or buffer solution a couple of times before starting or until the water absorbance is fairly flat. Then take another blank.
5. Wipe the measuring pedestal and measure the sample. Record the findings. Take at least 5 different points. Upon determining the concentration using Beer's law, take the average.
6. Have the last measurement be of water to ensure proper cleaning.

IV. Conductivity Meter

1. Take conductivity meter (YSI Pro30), and clean the probe with nano-water.
2. Make the needed buffer solutions.
3. Turn on the meter, and stick the probe in appropriate solution. Record the conductivity measured (make sure you record the proper units also).
4. Repeat steps until completion.
5. Clean the probe with nano-filtered water in the end.

V. ThT (thioflavin T) Assay at --- RPM

Objective: Conduct a ThT assay with 20μM $A\beta_{1\text{-}42}$ using 100 mM Sodium Phosphate buffer pH=7.4 at ---RPM

Method:

Prepare Aβ sample: 0.0271 mg $A\beta_{1\text{-}42}$,: 14.3 μL 5mM NaOH, 285.7 μL 100 mM Sodium Phosphate

$$Want: x\ \mu L\ 5mM\ NaOH\ and\ y\ \mu L\ 100mM\ Sodium\ Phosphate$$

Need: 500:10000 ratio of NaOH to Sodium Phosphate

Need Final Molarity of Aβ to be = 20μM

*Add 14.3 μL 5mM NaOH to get the 500:10000 ratio.

Therefore, 100 mM Sodium Phosphate should be 285.7 µL.

Prepare 1 mM ThT Stock for Assay:

Make 1 mM ThT solution made in di-water:

$$0.32mg * \frac{1\ mmol\ ThT}{318.87\ mg} = \frac{mmol}{1\ mM\ ThT} = 0.001\ \ liters$$

Prepare ThT Stock Solution for Assay: 4.929mL buffer, 0.071mL of 1mM ThT

Dilute 1 mM ThT to make a stock solution of 5 mL in 100 mM Sodium Phosphate buffer pH 7.4

Figure out the amount of stock solution needed for the ThT assay:

$$\frac{25\ \mu L\ AB * 20\ \mu M\ of\ AB}{200\ \mu L} = 2.5\ \mu M\ AB$$

Where 200 µL is the minimum volume required for the fluorometer

$$Want: 200\mu L\ volume$$

$$Have: 25\ \mu L\ of\ AB$$

Actual volume: 200µL-25 µL= 175 µL of stock solution needed

Find the molarity of the stock solution of ThT:

Need a 5:1 ratio of AB (amyloid beta) and ThT stock solution (due to previous experiments)

$$2.5\mu M\ AB * 5 = 12.5$$

$$200\mu L * 12.5\frac{\mu Mol}{L} = 175\ \mu l * Stock\ Solution$$

Where the stock solution in this case equals out to be 14.29 µM

Find out the amount of 1mM ThT solution and Phosphate buffer (use Equation 1):

$$14.29\mu M * 5ml = 1mM\ ThT * V$$

V=0.071 mL and therefore, we need 4.929 mL of buffer

Sample in Shimadzu RF Mini 150 Recording Fluorometer:

25 µL AB and 175 µL of ThT stock solution needed

Shaker Setting: 25°C and ---rpm

Procedures:

1. Take the non-stick surface micro-centrifuge tube containing 0.0271 mg $A\beta_{1-42}$ out of -80°C freezer. Put on ice in the hood.
2. Add 5 mM NaOH to tube and place on ice 10 minutes. (Make sure not too many ice or not in ice: potential chance it might freeze and ruin aggregation study)
3. Then add the buffer and let it stay for about 20 minutes on ice.
4. Turn on the mini-shaker at---- rpm and 25°C.
5. Turn on the fluorometer. Auto Zero the fluorometer using di-water. Make sure the optical filter in the fluorometer has the emission and excitation wavelength of 440nm and 490nm (respectively).
6. Run a blank run in the fluorometer of the ThT stock solution (noise). Record reading.
7. Take a time 0 reading of 25 µL $A\beta_{1-42}$ and 175 µL of ThT stock solution in the fluorometer.
    a. Make sure you add the ThT before the $A\beta_{1-42}$ for the sample in the cuvette.
    b. Add the $A\beta_{1-42}$ in the fluorometer and make sure it mixes well with the ThT in cuvette by pipetting the $A\beta_{1-42}$ in and out of the ThT.
    c. Also make sure the cuvette's window is facing the direction the light will hit it (in this case left side of the sample chamber).
    d. The actual reading will equal to be point reading subtracted by the blank run.
8. After taking the reading, put the rest of $A\beta_{1-42}$ sample in mini-shaker.
9. Clean the cuvette by vacuum.

10. Repeat step 7-9 for 9 different time point readings (make sure you make at least 30-70 µL of $A\beta_{1-42}$ left before last time point).

Note: to thoroughly clean the fluorometer cuvette:

1. Add 200 µl of 1M Sodium Hydroxide, let it sit in the cuvette for 5 minutes and vacuum it out the cuvette
2. Rinse with 200 µl di-water couple of times (2-3 times)
3. Add 200 µl methanol, let it sit in the cuvette for 1 minute and vacuum it out the vial
4. Wipe the outside of the cuvette to make sure it is clean and has no residue on it

VI. Changing Capillary from Capillary Cartridge in CE

Objective: Replace old capillary in the capillary electrophoresis machine.

Experimental Equipment:

Capillary

Window Maker Device

Wipes and DI Water

Capillary Electrophoresis Machine (aka P/ACE MDQ Glycoprotein System) and Computer Display:

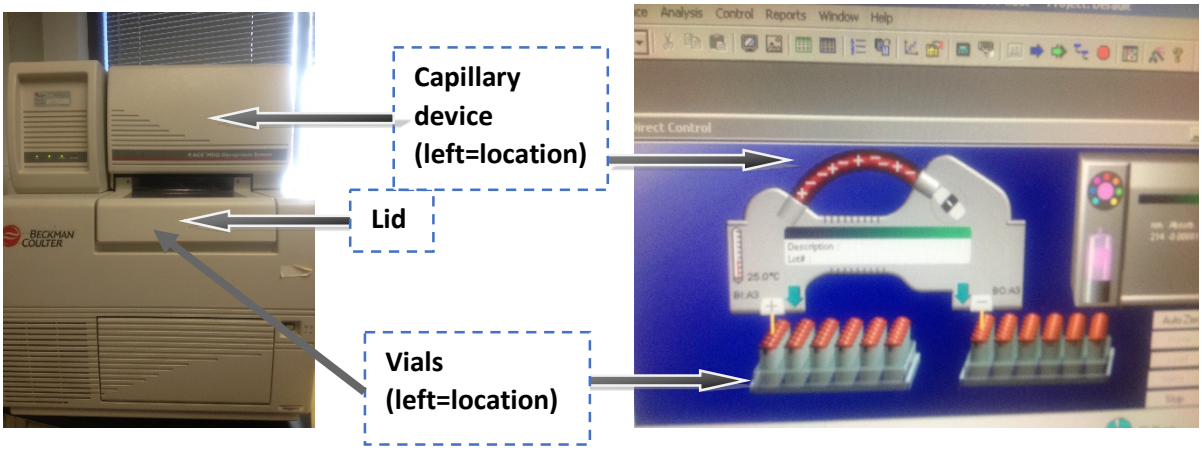

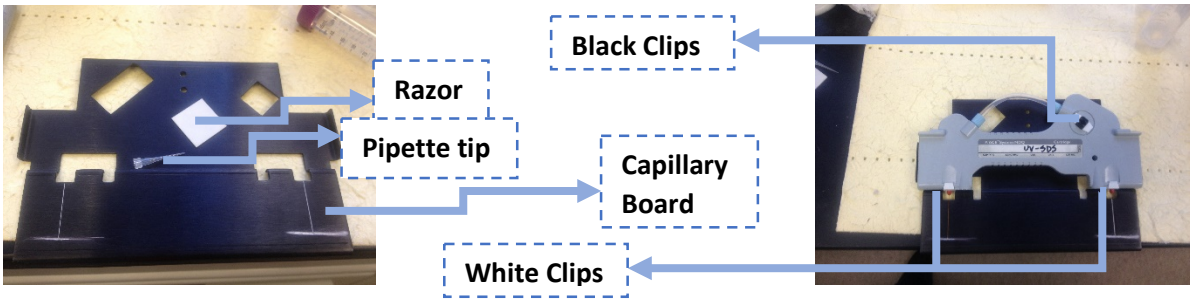

Procedure:

1. Open the lid from the Capillary Electrophoresis machine
2. Unscrew the two screws connecting the capillary cartridge to the equipment
3. Slowly pull the capillary cartridge up and out of its location
4. Take out the two white clips in the ends of the capillary on the device and take out the black clip- (the UV window clipper). To pull out the window clipper, push the click inward. Take out the black ring from the window clipper using a pipette tip. Set the black ring on a pipette tip.
5. Take the old capillary out (by pulling it out from one end) and dispose of it in the proper location.
6. Take a new set of capillary and put it through the capillary hole in the capillary device. Slowly insert the capillary until it comes out the other end. Take the capillary board (black cutter) and place it and the edge of the table (snugged tight to the end of the table). Place the capillary device on the top end on the capillary board and make sure the capillary reaches the right side mark (white horizontal line in the picture above) on the capillary board.
7. Cut the right side of the capillary according to the right side mark (white horizontal line in picture above) on the capillary broad using a razor blade.

8. Take the right side of the capillary and put it through the window maker until the capillary device is touching the window maker. Make sure the window maker is plugged in the switch and press the red button.
9. Hold the red button until the window maker's rings turn completely red and let go on the red button (upon completion of the rings turning red).
10. Take the capillary out of the window maker.
11. Take a task wipe (KIMWIPES-our lab usually uses this brand) and wet it in DI water.
12. Wipe the black region on the capillary (produced during the window maker steps). Make sure the black residue is completely off.
13. Push the capillary into the device until the window (step 12 area) is located in the middle region of the UV window in the capillary device.
14. Clip back on the two white clips by slowly moving it up the capillary.
15. Clip the black clip back on the capillary device and put the black ring in the window clipper.
16. Put the capillary device on the capillary broad in the middle of the board and cut both ends according to the mark.
17. Take the capillary device and put it in the Capillary Electrophoresis machine slowly.
18. Screw on the two side screws.

VII. CE Methods

For Water Polymer Rinse and Coat Sequence

a. Pre-Conditioning Wash Method Consist of:

Event	*Value (psi)*	*Duration (min)*	*Vial inlet side*	*Vial outlet side*	*Pressure Direction*	*Compound in vial*
Rinse-Pressure	50 psi	20 min	B1:C1	B0:C1	reverse	0.1M NaOH
Rinse-Pressure	20 psi	20 min	B1:C2	B0:C2	reverse	Water
Rinse-Pressure	20 psi	60 min	B1:C3	BO:C3	reverse	0.1M HCl
Rinse-Pressure	20 psi	10 min	B1:C2	B0:C2	reverse	Water

b. Polymercoating Method Consist of:

Event	*Value (psi)*	*Duration (min)*	*Vial inlet side*	*Vial outlet side*	*Pressure Direction*	*Compound in vial*
Rinse-Pressure	20 psi	15 min	B1:B1	B0:B1	reverse	Water
Rinse-Pressure	20 psi	15 min	B1:B2	B0:B2	reverse	0.1M HCl
Rinse-Pressure	50 psi	30 min	B1:B3	BO:B3	reverse	200 kDa PEO
Rinse-Pressure	20 psi	15 min	B1:B1	B0:B1	reverse	Water
Wait			B1:B4	B1:B4		Water

*Note: to make a method go to file->method->new and in each section (ex. Event) click the arrow in the right side of the first box below title to select the proper procedure.

For the Sample Run Sequence:

c. Water Polymer Rinse Method Consists of:

Event	*Value (psi)*	*Duration (min)*	*Vial inlet side*	*Vial outlet side*	*Pressure Direction*	*Compound in vial*
Rinse-Pressure	50 psi	10 min	B1:A1	B0:A1	reverse	Water
Rinse-Pressure	50 psi	10 min	B1:A2	B0:A2	reverse	Polymer separation matrix using 0.5% 50 kDa in separation buffer with 0.1% of 0.1% of 2000 kDa PEO

d. A4samplerun7kV Consists of:

Event	*Value*	*Duration*	*Vial inlet side*	*Vial outlet side*	*Pressure Direction*	*Compound in vial*
Rinse-Pressure	50 psi	5 min	B1:A2	B0:A2	reverse	Polymer separation matrix
Inject-Pressure	0.5 psi	-- sec	B1:A1	B0:A4	reverse	Inject sample
Separate-Voltage	7 kV	-- min	B1:A3	BO:A3	0.17MIN ramp, normal polarity	Separate in 100 mM sodium phosphate buffer pH=7.4

*Note: for the A5 sample run, changed A4 to A5 in the method procedure etc.

e. Final End Wash Method Consists of:

Event	*Value*	*Duration*	*Vial inlet side*	*Vial outlet side*	*Pressure Direction*	*Compound in vial*
Lamp-Off						
Rinse-Pressure	50 psi	10 min	B1:A1	B0:A1	reverse	Cleaning
Wait		1 min	B1:A4	BO:A4		Wait in water at end of experiment

VIII. Ohm's Law Experiment

Method:

Capillary Electrophoresis:

Utilizing P/ACE MDQ-UV Glycoprotein System 2006, conduct the experiment with 0.1M HCl, 0.1M NaOH, DI water, 0.5% 2000 kDa PEO, 100 mM sodium phosphate buffer (pH 7.4), and 0.5% 50 kDa PEO in 100 mM phosphate buffer (pH 7.4), wavelength of 214 nm, and at 7kV and 25°C.

Use CE Method:

Final End Wash Method

Water Polymer Rinse Method

Ohm's Law _kV (where I went from 1-20 kV)

Value	Duration	Type	Summary	Components
50.0 psi	10 min	Reverse	Water rinse	DI water
20.0 psi	10 min	Reverse	Phosphate buffer with PEO rinse	0.5% 50 kDa PEO in 100 mM buffer
_ kV	5 min		0.17 min ramp, normal polarity	100 mM sodium phosphate buffer

Procedure:

Conduct lab where my sequences were set up with a waterpolymerrinse method in between each Ohm's Law Method. The last method in each sequence was EndFinalWash.

IX. BSA Experiments on CE

Method:

Capillary Electrophoresis:

Utilizing P/ACE MDQ-UV Glycoprotein System 2006, conduct the experiment with 0.1M HCl, 0.1M NaOH, DI water, 0.5% 2000 kDa PEO, 100 mM sodium phosphate buffer (pH 7.4), and

0.5% 50 kDa PEO in 100 mM phosphate buffer (pH 7.4) with 0.1% of the 0.1% 2000 kDa PEO, wavelength of 214 nm, injection time=8 seconds, and at 7kV and 25°C.

Sample: 1 mg/ml BSA using various sodium phosphate buffer in sample (pH 7.4)

1. Dissolve the needed weigh of BSA in various sodium phosphate buffer concentrations in separate vials. (For storage, place in -20°C or -80°C)

Origin: Bi-gaussian method

Procedure:

For Experiment:

1. Make sample in proper sodium phosphate concentrations.
2. Make samples of just the sodium phosphate at the various concentrations (as blank buffer run).
3. Open program: 32 Karat
4. Click on MDQ-UV. If the direct control screen does not open automatically, click Control - go to Direct Control-Click View
5. Go to the light bulb, click it and turn it off
6. Click the load button and wait before opening the lid
7. Put 20 µl of the sample in the sample vial (with the spring) for the CE. Make sure all the vials are full with the needed solutions in the CE.
8. Close the lid

Blank Run consist of: WaterPolymerrinse Method, A4-30buffercheckingrun Method, WaterPolymerrinse Method, A5-30buffercheckingrun Method, FinalEndWashMethod (Sequence name: completebufferrun)

Each sample run consist of: WaterPolymerrinse Method, BSA Method, and FinalEndWashMethod (Method consists of pressure injection of 8 seconds and the separate voltage of 7kV for 10 minutes)

9. Turn on the light
10. Click the filter wheel and select the wavelength (214nm)
11. Click Auto Zero (make sure everything in working proper)
12. Click Control: Diagnostics: View

    Can see the amount of light going through 'window' in capillary (5 is a good rule of thumb #)
13. Run the buffer and sample sequences according to the stated methods earlier.

X. 30µM Amyloid Beta Sample using 100 mM or 40 mM Sodium Phosphate Buffer Method:

Capillary Electrophoresis:

Utilizing P/ACE MDQ-UV Glycoprotein System 2006, conduct the experiment with 0.1M HCl, 0.1M NaOH, DI water, 0.5% 2000 kDa PEO, 100 mM sodium phosphate buffer (pH 7.4), and 0.5% 50 kDa PEO in 100 mM phosphate buffer (pH 7.4) with 0.1% of the 0.1% 2000 kDa PEO, wavelength of 214 nm, injection time=13.3 seconds, and at 7kV and 25°C.

Sample: 30µM amyloid beta (1-42) using 100 mM sodium phosphate buffer in sample (pH 7.4), and 40 mM sodium phosphate buffer in sample (pH 7.4)

Make a 30µM $A\beta_{1\text{-}42}$ Sample Concentration:

1. Take 2 non siliconized micro-centrifuge tubes (non-stick tubes) containing 0.0271 mg $A\beta_{1\text{-}42}$ out of -80°C freezer. Add 5mM NaOH so that the 500:10000 ratio between

NaOH:100 mM/or 40 mM Sodium Phosphate is maintained (the ratio is similar to the one in Landers with 10:200 ratio)

$$Want: x\ \mu L\ 5mM\ NaOH\ and\ y\ \mu L\ 100mM\ Sodium\ Phosphate$$

Total volume= 200 µL

* 5mM NaOH = 9.52 µL to get the 500:10000 ratio.

Therefore, 100 mM or 40 mM Sodium Phosphate = 190.48 µL.

2. Let $A\beta_{1\text{-}42}$ solution in 5 mM NaOH for about 10 minutes on ice (due previous experimental findings)
3. Put the 190.48 µL of 100 mM or 40 mM Sodium Phosphate in 5mM NaOH and $A\beta_{1\text{-}42}$ solution and keep on ice for 20 minutes.

Shaker Setting: 25°C and 300 rpm

Origin: Bi-gaussian method

Procedure:

For Experiment:

1. Make amyloid beta sample in proper sodium phosphate concentrations.
2. Make samples of just the sodium phosphate at the various concentrations (as blank buffer run).
3. Open program: 32 Karat
4. Click on MDQ-UV. If the direct control screen does not open automatically, click Control - go to Direct Control-Click View
5. Go to the light bulb, click it and turn it off
6. Click the load button and wait before opening the lid

7. Put 20 µl of the sample in the sample vial (with the spring) for the CE. Make sure all the vials are full with the needed solutions in the CE.
8. Close the lid

Blank Run consist of: WaterPolymerrinse Method, A4-30buffercheckingrun Method, WaterPolymerrinse Method, A5-30buffercheckingrun Method, FinalEndWashMethod (Sequence name: completebufferrun)

Each sample run consist of: WaterPolymerrinse Method, 30 micrMolarsolution Method, and FinalEndWashMethod separately (Method consists of pressure injection of 13.3 seconds and the separate voltage of 7kV for 30 minutes)

9. Turn on the light
10. Click the filter wheel and select the wavelength (214nm)
11. Click Auto Zero (make sure everything in working proper)
12. Click Control: Diagnostics: View

    Can see the amount of light going through ‘window’ in capillary (5 is a good rule of thumb #)
13. For the Buffer Run Sequence:
    a. In the Sequence window, go to method section and select the needed methods (shown earlier)
14. For the sample sequence, make sure you run waterpolymerrinse method separately before the sample sequence. In the sample sequence, either have finalendwash method or lamp off method.

XI. Congo Red or Orange G Sample Preparation

Make a Congo red or Orange G Stock Solution:

1. Prepare a 16.7 µM Congo red or Orange G stock solution in di-water.

Make a 30µM $A\beta_{1\text{-}42}$ Sample Concentration:

1. Take a non-siliconized micro-centrifuge tubes (non-stick tubes) containing 0.0271 mg $A\beta_{1\text{-}42}$ out of -80°C freezer. Add 5mM NaOH so that the 500:10000 ratio between NaOH:100 mM/or 40 mM Sodium Phosphate is maintained

$$Want: x\ \mu L\ 5mM\ NaOH\ and\ y\ \mu L\ 100mM\ Sodium\ Phosphate$$

   Total volume= 200 µL

   * 5mM NaOH = 9.33 µL to get the 500:10000 ratio.

   Need 2% total volume to be inhibitor- 4 µL Congo red or Orange G stock solution

   Therefore, 40 mM Sodium Phosphate = 186.67 µL.

2. Add NaOH and after five minutes add 4 µL inhibitor stock solution to the amyloid beta. Let $A\beta_{1\text{-}42}$ solution in 5 mM NaOH and inhibitor for a total of about 10 minutes on ice (due previous experimental findings)
3. Put the 186.67 µL of 40 mM Sodium Phosphate in 5mM NaOH and $A\beta_{1\text{-}42}$ solution and keep on ice for 20 minutes.

Shaker Setting: 25°C and 300rpm

Origin Analysis: Bi-gaussian method

XII. Dot Blot Assay

Objective: Determine whether CE analysis shows similar results to dot blot analysis

Method:

Dot Blot Analysis:

Utilizing nitrocellulose membrane, primary antibodies: 6E10 (BioLegend), and OC (EMD Millipore), secondary antibodies: anti-mouse and rabbit (EMD Millipore), TBS-T(tris buffer saline with 0.01% Tween 20), sodium phosphate buffer at 100 mM and 40 mM pH 7.4, 5% milk in TBS-T, VWR Rocker, VWR Heating/Cooling Micro Plate Shaker, 4°C freezer, BCIP (5-bromo-4-chloro-3-indolyl phosphate) purchased by Amresco, NBT (Nitro blue tetrazolium chloride) purchased from Biotium.

Sample: 30µM amyloid beta (1-42) using 100 mM sodium phosphate buffer in sample (pH 7.4), and 40 mM sodium phosphate buffer in sample (pH 7.4)

Shaker Setting: 25°C and 300rpm

Method of Data Analysis: Image J

Procedures:

Dot Block Assay Set-Up:

1. Cut the necessary amount of 0.1 µm nitrocellulose membrane needed for the experiment. Make sure you touch the membrane as little as possible and use tweezers at the corners of the membrane to hold the membrane. Cut a small portion of a side of the membrane corner to help verify sample order of the membrane
2. Make 5% nonfat powdered milk solution in TBS-T (tris buffer saline with 0.01% Tween 20), make sure it is well mixed (can keep for about two days)

Note: To make TBS-T:

a. Prepare a 10X Stock 1 liter solution of TBS
    i. Get 500 mL di-water and add 66.1 g Tris-HCl, 9.7 g Tris-base, 875g NaCl and mix
    ii. Add 500 mL di-water to solution
    iii. Filter solution and store in 4°C refrigerator

3. Dot the membrane in the less shiny side and let it dry (about 15-20 minutes). The dot should contain at most 5 µL
4. Upon dotting the membrane for each aggregation time point, close container, put container in ziplock with drierite and place the container in the Tupperware. Place the Tupperware in the refrigerator in BELL 3131.
5. Repeat Steps 3-4 for each aggregation time point.
6. After the last time point, soak the membranes in and fill the container with enough bovine serum albumin (BSA) or in this case 5ml of 5% nonfat powdered milk to cover the membrane completely.

   Note: Make sure the membranes are dry before putting it in the container with the milk solution. If letting the membranes soak overnight, put the container on the shaker in the upstairs refrigerator or else at least soak the membranes for an hour. **In my case, added 5 ml of milk solution to container with membranes and put on VWR rocker with a tilt speed of 34 for an hour.**

Dot Block Protocol with Antibody

1. Drain the milk solution and wash with 5ml of TBS-T (Tris Buffer Saline and Tween 20) three times. Note: Make sure not directly on the membrane.

2. Add the primary antibody to the 5% milk solution (dilute). Do not put directly on the membrane but make sure membrane completely covered. Shake the container gently with the antibody. Put the container in the 4C refrigerator in Room 3133 for overnight with a tilt speed of 29-32.
    a. The dilution ratio are:
        i. Aβ1-16 specific 6E10 antibody- make sure assay is working correctly (sees amyloid beta in general, publish to show you know what you are doing) (1:2000 dilution)
        ii. Aβ fibril specific OC antibody (1:4000 dilution- see fibrils)
3. Drain the solution and wash 3 times with TBS-T to remove excess (cover the membrane).
4. Add secondary antibody same way.
    i. For OC use alkaline phosphatase-conjugated anti-rabbit IgG (1:4000 dilution) ***Note: if stock solution is diluted with glycerol than a 1:1500 dilution will be required for the same amount of antibody)
    ii. For 6E10 antibody use alkaline phosphatase-conjugated anti-mouse IgG (1:4000 dilution)
5. Incubate with gentle shaking on VWR rocker with tilt of 34 at room temperature for 1 hour.
6. Wash membranes 3 times in 1 X TBS-T. First two washes with 5 minutes interval. Last wash before start next step.
7. Make substrate solution (make enough for all membranes and cover with foil wrap):
    a. Add 15 ml of TBWS-T MgCl2 to test tube
    b. Add 0.1mL 50 mg/ml NBT solution in DMSO to test tube
    c. Add 0.05ml 50 mg/ml BCIP solution to same test tube

8. Remove TBS-T and add substrate solution
9. Have the membranes covered and incubate at room temperature with gentle agitation for 1-5 minutes depending when bands reach desired intensity *(if you notice purple precipitate the solution is probably done its job and you will only be adding color to the background)*.
10. To stop the reaction rinse with stop solution of 10% acetic acid and rinse with distilled water. Then take the membranes and put on Kimwipes but try to protect from light (light will cause signal to fade)

*Also conducted the experimentation without the freezing steps where after each time point the membranes were soaking in 5% milk solution and put in the refrigerator. Therefore, each time point consisted of a separate membrane. The milk solution was replaced every 12 hours.

XIII. TEM Imaging

Objective: Compare TEM with dot blot analysis

Method:

TEM Analysis:

Utilizing PELCO Slim Tweezer put handle carbon film on 300 mesh nickel grids (Electron Microscopy Sciences), parafilm, dry tissue paper, 2% Uranyl Acetate (Electron Microscopy Science), VWR Heating/Cooling Micro Plate Shaker, JEM-1011 Electron Microscope (JEOL)

Sample: 30μM amyloid beta (1-42) using 100 mM sodium phosphate buffer in sample (pH 7.395), and 40 mM sodium phosphate buffer in sample (pH 7.4)

Shaker Setting: 25°C and 300rpm

Method of Data Analysis: AMT software

Procedures:

TEM sample preparation:

1. Pipette 3μL of sample onto a parafilm. Put the shiny side of the grid onto the sample using slim tweezers. The dull side consist of the formvar coated grids which provides better sticking ability of grid and sample; however, due to experiments conducted by fellow researchers, the shiny side provides better results. Important Note: be carefully with the tweezers to avoid damaging the grids. Carefully remove grid from container-if move the grid container without the lid, the grids have a potential to fly off. Cannot use grids that have fallen etc.
2. After 1-2 minutes, remove the grid and dry it by gently tapping it to a filter paper from the grids sides.
3. Put the shiny side of the grid onto 3μL of 2% uranyl acetate. Uranyl acetate is a toxic radioactive chemical that is made from depleted uranium. Though uranyl acetate utilized in diluted, avoid long term exposure to the chemical. Important Note: Uranyl acetate consists of slight odor.
4. After 45 seconds to 90 seconds, remove the grid and dry it by gently tapping it to the filter paper.
5. Put the shiny side facing up in a glass container to further analysis using a TEM.

TEM Analysis:

6. Make sure the TEM has enough liquid nitrogen in it. Be careful while pouring in the liquid nitrogen. Wear proper gloves, avoid pouring onto skin- can cause cool burns.
7. In the sample region, take the sample holder out of the container. Note: Do not touch area with the ruby with hands.

8. Use thick/ normal tweezers for opening the sample lid. To open, place the tweezer close to the lid indenture and use that to slant- lift upwards.
9. Put in the sample in the 1 and 2 position if have more than one sample. Make sure sample is in the middle by looking at it through a microscope. Close the lid.
10. Turn on the software AMT on the computer. Make sure beam is facing the right direction.
11. Take the sample holder and slowly insert into the TEM location until the first stopping location (hear a click)
12. Wait until the green light goes off a 2nd time, and turn the holder clockwise. Then slowly guide the place holder into the TEM.
13. Turn on the filament and gradually turn the filament node to see beam in the microscopy area
14. Condense the beam inward into a little circle by increasing the magnification
15. Saturate the filament by turning the filament node (to 77 or when images of filament has disappeared)
16. Analysis the sample by moving throughout the grid and changing the magnification. Once found an image, bring beam down and switch beam towards the computer.
17. On the computer, click live image and make sure the beam has an adequate intensity.
18. After saving the image, can repeat procedure. Once imaging is complete, make sure the magnitude is at 800X, the microscope image is at the center of the grid and leave the sample node in the 1 position.
19. Bring the filament beam down by turning the filament node all the way down to zero.
20. Turn off the filament.

XIV. CE Centrifugation Experiment

Objective: Determine cutoff molecular weight for both 60 μM $A\beta_{1-42}$ solution using either 100 mM or 40 mM sodium phosphate buffer and 5 mM NaOH

Method:

Capillary Electrophoresis:

Utilizing P/ACE MDQ-UV Glycoprotein System 2006, conduct the experiment with 0.1M HCl, 0.1M NaOH, DI water, 0.5% 2000 kDa PEO, 100 mM sodium phosphate buffer (pH 7.395), and 0.5% 50 kDa PEO in 100 mM phosphate buffer (pH 7.395) with 0.1% of the 0.1% 2000 kDa PEO, wavelength of 214 nm, and at 7kV and 25°C.

Make a 60μM Aβ1-42 Sample Concentration:

1. Take 2 non siliconized micro-centrifuge tubes (non-stick tubes) containing 0.0271 mg Aβ1-42 out of -80°C freezer. Add 5mM NaOH so that the 500:10000 ratio between NaOH:40 mM Sodium Phosphate is maintained

$$Want: x\ \mu L\ 5mM\ NaOH\ and\ y\ \mu L\ 40mM\ Sodium\ Phosphate$$

Total volume= 100.05 μL

* 5mM NaOH = 4.8 μL to get the 500:10000 ratio.

Therefore, 40 mM Sodium Phosphate = 95.25 μL.

2. Let $A\beta_{1-42}$ solution in 5 mM NaOH for about 10 minutes on ice (due previous experimental findings)
3. Put the 95.25 μL of 40 mM Sodium Phosphate in 5mM NaOH and $A\beta_{1-42}$ solution and keep on ice for 20 minutes.

Centrifuge Setting: 14,100 X g (14.5 rpm)

Origin Analysis: Bi-gaussian method

Procedure:

For Experiment:

1. Put the centrifuge in the refrigerator (4°C). This will help potentially avoid the occurrence of $A\beta_{1-42}$ aggregation due to heating.
2. Wash filter with 70% of ethanol at 14.5 rpm for 5 minutes (ethanol should be completely filtered through).
3. Make sure filter/ vial does not contain any ethanol after wash.
4. Wash filter with di-water at 14.5 rpm for 3 minutes.
5. Make sure filter/ vial does not contain any water after wash.
6. Wash filter with buffer at 14.5 rpm for 6 minutes (buffer should be completely filtered through).
7. Make sure filter/ vial does not contain any buffer after wash.
8. Take --µl at 0 hour of 40 mM sodium phosphate buffer amyloid beta sample and put in --kDa filter.
9. Put the filter vial in the centrifuge and set to the proper conditions. (14.5 rpm and 5 minutes)
10. Transfer the sample from the filter (retenate) or the sample that comes out of the filter in two different nonstick tubes (filtrate).
11. Open program on computer: 32 Karat
12. Click on MDQ-UV. If the direct control screen does not open automatically, click Control - go to Direct Control-Click View
13. Go to the light bulb, click it and turn it off
14. Click the load button and wait before opening the lid

15. Put sample in CE (have control and sample vials).
16. Put filtrate in the sample vial (with the spring) for the CE. Make sure all the vials are full with the needed solutions in the CE. Run sample in CE after centrifugation.
17. Close the lid

Run consist of 0.5psi pressure injection of 8 seconds.

18. Turn on the light and click the filter wheel and select the wavelength (214nm)
19. Click Auto Zero (make sure everything in working proper)
20. Click Control: Diagnostics: View

    Can see the amount of light going through 'window' in capillary (5 is a good rule of thumb #)

21. For the Sample Run Sequence:
    a. In the Sequence window, go to method section and select the needed methods (shown earlier)
22. Take the next sample and repeat procedure.
23. Take an un-filtered $A\beta_{1-42}$ sample for each time point as well.